Natland, J.H., Dick H.J.B., Miller, D.J., and Von Herzen, R.P. (Eds.)
Proceedings of the Ocean Drilling Program, Scientific Results Volume 176

9. The Composition and Origin of Igneous and Hydrothermal Veins in the Lower Ocean Crust—ODP Hole 735B, Southwest Indian Ridge[1]

Paul T. Robinson,[2] Jörg Erzinger,[2] and Rolf Emmermann[2]

ABSTRACT

During Legs 118 and 176, Ocean Drilling Program Hole 735B, located on Atlantis Bank on the Southwest Indian Ridge, was drilled to a total depth of 1508 meters below seafloor (mbsf) with nearly 87% recovery. The recovered core provides a unique section of oceanic Layer 3 produced at an ultraslow spreading ridge. Metamorphism and alteration are extensive in the section but decrease markedly downward. Both magmatic and hydrothermal veins are present in the core, and these were active conduits for melt and fluid in the crust. We have identified seven major types of veins in the core: felsic and plagioclase rich, plagioclase + amphibole, amphibole, diopside and diopside + plagioclase, smectite ± prehnite ± carbonate, zeolite ± prehnite ± carbonate, and carbonate. A few epidote and chlorite veins are also present but are volumetrically insignificant. Amphibole veins are most abundant in the upper 50 m of the core and disappear entirely below 520 mbsf. Felsic and plagioclase ± amphibole ± diopside veins dominate between ~50 and 800 mbsf, and low-temperature smectite, zeolite, and prehnite veins are present in the lower 500 m of the core. Carbonate veinlets are randomly present throughout the core but are most abundant in the lower portions. The amphibole veins are closely associated with zones of intense crystal plastic deformation formed at the brittle/ductile boundary at temperatures above 700°C. The felsic and plagioclase-rich veins were formed originally by late magmatic fluids at temperatures above 800°C, but nearly all of these have been overprinted by intense

[1]Robinson, P.T., Erzinger, J., and Emmermann, R., 2002. The composition and origin of igneous and hydrothermal veins in the lower ocean crust—ODP Hole 735B, Southwest Indian Ridge. *In* Natland, J.H., Dick, H.J.B., Miller, D.J., and Von Herzen, R.P. (Eds.), *Proc. ODP, Sci. Results,* 176, 1–66 [Online]. Available from World Wide Web: <http://www-odp.tamu.edu/publications/176_SR/VOLUME/CHAPTERS/SR176_09.PDF>. [Cited YYYY-MM-DD]
[2]GeoForschungsZentrum Telegrafenberg, D-14473 Potsdam, Germany. Correspondence author: **paul.robinson@kvab.be**

Initial receipt: 4 May 2000
Acceptance: 15 December 2001
Web publication: 31 May 2002
Ms 176SR-019

hydrothermal alteration at temperatures between 300° and 600°C. The zeolite, prehnite, and smectite veins formed at temperatures <100°C. The chemistry of the felsic veins closely reflects their dominant minerals, chiefly plagioclase and amphibole. The plagioclase is highly zoned with cores of calcic andesine and rims of sodic oligoclase or albite. In the felsic veins the amphibole ranges from magnesio-hornblende to actinolite or ferro-actinolite, whereas in the monomineralic amphibole veins it is largely edenite and magnesio-hornblende. Diopside has a very narrow range of composition but does exhibit some zoning in Fe and Mg. The felsic and plagioclase-rich veins were originally intruded during brittle fracture at the ridge crest. The monomineralic amphibole veins also formed near the ridge axis during detachment faulting at a time of low magmatic activity. The overprinting of the igneous veins and the formation of the hydrothermal veins occurred as the crustal section migrated across the floor of the rift valley over a period of ~500,000 yr. The late-stage, low-temperature veins were deposited as the section migrated out of the rift valley and into the transverse ridge along the margin of the fracture zone.

INTRODUCTION

Ocean Drilling Program (ODP) Hole 735B is situated on top of Atlantis Bank, an uplifted and unroofed section of lower ocean crust (Fig. **F1**). Massive and foliated gabbros are exposed on the bank in 650–700 m of water. Hole 735B, drilled during Legs 118 and 176, penetrated 1508 m into the section with an average recovery of 87% (Robinson, Von Herzen, et al., 1989; Shipboard Scientific Party, 1999; Dick et al., 2000). Most of the unrecovered core was in the upper 100 m of the hole or in fault zones located at various levels in the section. Thus, for much of the drilled sequence core recovery was close to 100%, providing a nearly complete sample of much of oceanic Layer 3. Based on variations in texture and mineralogy, 12 major lithologic units are recognized in the section, ranging from 39.5 to 354 m thick (Robinson, Von Herzen, et al., 1989; Shipboard Scientific Party, 1989, 1999). The principal lithologies include troctolite, troctolitic gabbro, olivine gabbro and microgabbro, gabbro, gabbronorite and Fe-Ti oxide gabbro, gabbronorite, and microgabbro. Highly deformed mylonites, cataclasites, and amphibole gneisses are locally present, as are small quantities of pyroxenite, anorthositic gabbro, and trondhjemite.

Igneous and hydrothermal veins are abundant and widely distributed throughout the drilled section, but most are present in the upper 800 m. Individual veins were not logged during Leg 118, but the area percentages of the different vein types were estimated later (Dick et al., 1991). During Leg 176, each vein in the core was logged and its composition and dimensions were recorded. Nearly 3000 veins were logged in the core from the lower 1053 m of the hole (Table **T1**). Smectite veins are the most numerous, making up nearly half the total number, followed in order of abundance by amphibole, amphibole + plagioclase, carbonate, plagioclase, and felsic veins. These six varieties make up 92% of the total veins logged during Leg 176, and only three other varieties comprise >1% each.

Using data from both legs, we estimated the area percentage of veins for the entire section (Fig. **F2**). Although smectite veins are the most numerous, felsic and amphibole veins are far more voluminous. Felsic veins alone make up ~38% by area, and amphibole and amphibole +

F1. Location of Hole 735B on Atlantis Bank, Southwest Indian Ridge, p. 26.

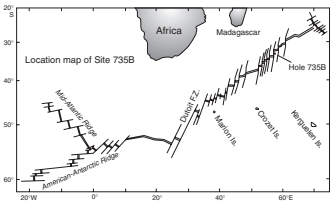

T1. Vein types, p. 38.

F2. Area percentages of different vein types, p. 27.

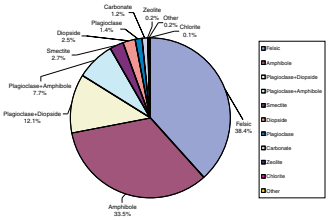

plagioclase veins combined make up ~41%. Diopside and plagioclase + diopside veins combined make up nearly 15% by area, and all the rest account for <6%.

The veins listed in Table T1 were identified macroscopically on the basis of their dominant mineralogy. Detailed petrographic examination revealed considerable overlap in mineralogy among the different veins; for example, most diopside and plagioclase veins contain at least small amounts of amphibole, many plagioclase veins contain significant amounts of quartz, and many smectite veins have small amounts of carbonate and prehnite.

Compositional zoning in some veins further complicates the classification. Typically, though not always, relatively high-temperature minerals are present along the vein walls and lower temperature minerals near the center. In a few cases, veins with relatively high-temperature mineral assemblages have reopened and the new crack is filled with low-temperature minerals such as smectite, carbonate, or zeolite.

Based on our thin section descriptions, we recognize seven major types of veins: felsic and plagioclase rich, plagioclase + amphibole, amphibole, diopside and diopside + plagioclase, smectite ± prehnite ± carbonate, zeolite ± prehnite ± carbonate, and carbonate. A few epidote and chlorite veins are also present but are volumetrically insignificant. Although the groups are named for their dominant mineralogy, most veins contain at least a small percentage of several other minerals. Most of the veins show no obvious correlation with primary lithology, although felsic varieties are most abundant in the oxide gabbros of lithologic Unit IV.

The vein assemblage described here is quite different from that recovered from Hess Deep gabbros in ODP Hole 894. The three main types recovered from that section are amphibole veins, composite veins containing mixtures of chlorite ± prehnite ± epidote ± titanite ± clay minerals, and smectite ± chlorite ± zeolite ± calcite veins (Mével, Gillis, Allen, and Meyer, 1993; Manning and MacLeod, 1996; Früh-Green et al., 1996). The abundant felsic, plagioclase + amphibole, and plagioclase + diopside veins in Hole 735B appear to be entirely absent from the Hess Deep section.

PETROGRAPHY AND MINERALOGY

Felsic and Plagioclase Veins

By number, felsic and plagioclase veins comprise only a few percent of the total but they make up nearly 40% by area (Table T1; Fig. F2). Thin section examination reveals no significant differences between felsic and plagioclase veins, but because they were logged separately during core description, we retain the terminology.

Felsic material may form irregular patches 1–3 cm across, anastomosing veinlets 2–3 mm wide, or single veins normally 5–10 mm wide (Pl. P1). In all cases, the veins or patches have sharp, well-fined contacts with the host rock. Many of the felsic veins are associated with oxide gabbros in lithologic Unit IV, and they are most abundant in the upper 500 m (Fig. F3). They decrease rapidly downhole and are virtually absent below ~1250 meters below seafloor (mbsf).

The felsic and plagioclase veins consist predominantly of plagioclase, with lesser amounts of amphibole, biotite, and quartz (Pls. P1, P2). Many also contain trace amounts of ilmenite, titanite, zircon, albite, ap-

P1. Felsic and plagioclase + amphibole and plagioclase + diopside veins, p. 62.

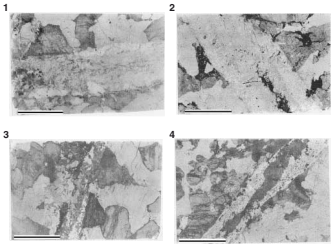

F3. Downhole plots of vein abundance, p. 28.

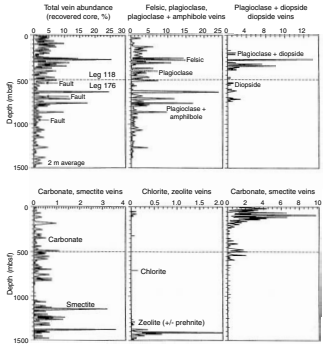

P2. Felsic and plagioclase-rich veins showing strongly zoned plagioclase crystals, p. 63.

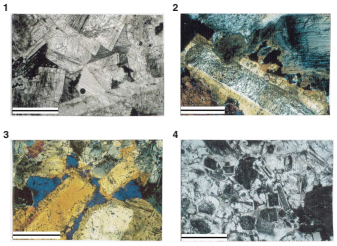

atite, and epidote as well as variable quantities of late-stage minerals such as chlorite, clay minerals, zeolites, and carbonate. A few have narrow, 2- to 3-mm-wide bands of amphibole + diopside in the center (Pl. **P1,** fig. 3) but most lack clinopyroxene. Narrow bands of greenish brown amphibole along the vein walls are common, particularly where the vein cuts clinopyroxene crystals in the host rock (Pl. **P3,** figs. 3, 4).

Plagioclase is present in two modes in the felsic veins: as myrmekitic intergrowths with quartz and minor K-feldspar and as large, strongly zoned crystals. Myrmekite is relatively rare, present in <5% of the veins examined in thin section. A typical example of a myrmekite vein (Sample 176-735B-124R-1, 111–115 cm) has narrow bands of greenish brown amphibole and minor oxide along the margins, grading inward into a zone containing large, zoned plagioclase crystals and quartz, which in turn grades into myrmekite. The myrmekite varies significantly in grain size from very fine to relatively coarse (quartz blebs up to 0.5 mm in diameter).

Large, concentrically zoned plagioclase crystals are present in nearly every felsic vein examined (Pl. **P2**). They are commonly subhedral, blocky crystals ranging from 2 to 10 mm across. Most have pitted cores of andesine containing small inclusions of amphibole, chlorite, or dark aphanitic material and clear white rims of albite and oligoclase. In some cases, the plagioclase is extensively replaced by green or brown chlorite, locally accompanied by minor epidote or carbonate. Narrow, irregular veinlets of colorless albite and oligoclase are commonly present, and albite may replace, as well as rim, the more calcic cores.

Most of these plagioclase-rich veins have relatively high porosities, suggesting corrosion of the grains by hydrothermal fluids. The resulting pore space may be open or, more commonly, partly filled with Na-plagioclase and quartz (Pl. **P2**).

The quartz in the felsic veins is typically present as small, irregular interstitial grains, ranging from 0.1 to 1 mm across. Commonly, the quartz grains, although physically separated, are in optical continuity, forming large, almost poikilitic masses (Pl. **P2,** fig. 3). The quartz is typically concentrated in the centers of the veins where the porosity is highest. In some samples, the quartz itself is rimmed and partly replaced by light brown smectite. Smectite, chlorite, prehnite, and zeolites may also fill some of the spaces between the plagioclase grains.

Almost all of the veins that contain significant amounts of quartz (>5 modal%) also contain a few crystals of mica, up to 5 mm across. The mica is typically yellowish brown biotite or phlogopite, and it is present either as single crystals or as rims on amphibole. The mica may also be associated with small amounts of iron oxides and titanite.

Trace amounts of zircon are also present in the felsic and plagioclase veins. It forms small, euhedral crystals usually ~0.1 mm across, typically enclosed in plagioclase.

Amphibole Veins

Amphibole veins are virtually confined to the upper 600 m of the section and most are present in the upper 250 m (Fig. **F3**). They are most abundant in highly sheared gabbros, particularly in the amphibole gneisses near the top of the hole. Most are 0.2–3 mm wide, have sharp but irregular contacts, and are oriented at high angles to the foliation (Pl. **P4,** fig. 1). They both cut and are cut by the foliation in the host rocks. Many are small, discontinuous features that extend for only a few centimeters, although some may be several meters in length.

P3. Plagioclase + diopside and plagioclase + amphibole veins, p. 64.

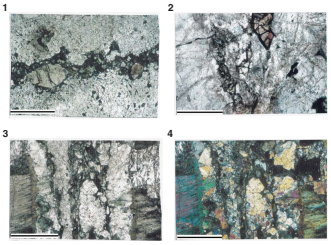

P4. Various vein minerals, p. 65.

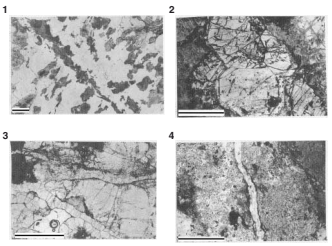

Small veins commonly are not continuous across clots of colorless amphibole after olivine and orthopyroxene but, rather, merge into them.

These veins consist almost entirely of small, subhedral crystals of brown to greenish brown amphibole, 0.2 to 1 mm across, in some cases accompanied by small amounts of plagioclase. The amphibole crystals may have a random orientation or they may be aligned along the length of the vein. Optical zoning is not visible in thin section, and most amphibole grains are compositionally homogeneous. Some of the amphibole is rimmed by green chlorite.

Plagioclase + Amphibole Veins

Plagioclase + amphibole veins are the third most abundant variety in Hole 735B (Table **T1**) and make up nearly 8% by area (Fig. **F2**). They are primarily present between 550 and 950 mbsf, that is, below the monomineralic amphibole veins and below most of the plagioclase + diopside veins (Fig. **F3**). Most of these veins consist dominantly of plagioclase, with only small amounts of amphibole, and hence are difficult to distinguish macroscopically from plagioclase or felsic varieties. A few contain small relict grains of diopside, completely surrounded by amphibole, suggesting that these two types of veins are gradational.

The plagioclase + amphibole veins typically range from ~2 to 10 mm in width and have sharp boundaries with the host rock (Pl. **P1,** figs. 3, 4). Typically, where these veins cut clinopyroxene in the wall rock, a narrow band of amphibole is developed along the contact (Pl. **P3,** figs. 3, 4); where the veins cut plagioclase, the contact is marked by secondary plagioclase. Many of the veins are compositionally zoned with alternating bands of amphibole and plagioclase (Pl. **P3,** figs. 3, 4). In some cases, the amphibole may be present as a discrete band along the center of the vein (Pl. **P1,** figs. 3, 4).

The plagioclase in these veins typically forms subhedral, blocky, strongly zoned crystals, often with a pitted appearance. The plagioclase-rich portions are typically quite porous, with many open spaces between the grains. Nearly all of these veins also contain small amounts of titanite, which forms subhedral to euhedral grains, typically close to the vein wall (Pl. **P3,** fig. 2). Chlorite is present in about a third of the veins, rimming amphibole or filling spaces between the plagioclase grains.

The amphibole along the vein walls is greenish brown in color and commonly forms ragged grains oriented perpendicular to the wall. Most veins also contain scattered subhedral to euhedral crystals of either brownish green or green amphibole intergrown with the plagioclase. Many of these grains, particularly the larger ones, exhibit some optical zoning, from brown or greenish brown in the cores to brighter green on the margins. The most spectacular example of zoning is from a small felsic patch in Sample 176-735B-202R-7, 96–101 cm. In this patch, amphibole forms clots up to 5 mm across that replace plagioclase. The amphibole adjacent to the plagioclase is dark brown, but it grades rapidly into light brown material and then into green amphibole (Pl. **P5,** fig. 1). The green amphibole also exhibits strong zoning.

A few of the plagioclase + amphibole veins contain small patches of dark, very poorly crystallized material with tiny skeletal needles of bright green actinolite.

P5. Vein minerals, p. 66.

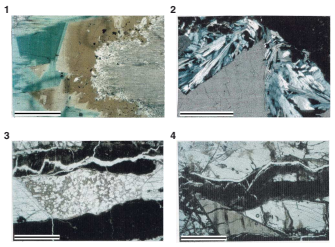

Diopside and Plagioclase + Diopside Veins

These veins are particularly abundant in a 235-m-thick interval between ~165 and 400 mbsf, but several smaller clusters are also present between 460 and 750 mbsf (Fig. F3). Most are 2–10 mm wide and typically have sharp boundaries with the host rocks, which are chiefly gabbro and olivine-bearing gabbro (<5% olivine) or, more rarely, olivine gabbro.

The diopside is typically present as irregular to tabular, light green to colorless grains along or near the vein walls, but in a few samples it forms a 1-mm-wide band down the center of the vein (Pl. P3, fig. 1). Large (up to 4 mm), euhedral, zoned crystals are present in a few veins, for example, Sample 176-735B-69R-5, 31–41 cm (Pl. P4, fig. 2). Many of the grains are pitted and irregular, and most are rimmed and partly replaced by greenish brown amphibole. Typically, diopside makes up no more than 5 to 10 modal% of a given vein but can be up to 90%. It is invariably associated with intermediate plagioclase, which makes up the bulk of most veins, and with variable amounts of amphibole. Other common minerals in these veins include chlorite, epidote, titanite, Na-plagioclase, clay minerals, and zeolites. Quartz and biotite have not been found in the diopside-bearing veins. The chlorite is nearly always in the groundmass of the vein, filling spaces between plagioclase crystals. Na-plagioclase rims and fills spaces between more calcic plagioclase grains, producing highly zoned crystals like those in the felsic and plagioclase-rich veins. In a few cases, it also fills narrow veinlets or cracks cutting through the other grains. Epidote is present in only trace amounts, usually as an alteration product of plagioclase. At least a few grains of titanite are present in most diopside-bearing veins (Pl. P3, fig. 1), and in some cases they are associated with ilmenite.

Smectite ± Prehnite ± Carbonate Veins

Smectite veins are present throughout the Hole 735B core but are best developed in the lower 500 m of the section and in a 260-m-thick interval between 575 and 835 mbsf (Fig. F3). Even in the lower 500 m of the section, however, their distribution is uneven, with a concentration of veins between 1230 and 1330 mbsf and a barren zone between 1340 and 1380 mbsf (Fig. F3). Although abundant in number (Table T1), most of these veins are simply minute, smectite-lined cracks <1 mm wide, and they make up only ~3% of the total area of the core (Fig. F2). A few smectite + carbonate and smectite + zeolite veins are also present, but these are less abundant. The smectite veins may be present either as individual features or as narrow cracks in the center of felsic veins. In some cases, they form networks of hairline cracks, particularly in plagioclase where the host mineral is partly replaced.

The well-developed smectite veins in the lower part of the hole are generally 2–5 mm wide and have relatively sharp contacts (Pl. P5, fig. 4), except where the vein intersects olivine. Where that happens, the olivine is extensively altered to smectite + magnetite + pyrite, whereas adjacent plagioclase and clinopyroxene are little affected. Veins between ~575 and 835 mbsf are filled with dark green smectite, commonly accompanied by variable amounts of pyrite. Those deeper in the hole consist of light green or white, well-crystallized smectite, with or without prehnite. In most cases, the smectite crystals are oriented perpendicular to the vein walls, whereas prehnite grains have a random orientation. Where the two are present together, smectite lines the vein

walls and prehnite fills the center. Small amounts of carbonate are commonly included in these veins (Pl. P5, fig. 4), but other minerals are absent.

Zeolite ± Prehnite ± Carbonate Veins

Separate zeolite veins are relatively rare and make up <2% of the total number (Table T1). However, zeolites are also present as minor groundmass phases in felsic veins and occasionally they fill late-stage cracks in such veins (e.g., Sample 118-735B-84R-6, 31–41 cm) (Pl. P4, fig. 4). Most zeolite veins are present in the lower part of the hole between ~1385 and 1455 mbsf, where they are associated with smectite and prehnite veins. The zeolite veins are typically 1–2 mm wide, 10–20 mm long, and have relatively sharp but irregular boundaries. They are filled primarily with sheaflike clusters of light brown natrolite crystals, sometimes accompanied by smectite or carbonate (Pl. P5, figs. 2, 3). A few thomsonite veins are present in the lower 100 m of the core, but this mineral is most commonly present in the groundmass of felsic veins.

Prehnite veins are restricted to the lower 200 m of the core and are most abundant between ~1300 and 1450 mbsf. They are similar to the zeolite veins in size and appearance, and the two are typically present together. Many of the prehnite veins are zoned, with thin bands of smectite along their margins. The cores may be filled with prehnite alone or with mixtures of prehnite, zeolite, and minor carbonate. The prehnite is typically present as small, colorless, tabular crystals randomly oriented in the vein.

Carbonate Veins

Carbonate veins are widespread and abundant in the core but make up <2% of the total area (Table T1). They are concentrated in a 100-m-thick interval between 500 and 600 mbsf, which is characterized by brittle deformation and by extensive low-temperature groundmass alteration (Fig. F3). In other parts of the core, carbonate veins are typically present in small clusters and are associated with smectite, zeolite, and prehnite veins. Wherever carbonate veins are abundant, the adjacent host rock is reddish in color because of oxidation of iron in the silicate minerals.

Most of these veins are <2 mm wide, and they rarely extend for more than 10–15 cm in the core (Pl. P4, fig. 3). Many are just hairline cracks that radiate outward from an irregular mass of groundmass carbonate. The carbonate in these veins consists either of minute fibers oriented perpendicular to the vein walls or of small anhedral, interlocking crystals. In addition to carbonate many of these veins contain small amounts of zeolite, prehnite, and, especially, smectite. In such mixed veins the carbonate is usually present in the center and appears to be the latest mineral deposited (Pl. P5, figs. 3, 4). Four of the logged veins consist of mixtures of carbonate and iron oxyhydroxide similar to that replacing olivine in the host rock.

Other Veins

A few veins of quartz, chlorite, and epidote are also present in the core, but these are rare. Eight quartz veins were logged, mostly between 1264 and 1505 mbsf, and three epidote veins are present, the largest of which is at 656.4 mbsf. The quartz veins are <2 mm wide, ~10 cm long,

and have sharp, planar contacts. A little smectite is present along the vein walls. The only significant epidote vein is ~15 mm wide and 20 cm long, pinching out downward in the core. It is filled with a mixture of epidote and amphibole and has a chloritic halo 1–2 cm wide.

Chlorite is relatively common in the groundmass of many felsic and plagioclase veins, but only a few separate chlorite veins were recognized, most of which are present in the lower 50 m of the core (Fig. F3). A cluster of five small chlorite veins are present in Core 176-735B-121R at 721 mbsf. Those in the lower part of the hole typically contain small amounts of smectite, prehnite, or zeolite along with the chlorite.

VEIN MINERALOGY

The principal vein minerals in the Hole 735B core are, in order of abundance, plagioclase, amphibole, smectite, diopside, and quartz. All of the other minerals such as biotite, chlorite, zeolite, prehnite, titanite, ilmenite, oxyhydroxides, zircon, apatite, K-feldspar, carbonate, and epidote are typically present in only trace amounts.

Feldspar

Plagioclase is the most common and abundant vein mineral in Hole 735B. It is primarily present in felsic, plagioclase + diopside, and plagioclase + amphibole veins but can also be present in narrow monomineralic veinlets of Na-rich plagioclase (Robinson et al., 1991). In felsic veins, it commonly forms myrmekitic intergrowths with quartz and is accompanied by small amounts of titanite, zircon, and apatite. In plagioclase-rich veins with diopside or amphibole, it forms relatively large (1–3 mm), subhedral, strongly zoned grains, commonly with pitted and corroded cores. The monomineralic plagioclase veins consist of narrow, 0.2- to 0.3-mm-wide bands of albite or sodic oligoclase that cut more calcic plagioclase grains. Individual crystals are not visible in these veins.

Based on 439 microprobe analyses, the vein plagioclase ranges in composition from $An_{49.4}$ to $An_{0.2}$ and averages $An_{16.8}$ (Table T2; Fig. F4). There are no systematic compositional variations in the plagioclase with depth in the hole, with vein type, or with position within the vein. The variations in composition primarily reflect zoning of individual crystals. Most grains have cores of oligoclase-andesine ($An_{25–35}$) and rims of albite-oligoclase ($An_{5–15}$). Some of the cores are as calcic as An_{49} but this is rare. In such cases, the rims are typically sodic andesine (~$An_{30–35}$).

Plagioclase compositions are similar in felsic, plagioclase + diopside, and plagioclase + amphibole veins (Table T2) and show no clear patterns within individual veins. Where a vein cuts a preexisting plagioclase crystal in the host rock, the host mineral is replaced by more sodic plagioclase along a very sharp boundary. Plagioclase in monomineralic veins is typically internally uniform but varies in composition from vein to vein (Table T2).

The K_2O content of the plagioclase is very low but increases gradually as the An content decreases, reaching a maximum at ~An_{15} (Fig. F5). It then decreases to trace amounts in albite. Pure K-feldspar is very rare in Hole 735B veins, having been identified only in a few felsic veins and one smectite + prehnite vein (Sample 176-735B-183R-3, 69–78 cm). In

T2. Feldspar by microprobe, p. 39.

F4. Compositions of vein plagioclase, p. 29.

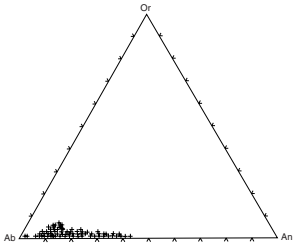

F5. Classification of brown and green vein amphiboles, p. 30.

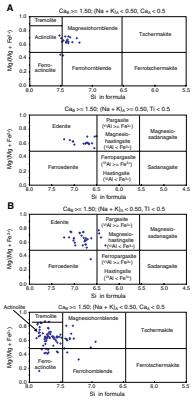

the felsic veins it is largely present as fine-grained interstitial material between plagioclase grains; in the smectite + prehnite vein it is present as a narrow band of aphanitic material along the vein margin.

Amphibole

Amphibole is the second most abundant vein mineral in Hole 735B, forming both monomineralic and plagioclase + amphibole veins. Small quantities of amphibole are also present in most diopside and diopside + plagioclase veins and in irregular felsic patches in the gabbros. Representative microprobe analyses for brown and greenish brown vein amphiboles are given in Table T3, and those for green vein amphiboles are given in Table T4. The amphibole nomenclature is based on the International Mineralogical Association (IMA) classification of Leake et al. (1997). The cation proportions and ferric/ferrous iron ratios were calculated using the program of Currie (1997) that also assigns Mg and Fe to the appropriate sites by assuming constant distribution coefficients for these elements among the possible sites.

T3. Amphibole by microprobe, p. 43.

T4. Green amphibole by microprobe, p. 44.

Optically, the amphibole forms three major groups based on color: colorless to green, greenish brown to brownish green, and dark brown. These three groups are distinguished chemically primarily on their TiO_2 contents; in colorless and green amphiboles TiO_2 is typically <0.50 wt%, in greenish brown to brownish green varieties it ranges from 0.5 to 1.5 wt%, and in dark brown varieties it is >2 wt% (Tables T3, T4). A few green amphiboles have unusually high TiO_2 contents, up to 2.37 wt% (Table T4), but these are rare. In the IMA classification scheme the colorless to green amphiboles are primarily actinolite, whereas the greenish brown, brownish green, and dark brown varieties are magnesio-hornblende or edenite, depending on the Na and K contents (Fig. F5).

The monomineralic amphibole veins at the top of the section consist chiefly of greenish brownish to brown magnesio-hornblende and edenite, the two differing only in having slightly different amounts of Na in the X position (Table T3; Fig. F5A). Individual grains show no optical zoning and are essentially homogeneous. Likewise, there is little variation among grains within a single vein, although there is some variation from sample to sample. For example, vein amphibole in Sample 176-735B-12R-1, 50–55 cm, is a dark brown, high-TiO_2 variety, whereas most of the others are green to greenish brown in color, with low TiO_2. The main compositional variation in the brown amphiboles is in the iron/magnesium ratio, with Mg numbers ranging from 45 to 72 (Table T3).

The monomineralic amphibole veins are most commonly present in foliated metagabbros composed of alternating bands of plagioclase and amphibole. These amphibole bands formed by replacement of clinopyroxene during brittle-ductile deformation. In these rocks there is typically no significant chemical difference between the vein amphibole and that in the foliated host rock (cf. Vanko and Stakes, 1991).

In plagioclase-amphibole and felsic veins, most of the amphibole is present as selvedges along vein walls or as replacements of hydrothermal diopside. These amphiboles are typically green to brownish green magnesio-hornblende to actinolite, although some are edenite. Brownish green and dark brown amphiboles are present in a few veins and, where present, are commonly zoned, with a brown core and a narrow green rim.

A few individual subhedral amphibole crystals are also scattered through the matrix of most felsic and plagioclase veins, although they are not abundant. These are characteristically either bright bluish green or dark brown in color and are commonly accompanied by small crystals of ilmenite and titanite. Some of these are partially altered to, or accompanied by, yellowish brown mica. The bright green amphibole is typically rich in Al_2O_3 and TiO_2, whereas the dark brown varieties are characterized by relatively high TiO_2 and intermediate Al_2O_3 contents (Tables **T3, T4**). The green amphibole is mostly actinolite with smaller amounts of ferro-actinolite, ferro-hornblende, and magnesio-hornblende (Fig. **F5B**). As in the veins higher in the section, the brown amphibole is mostly edenite with small variations in Fe/Mg ratios (Table **T3;** Fig. **F5A**).

A few very high iron amphiboles (FeO = 30–31.5 wt%) are also present in several veins (e.g., Samples 176-735B-144R-6, 35–47 cm, and 119R-5, 62–68 cm), a feature also noted by Vanko and Stakes (1991). These are bright green ferro-actinolite and ferro-hornblende intergrown with plagioclase in felsic veins.

Diopside

Diopside typically forms anhedral, blocky crystals along vein margins, where it is almost always associated with intermediate plagioclase and greenish brown amphibole. In a few veins it forms euhedral, zoned crystals up to 2 mm across (Pl. **P4,** fig. 2). Most crystals are light green but a few are colorless, and most contain solid and fluid inclusions that give the crystals a pitted appearance.

Overall, the diopside is very uniform in composition, forming a tight cluster in the pyroxene quadrilateral. Most grains cluster closely around 50% Wo and vary only in their Fe/Mg ratios (Table **T5;** Fig. **F6**). Most of the diopside is compositionally homogeneous, although a few large euhedral grains show weak zoning in Fe and Mg (Table **T5**). Al_2O_3 contents range from 0.04 to 1.19 wt%, CaO is between 22.5 and 24.5 wt%, and Na_2O is typically <0.5 wt%. Alumina and silica show a weak inverse relationship. TiO_2, Cr_2O_3, and MnO contents are negligible and do not vary systematically with other oxides. The largest variations are in FeO contents, with Mg numbers ranging from 63 to nearly 87 (Table **T5**). The euhedral crystals have very narrow oscillatory zones that span the range of composition among crystals and become slightly more iron rich toward the rims. Many of these crystals have a narrow band of clay between the outermost band and the main part of the grain, but it is not clear when the clay formed, that is, before or after deposition of the outermost band. Nearly all the analyzed grains have totals <100%, even though clinopyroxene in the wall rock, analyzed during the same run, is close to an ideal composition. This suggests that these vein diopsides may contain small amounts of H_2O or other volatiles as submicroscopic inclusions.

The absence of nonquadrilateral components in the diopside compared to igneous clinopyroxene indicates formation in a lower-temperature hydrothermal environment, that is, >300°C (Bird et al., 1984, 1986; Manning and Bird, 1986).

T5. Diopside by microprobe, p. 47.

F6. Compositions of vein diopside, p. 31.

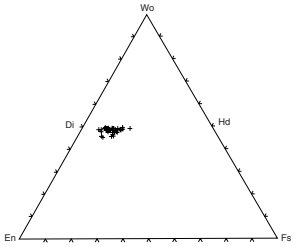

Mica

Mica occurs only in felsic or plagioclase-rich veins, where it forms subhedral, somewhat ragged crystals 1–3 mm long. It is typically strongly pleochroic, from yellow to dark brown, but a few grains are reddish brown in color, presumably reflecting oxidation. Although there is no clear compositional demarcation between phlogopite and biotite (Deer et al., 1992), phlogopite generally has high MgO, low TiO_2, and little Al substituting for Fe and Mg in the Y position. Based on their strong pleochroism and the high FeO and TiO_2 contents, most of the micas in Hole 735B veins are classified as biotite, although a few are relatively Mg rich (Table T6). However, very few of these micas have Al^{VI} in their formulas.

T6. Mica by microprobe, p. 48.

Most of the analyzed grains are uniform in composition without observable zoning. However, in a few cases, rims of crystals are slightly more Fe rich than the cores (e.g., Sample 176-735B-149R-4, 82–87 cm) (Table T6). SiO_2, Al_2O_3, and K_2O contents are relatively constant, whereas TiO_2, FeO, and MgO show significant variations from grain to grain. TiO_2 contents are generally between 3 and 4 wt% but range from 0.28 to 4.25 wt% (Table T6). Mg numbers range from 37.2 to 59.1. Compositional variations do not correlate with color; the red grains have essentially the same composition as the other crystals.

Chlorite

In Hole 735B, chlorite is typically present as irregular patches in the groundmass of felsic or plagioclase-rich veins. In a few cases, it rims amphibole or mica or partially replaces plagioclase. Although widely distributed, it rarely makes up more than 1 modal% of any given vein.

Most of the chlorite is light green or colorless, but brown varieties are locally present. Although it is difficult to obtain reliable microprobe analyses of such fine-grained hydrous minerals, the data reported in Table T7 are very consistent. Duplicate analyses within any patch show only minor differences, and these are primarily in the Fe/Mg ratios (Table T7). All of the analyzed grains are very close to an ideal formula with 20 cations when calculated on the basis of 36 (O, OH).

T7. Chlorite by microprobe, p. 49.

As expected, chlorite compositions vary widely from vein to vein, ranging from 24.76 to 30.52 wt% SiO_2 and from 16.21 to 20.10 wt% Al_2O_3. FeO and MgO also vary widely and are negatively correlated. Most other oxides are present in very small quantities, although MnO is as high as 1.45 wt% in one specimen. There are no systematic variations in chlorite compositions, either with depth in the hole or with mode of occurrence within individual veins.

Quartz

Quartz is a common, although not voluminous, mineral in many felsic and plagioclase-rich veins. In felsic veins with a myrmekitic texture, the quartz forms small blebs and irregular patches intergrown with sodic plagioclase and is more or less regularly distributed throughout the vein. The more common occurrence is as irregular masses in the groundmass of plagioclase veins, where it forms small, anhedral grains that are in optical continuity over distances to 1–3 mm. Typically, the quartz is colorless to white and lacks inclusions. In a few cases, it is marginally replaced by yellowish brown clay minerals.

As expected, the quartz consists of nearly pure SiO_2, occasionally accompanied by trace amounts of Al_2O_3, TiO_2, FeO, or CaO (Table T8). The nonsilica components never exceed 0.19 wt% and do not vary with the mode of occurrence of the quartz.

T8. Quartz by microprobe, p. 51.

Epidote

Epidote occurs in many plagioclase-rich veins but is typically present in very small quantities (<1 modal%). Most commonly, it replaces the cores of plagioclase crystals, but in a few cases it is present as discrete clusters of grains within the vein matrix. It is typically white to very pale brown in color and forms subhedral to anhedral crystals 0.1 to 0.5 mm across. In Sample 176-735B-120R-1, 85–91 cm, epidote forms subhedral, prismatic to bladed crystals up to 4 mm long. These are in a matrix of dark brown, aphanitic material and are associated with plagioclase, diopside, and chlorite.

The epidote has nearly constant SiO_2 and CaO but varies significantly in iron and alumina (Table T9). In nearly all of the analyzed grains, silica fills the tetrahedral position; thus, the aluminum is all in sixfold coordination. Iron in epidote can be assumed to be mostly in the ferric state and thus to also occur in sixfold coordination. This assumption is supported by the strong negative correlation of Fe_2O_3 and Al_2O_3 in the analyzed grains (Fig. F7). Fe_2O_3 contents range from 3.14 to 10.56 wt% and Fe_2O_3/Al_2O_3 ratios range from 0.10 to 0.41 (Table T9). Although there are no systematic downhole variations in composition, the high-iron epidotes are present in the deepest levels in the hole (>700 mbsf). However, they are associated with relatively low-iron varieties in the same sample (Table T9).

T9. Epidote by microprobe, p. 52.

F7. Fe_2O_3 vs. Al_2O_3 in vein epidote, p. 32.

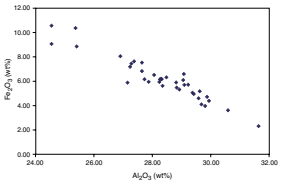

None of the epidote grains show optical zoning, even though compositional zoning is apparent from the microprobe analyses. This is particularly apparent in Sample 176-735B-120R-1, 86–91 cm, where iron contents within single crystals range from just under 6 to over 10 wt% (Table T9).

Prehnite

Prehnite is present only in the lower part of the hole in composite veins with smectite and carbonate. These veins typically have narrow bands of greenish brown smectite along the margins and have prehnite, with or without carbonate, in the central part. The prehnite forms colorless to very light brown bladed crystals, 0.1–0.2 mm long, typically aligned subparallel to the vein axis. All of the analyzed prehnite is very uniform in composition and shows no evidence of zoning within individual minerals or within veins, nor is there any variation in composition with depth (Table T10).

T10. Prehnite by microprobe, p. 53.

Opaque Minerals

Ilmenite is by far the most abundant opaque mineral in Hole 735B veins, but trace amounts of magnetite, hematite, and sulfide may also be present. Ilmenite is almost exclusively present in the felsic and plagioclase-rich veins, where it forms individual anhedral grains, usually 0.2–0.5 mm across, or anhedral aggregates along the vein margins. In the latter case, the ilmenite may extend from the vein into the host

gabbro. It can occur alone or, more commonly, in small clots associated with green or brown amphibole, titanite, and rare biotite.

The ilmenite is quite uniform in composition, consisting almost entirely of FeO and TiO_2 with minor amounts of MnO (up to 2.45 wt%) and MgO (up to 0.88 wt%) (Table T11). Formulas calculated on the basis of six oxygens have slightly high iron because all of the iron was calculated as Fe^{+2}. Compared to ilmenite in the host rock, the vein ilmenite has somewhat higher MnO and lower TiO_2 and MgO.

T11. Ilmenite by microprobe, p. 54.

Minute grains of secondary sulfide are commonly associated with ilmenite in the veins, particularly along grain boundaries. Pyrite or pyrrhotite and chalcopyrite are the most common varieties but are present in only trace amounts.

A few veins also have small amounts of reddish brown ferric oxide, either rimming some of the ilmenite grains or as small patches associated with carbonate in the vein matrix. The distribution of ferric oxide in the core is directly related to the abundance of carbonate veins, but most of the oxide replaces olivine or orthopyroxene in the host rock rather than occurring in veins.

Zeolites

In Hole 735B, zeolites are primarily present in the groundmass of felsic or plagioclase-rich veins, where they are associated with, and appear to replace, dark, aphanitic material. In a few veins they fill late-stage cracks cutting through the centers of felsic and plagioclase veins. The zeolites are associated with amphibole, chlorite, clay minerals, prehnite, and, rarely, carbonate.

Two zeolite species are recognized in these veins: natrolite and thomsonite. Both are typically present as small, radiating clusters of white to light brown acicular crystals (Pl. P5, fig. 2), although natrolite also forms minute white prismatic crystals with square cross sections (Pl. P5, fig. 3). For zeolites, both of these minerals are relatively uniform in composition (Table T12). Natrolite averages about 50 wt% SiO_2, 27 wt% Al_2O_3, and 10 wt% Na_2O. CaO is typically <1 wt% but ranges up to 2.41 wt% (Table T12). Thomsonite has significantly higher CaO and lower SiO_2 and Na_2O than natrolite. CaO/Na_2O ratios vary widely in the thomsonite, ranging from 0.21 to 0.45.

T12. Zeolites by microprobe, p. 55.

Apatite

Apatite is a common constituent of many of the shear zones impregnated with Fe-Ti oxide melts but is relatively rare as a vein mineral. It is restricted to felsic and plagioclase-rich veins, where it forms small (usually <0.1 mm) subhedral to euhedral grains in the matrix. The apatite crystals occur either singly or in small clusters, sometimes associated with titanite or ilmenite. They are relatively uniform in composition but contain small amounts of SiO_2, Al_2O_3, and Na_2O (Table T13).

T13. Apatite and zircon by microprobe, p. 56.

Zircon

Approximately half of the felsic and plagioclase veins examined contain trace amounts of zircon. The zircon is present as minute (0.05 mm or less), colorless, euhedral crystals sometimes associated with apatite. Only rarely is there more than one grain per thin section of a vein. The

zircon is relatively uniform in composition, the major variation being in P_2O_5, which ranges from 0 to a maximum of 2.27 wt% (Table T13).

Titanite

Virtually every felsic and plagioclase-rich vein in Hole 735B core has at least small quantities of titanite. The titanite typically forms subhedral to euhedral crystals from 0.1 to 1 mm across that are almost always associated with ilmenite or green or brown amphibole. Most grains are colorless to very light brown but some have red pleochroic cores, suggesting high rare earth element concentrations (Pl. P3, fig. 2). The grains may be randomly distributed in the veins but are most abundant near the vein walls. In a few cases they are concentrated in narrow bands or fractures.

The titanite is very uniform in its bulk composition (Table T14), showing only small variations in FeO and Al_2O_3. Some of the red pleochroic crystals have La_2O_3 contents up to 0.67 wt%.

T14. Titanite by microprobe, p. 57.

Clay Minerals

Late-stage smectite-coated cracks are common throughout Hole 735B core and some amphibole veins in the upper part contain bands of smectite, but significant clay mineral veins are present only in the lower parts of the section. In these veins, the clay minerals are commonly associated with prehnite and carbonate. In most veins, the clay minerals form platy or tabular crystals oriented perpendicular to the vein walls. Where they occur with other minerals, the clay minerals typically line the vein walls, whereas carbonate and prehnite fill later cracks. Clay minerals are also present in small quantities in felsic veins, where they partly replace plagioclase or other minerals in the groundmass. In a few of these veins, very light brown clay minerals replace quartz in the groundmass.

Most of the analyzed clay minerals are high-magnesia smectite, although a few green varieties have relatively high iron (Table T15). Neither the Fe- nor Mg-rich clay minerals are associated with ferromagnesian minerals, and generally the composition is independent of the host mineral. Exceptions to this rule are found in Samples 176-735B-203R-2, 11–16 cm, and 210R-5, 116–120 cm, where what appears optically to be a clay mineral is actually partly altered plagioclase. A few clay mineral samples with high CaO (not shown in Table T15) contain small amounts of finely divided carbonate.

T15. Clay minerals by microprobe, p. 58.

Carbonate

Small amounts of carbonate are widely scattered in the Hole 735B veins. The carbonate either replaces groundmass minerals or forms narrow, discrete veins. In both cases, it is typically associated with clay minerals, zeolites, or prehnite. Most of the carbonate, particularly that in discrete veins, is white, but some of the material is light brown or is intimately intermixed with light brown clay minerals. It is entirely calcite in composition, having a maximum of 5.67 wt% MgO and only trace amounts of FeO, MgO, SiO_2, and SrO (Table T16).

T16. Carbonates by microprobe, p. 59.

VEIN GEOCHEMISTRY

Sixteen relatively large veins and one irregular felsic patch in gabbro were selected for chemical analysis. The vein material was carefully separated from the host rock, crushed in an agate mortar, and analyzed by standard X-ray fluorescence (XRF) techniques for major oxides and some of the abundant trace elements (Table T17). The same powders were then analyzed by inductively coupled plasma–mass spectrometry (ICP-MS) for the remaining trace elements, and H_2O and CO_2 were measured using a CHN analyzer. The sample preparation and all analyses were carried out at the GeoForschungsZentrum, Potsdam, Germany.

T17. Vein composition, p. 60.

Twelve of the analyzed veins are classified as felsic, three are plagioclase + diopside, and one is plagioclase + amphibole. Seven of the felsic veins (Samples 176-735B-90R-3, 38–44 cm; 90R-4, 55–58 cm; 90R-4, 84–88 cm; 124R-1, 111–115 cm; 135R-3, 68–72 cm; 130R-3, 52–58 cm; and 138R-4, 59–63 cm) contain 5 modal% or more of quartz and three (Samples 176-735B-150R-7, 93–100 cm; 157R-7, 1–5 cm; and 161R-7, 78–84 cm) have traces of quartz in the groundmass. One of the plagioclase + diopside veins (Sample 176-735B-120R-2, 99–104 cm) contains ~15 modal% of chlorite. Sample 176-735B-202R-7, 99–101 cm, is a felsic patch rather than a discrete vein. It consists chiefly of light green, very fine grained, poorly crystallized material with a few large zoned crystals of green and brown amphibole.

Because the veins have a rather simple mineralogy dominated by plagioclase, they exhibit a relatively narrow range of composition. Silica contents range from 53 to 74 wt% and reflect the abundance of quartz. Except for two diopside-rich veins (Samples 176-735B-120R-2, 99–104 cm, and 123R-6, 140–146 cm), SiO_2 and Al_2O_3 show a strong negative correlation, reflecting both the relative proportions of quartz and plagioclase and the more sodic nature of the plagioclase in the quartz-rich veins. Both Fe_2O_3 and MgO are low in all but the diopside-rich veins and correlate positively with the abundance of amphibole. CaO is relatively high in many of these veins, commonly between 2 and 5 wt% and up to more than 12 wt% in the most diopside-rich specimen. K_2O is very low in all the veins, ranging from 0.01 to 0.43 wt%. This reflects the nearly complete absence of K-feldspar and the sparse presence of mica in these rocks. A few flakes of yellowish brown to reddish biotite are present in Samples 176-735B-135R-3, 68–72 cm; 138R-4, 59–63 cm; and 157R-7, 1–5 cm, the veins with the highest K_2O. Likewise, Rb is very low, generally <1 ppm. The highest Rb is 4 ppm, and that is in the sample with the highest K_2O. Despite the presence of a few grains of titanite in most of these veins, TiO_2 contents are also very low (maximum = 0.27 wt%). Samples 176-735B-135R-3, 68–72 cm, and 157R-7, 78–84 cm, have a few grains of apatite, just enough to produce very small increases of P_2O_5 compared to the other veins. All of the analyzed samples contain some CO_2 (0.29–2.60 wt%), suggesting the presence of carbonate. No carbonate was identified optically in these veins, but some finely disseminated material might be present in the groundmass. However, there is only a weak correlation between CO_2 and CaO contents, and the samples with the highest CO_2 show no particular enrichment in CaO. This suggests that the CO_2 resides in some other phase, perhaps in sparse clay minerals, zeolites, or poorly crystallized matrix materials that are present in a few samples. Except in Sample 176-735B-120R-2, 99–104 cm, which has abundant chlorite in the matrix, water contents are relatively low, mostly <1 wt%.

Most of the trace elements, except for Ba, Sr, Zr, Y, Zn, Ni, and Ga, have very low concentrations. Ba averages ~30 ppm but is significantly higher in the two siliceous quartz-plagioclase veins (Table T17). Sr ranges from 35 to 194 ppm (40–197 ppm by ICP-MS) and shows a good positive correlation with CaO except in the diopside-rich samples. Zr values determined by XRF (33–1720 ppm) are significantly higher than those determined by ICP-MS (3–30 ppm). The differences suggest that zircon was not completely digested during preparation for ICP-MS analysis. Because the XRF values correlate best with the observed modal distribution of zircon, we believe that they are the most accurate. If zircon was not completely dissolved during sample preparation for the ICP-MS analyses, other elements such as Hf, Pb, U, and Th, which typically concentrate in zircon, are probably also underrepresented and thus are not reported here. Yttrium values have a narrow range of variation (19–136 ppm) and show no correlation with Zr. Concentrations of Zn range from <10 to 358 ppm, and the few high values probably reflect small amounts of secondary sulfides that are present in some of the veins. Ni values are relatively high (up to 87 ppm) in some felsic veins composed chiefly of plagioclase and quartz. This suggests that small amounts of olivine may have been incorporated into the vein sample during preparation.

Because the geochemistry of the veins is strongly controlled by the vein mineralogy, we produced geochemical maps of four veins in order to show the zoning and distribution of elements within the veins. The geochemical maps were produced using the Cameca SX-100 microprobe at the GeoForschungsZentrum, Potsdam, Germany, using both energy-dispersive and wavelength-dispersive spectrometers. Spot spacing was 30 µm, small enough to sample all but the finest crystals.

Sample 176-735B-124R-1, 111–115 cm, is a quartz-plagioclase vein, ~2 cm wide, with a myrmekitic texture. Element maps of this vein reveal sharp, distinct vein walls and strong zoning within the vein (Fig. F8). The vein walls are clearly delineated in Figure F8 by the presence of calcic plagioclase, indicated by high Ca and Al. Along the vein walls are very narrow bands of amphibole characterized by moderate levels of Al, Ca, and Si, followed inward by a bands of sodic plagioclase about 2 mm wide. The myrmekitic intergrowths of quartz and sodic plagioclase (clearly visible in the plot of Si) form two parallel bands, each about 5–7 mm wide. These are followed inward by narrow felsic bands, 1–1.5 mm wide, without quartz. The center of the vein is composed of greenish brown amphibole with a few very small grains of ilmenite.

Sample 176-735B-123R-6, 140–144 cm, illustrates the compositional zoning in a typical plagioclase + diopside vein (Fig. F9). The vein margin (upper left) is sharp and marked by a significant change in plagioclase composition. The boundary in the lower right is against epoxy. Small amounts of diopside are present along the vein wall in the upper left, but most of the vein is filled with sodic plagioclase ($An_{0.9–22.5}$). The distinct band, 1–2 mm wide, near the center of the vein consists of diopside and minor plagioclase in a matrix of black to dark brown aphanitic material. Overall, the plagioclase in this vein is quite uniform in composition, with very little zoning, although there is a very narrow band along the margin with slightly elevated Na.

Sample 176-735B-161R-7, 77–83 cm, is an excellent illustration of a coarse-grained, plagioclase-rich vein with a strong hydrothermal overprint (Fig. F10). Again, the margin of the vein is sharp against calcic plagioclase and clinopyroxene in the host rock. The large plagioclase crystals within the vein are subhedral to euhedral and strongly zoned,

F8. Abundances of Ca, Si, Al, and Mg in a felsic vein with myrmekitic texture, p. 33.

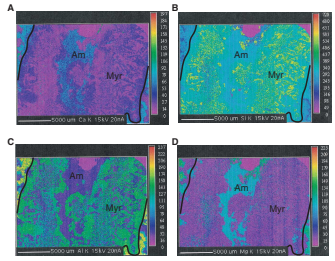

F9. Abundances of Mg, Si, Al, and Na in a plagioclase + diopside vein, p. 34.

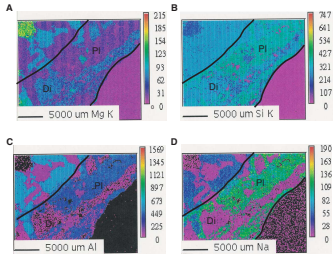

F10. Variations of Al and Na in plagioclase crystals in a plagioclase-rich vein, p. 35.

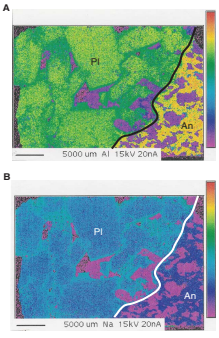

particularly at the edges, clearly becoming more sodic. In thin section, the cores are pitted and corroded, whereas the rims are clear and smooth. The spaces between the grains may be open or filled with minor amphibole and quartz.

Strong zoning of plagioclase is also observed in Sample 176-735B-120R-2, 99–104 cm (Fig. F11). Subhedral crystals up to 5 mm long have relatively calcic cores and sodic rims. The large clinopyroxene grain in the upper right part of the map has a narrow rim of chlorite, and hairline cracks in the vein plagioclase are also filled with chlorite. The central part of the vein is filled with dark brown to black aphanitic material, probably a clay mineral.

F11. Variations in Al in a plagioclase-rich vein, p. 36.

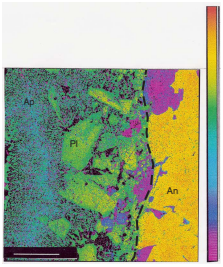

TEMPERATURES OF VEIN FORMATION

Estimating the temperatures of formation of the veins in Hole 735B is very difficult because few, if any, veins contain equilibrium mineral assemblages. Most of the amphibole veins are monomineralic, and all of the felsic and plagioclase-rich veins contain mixtures of minerals ranging from relatively high-temperature plagioclase + quartz assemblages to low-temperature mixtures of clay minerals, zeolites, and carbonate. An even greater problem is that nearly all of the relatively high-temperature minerals are moderately to strongly zoned, making it extremely difficult to identify equilibrium pairs. Plagioclase in the veins varies from a maximum of about An_{43} to a minimum of $An_{0.5}$, and the full range of variation is commonly present within individual crystals. Although not as strongly zoned, amphiboles exhibit color variations from brown or dark brown in the core to green or light green on the rim, corresponding to varying contents of alumina and iron.

The monomineralic amphibole veins are restricted to ductilely deformed metagabbros that were formed under the equivalent to granulite and amphibolite facies conditions. The amphibole veins both crosscut and are cut by the gneissic and mylonitic foliation in these rocks, suggesting that ductile and brittle deformation occurred penecontemporaneously (Dick et al., 1991; Stakes et al., 1991).

In those rocks with neoblasts of both clinopyroxene and orthopyroxene, equilibrium temperature calculations suggest that the earliest deformation and metamorphism took place under anhydrous granulite facies conditions between 849° and 908°C (Stakes et al., 1991). The amphibole gneisses mark the start of hydrous metamorphism and formed at temperatures between ~590° and 720°C (Stakes et al., 1991), roughly the same temperature range calculated for sparse amphibole + plagioclase veins in this interval (see below). We infer, based on their textural relations, that the monomineralic amphibole veins formed essentially at the brittle–ductile transition, which is believed to lie everywhere in the ocean basins between 700° and 800°C (Phipps Morgan and Chen, 1993). The temperature estimates for the amphibole veins in Hole 735B are in good agreement with those of Manning et al. (1999) for amphibole + plagioclase veins in gabbros from Hess Deep (687°–745°C).

For amphibole + plagioclase veins we applied the geothermometers of Holland and Blundy (1994) with some success, despite the problems of identifying equilibrium assemblages. Holland and Blundy (1994) present two amphibole-plagioclase geothermometers: an edenite-tremolite thermometer that requires silica saturation in the system and an edenite-richterite thermometer that can be applied to either silica-saturated or unsaturated samples.

Most of the amphibole + plagioclase veins in the section also contain quartz, suggesting a silica-saturated environment. However, petrographic examination indicates that the quartz is almost invariably present as a late-stage mineral filling interstices between zoned and pitted plagioclase crystals and thus is not part of an equilibrium assemblage. Only in a few veins with well-developed myrmekitic textures is the quartz clearly intergrown with plagioclase. To test this interpretation, we applied both geothermometers to the same data and compared the results. In nearly every case the edenite-tremolite thermometer, which requires silica saturation, produced temperatures 50°–60°C higher than the edenite-richterite thermometer even though quartz is present in the veins. Holland and Blundy (1994) predict such a discrepancy for samples lacking silica saturation. In this situation, the lower temperature is taken as the equilibrium temperature and the higher temperature is offset because α_{SiO_2} is <1.0. Where both thermometers were applied to clearly silica-saturated samples, they gave virtually identical temperatures. Thus, all reported temperatures are based on the edenite-richterite geothermometer.

In order to deal with compositional variations in the vein plagioclase and amphibole, we applied the edenite-richterite thermometer in two ways. First, we attempted to match the Fe-rich amphibole rims with sodic plagioclase rims and the Fe-poor amphiboles with calcic plagioclase cores. Second, we calculated the range of temperature based on all amphibole and plagioclase vein compositions and took the mean value. The resulting temperatures, which are estimated to be accurate to ±40°C, range from a high of 834°C to a low of 525°C (Fig. **F12**). Pressure effects are assumed to be negligible since this crustal section was probably never more than 1–2 km below the seafloor (Dick et al., 1992). The highest temperatures are from veins with the most calcic plagioclase, assumed to be the closest to the original composition. The lowest temperatures are based on the most sodic plagioclase rims, clearly formed by hydrothermal processes. The mean temperature for all the veins is 674°C (standard deviation = 77°C). These temperatures are slightly higher than those estimated by Vanko and Stakes (1991) for the formation of amphibole + plagioclase veins in the upper part of the section. Using the geothermometers of Spear (1980) and Plyusnina (1982), they obtained temperatures between 520° and 640°C for andesine-bearing (An_{31}) veins very similar to those described here. They reported temperatures of <500°C for albite and oligoclase assemblages in brecciated horizons. A small trondhjemite intrusion registered temperatures between ~500° and 550°C (Vanko and Stakes, 1991).

The temperatures of formation for the diopside and diopside + plagioclase veins can be estimated in two ways. The diopside compositions plot in a tight cluster on the pyroxene quadrilateral (Fig. **F6**) and lie well below the 500°C temperature contour of Bird et al. (1986). Homogenization temperatures of fluid inclusions in diopside range from 310° to 420°C for three diopside + plagioclase veins in the upper part of Hole 735B (Vanko and Stakes, 1991). Interestingly, homogenization temperatures for plagioclase from the same veins are significantly lower (200°–290°C). The temperatures obtained for the diopside + plagioclase veins are significantly lower than those obtained from the amphibole + plagioclase veins, and are clearly in the hydrothermal range.

Temperatures for the other veins can only be estimated from their mineral assemblages. Greenschist minerals such as epidote, chlorite, and actinolite probably formed at temperatures of 300°–450°C. These are volumetrically insignificant and are present chiefly as replacements

F12. Formation temperatures calculated from plagioclase-amphibole pairs, p. 37.

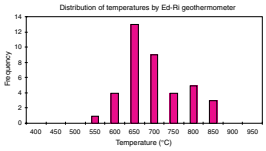

of higher-temperature vein minerals. Smectite and zeolite (thomsonite and natrolite) veins presumably formed at temperatures <50°C, and the carbonate veins probably formed at temperatures close to ambient seawater. When these phases are present in relatively high-temperature veins, they always fill late-stage fractures or replace the higher-temperature minerals. Prehnite is closely associated with smectite and carbonate probably formed at similar temperatures.

ORIGIN OF HOLE 735B VEINS

It is clear that the veins in Hole 735B span the entire range of temperatures from magmatic to ambient seawater and thus provide a unique record of the cooling of this crustal segment and the fluids circulating through it. Alteration of the Hole 735B rocks reflects penetration of aqueous fluids into the section and the veins provided pathways by which fluids were able to migrate through the crust. It is clear, however, that in most cases, the fluids passing through the veins did not interact extensively with the immediately adjacent host rock. The vein walls are sharp and the geochemical maps of the veins clearly indicate an abrupt chemical boundary. The only exception to this rule seems to be where olivine was present in the vein wall. In such cases, the olivine is typically replaced by talc and colorless amphibole when adjacent to medium- or high-temperature veins and by carbonate and Fe oxyhydroxides when adjacent to carbonate veins.

Most of the groundmass alteration in the plutonic rocks occurs in areas that have undergone significant brittle or ductile deformation. Cataclastic zones associated with faults are always highly altered, and zones of brittle-ductile deformation show weak to strong metamorphism and alteration. Where brittle-ductile deformation is sparse or absent, for example, in the lower 500 m of the hole, background alteration is weak to nonexistent.

Although crosscutting vein relationships are rarely observed in the Hole 735B core (except for low-temperature, late-stage veins), we infer a vein sequence based on texture, mineralogy, and estimated temperature of formation. The felsic and plagioclase-rich veins are inferred to be the earliest in the sequence. Most of these are 5–10 mm wide and have sharp contacts with the host rock, indicating that they formed by brittle fracture. Some are present as anastomosing networks that splay outward from irregular felsic patches. The felsic and plagioclase-rich veins are most abundant between ~250 and 850 mbsf, and many are associated with the Fe-Ti oxide gabbros in lithologic Unit IV. Their compositions and temperatures of formation strongly indicate that most, if not all, of these veins were originally magmatic. All of these veins are plagioclase rich with relatively high Al_2O_3 and, hence, are not likely to be hydrothermal. Some have well-developed myrmekitic textures and many contain small quantities of zircon and apatite, suggesting a late-magmatic origin. Their temperatures of formation, according to the edenite-richterite geothermometer of Holland and Blundy (1994), range from 834° to 525°C with a mean of 674°C (standard deviation = ±77°C). The highest temperatures are believed to approximate the original temperatures of formation, whereas the lower temperatures reflect the strong hydrothermal overprint observed in most of these veins.

It is clear that these veins continued to act as pathways for migration of high-temperature hydrothermal fluids long after their igneous formation. The original, relatively calcic plagioclase was corroded and re-

sorbed, producing a porous texture in many samples. Oligoclase and albite were deposited on the rims of the original plagioclase, producing strongly zoned, euhedral crystals. As temperatures decreased further, quartz was deposited between the plagioclase crystals and some of the plagioclase was altered to epidote. In some veins, new cracks developed that were filled with diopside, actinolite, and even lower-temperature zeolites or carbonate. Thus, the felsic and plagioclase-rich veins span a wide temperature range from late magmatic (>700°C) to near ambient seawater. Although they formed originally during the late stages of igneous crystallization, they remained as fluid pathways long after the crustal section had migrated out of the axial zone.

The next to form were presumably the monomineralic amphibole veins, although these may have overlapped with the felsic and plagioclase-rich veins. The amphibole veins are clearly associated with the intense deformation and metamorphism of the gabbros, particularly in the upper 70 m of the hole. Because the well-developed foliation in these rocks both cuts and is offset by the amphibole veins, brittle and ductile deformation were clearly penecontemporaneous. The ductile deformation and metamorphism of the gabbros began at high temperatures (849°–908°C) shortly after their formation. The amphibole gneisses mark the start of hydrous metamorphism and occurred at temperatures between ~590° and 720°C (Stakes et al., 1991), roughly the same temperature range calculated for sparse amphibole + plagioclase veins in this part of the section.

The amphibole veins in Hole 735B are presumed to have formed from the same fluids as those involved in metamorphism of the gabbros. ^{18}O depletion in the plagioclase and amphibole from the amphibole gneisses suggest that these were seawater-dominated fluids (Stakes et al., 1991) that gained access to the gabbro as it was being deformed by a detachment fault at the ridge axis.

Diopside and diopside + plagioclase veins formed at somewhat lower temperatures than either the felsic or amphibole veins and appear to be entirely hydrothermal in origin. Diopside is present either in nearly monomineralic veins or as a minor phase in felsic and plagioclase-rich veins. The estimated temperatures of formation (310°–420°C) are clearly within the hydrothermal range.

The diopside veins are very similar to those reported from the Skaergaard Intrusion by Bird et al. (1986), which have been attributed to brittle deformation associated with subsolidus cooling. Bird et al. (1986) found that formation of diopside was favored where the vein fluids had high Ca/Mg ratios, whereas amphibole formed when the ratios were low. Early precipitation of amphibole would quickly increase the Ca/Mg ratio of the fluid, leading to the formation of diopside.

The other veins in Hole 735B have relatively low temperatures of formation, and most are clearly hydrothermal in origin. A few greenschist facies minerals, such as chlorite, actinolite, epidote, and albite, are present in the groundmass of some felsic veins but rarely form separate veins. They appear to have formed by interaction between cooling fluids and the common silicate minerals in the veins, particularly plagioclase, amphibole, and diopside. Prehnite, smectite, and zeolite veins are common only in the lower part of the section where they are hosted in relatively fresh olivine gabbro. In some cases, these minerals fill new cracks in felsic or plagioclase-rich veins; in others they are present as separate veins. Carbonate veins are irregularly distributed throughout the core and are associated with oxidation of iron in pyroxenes and

olivine. They are believed to represent circulation of seawater through late cracks.

DYNAMIC MODEL FOR VEIN FORMATION

Here, we adopt a dynamic model for vein formation in the crustal section underlying Atlantis Bank similar to that proposed by Dick et al. (1991), Robinson et al. (1991), and Dick et al. (1992). The felsic and plagioclase-rich veins must have formed very early as late magmatic melts penetrated a crystalline mush. The sharp planar boundaries of these veins indicate that the rocks were deforming in a brittle fashion and that there was little interaction between the veins and the wall rocks. As the late-stage melts cooled and evolved, they became more fluid rich, perhaps mixing somewhat with seawater. These late-magmatic or hydrothermal fluids, with temperatures generally between 600° and 700°C, followed the original cracks formed by brittle deformation, significantly modifying the original vein mineralogy.

Early in the crystallization history of the crustal section, a detachment fault developed in the newly formed crust as spreading continued. The main detachment fault is marked by the roughly 70 m of amphibole schists and gneisses at the top of the section, which are characterized by well-developed porphyroclastic and mylonitic textures. Considering that these rocks and the monomineralic amphibole veins within them formed essentially at the brittle–ductile transition, this deformation must have taken place largely at the ridge axis. Although some shear zones are present deeper in the hole, the intensity of high-temperature crystal-plastic deformation decreases significantly with depth, as does the abundance of amphibole veins and the extent of groundmass alteration (Shipboard Scientific Party, 1999). The abundance of amphibole in the zones of crystal-plastic deformation indicates that these zones were major conduits for hydrothermal fluids. The remarkably fresh nature of the lower 500 m of core indicates that very few fluids penetrated this part of the section and those that did probably had temperatures <100°C. Thus, there is clearly a close link between high-temperature crystal-plastic deformation and alteration in the Hole 735B gabbros. Brittle fracture of the crust appears to have played a less important role.

It is very difficult to constrain the rate of cooling of this crustal segment, which would have depended primarily on the spreading rate and the amount of seawater that penetrated the crust. The current rift valley on this portion of the Southwest Indian Ridge is ~8 km wide, and the spreading rate to the south of the ridge axis has been 8.5 ± 1.2 mm/yr for the last 25 m.y. (A. Hosford, pers. comm., 2000). If the rift valley was the same width at 11–12 Ma when the Atlantis Bank crust was formed, it would have taken roughly 500,000 yr for the crustal segment to migrate across the valley floor and reach the rift valley walls. The downward decrease in the intensity and temperature of alteration suggests that cooling of the crust was relatively rapid. Detachment faulting associated with the crystal-plastic deformation at the top of the section would have thinned the crust and allowed penetration of cold seawater, leading to rapid cooling.

Circulation of high-temperature hydrothermal fluids would presumably have ceased by the time the crustal segment reached the edge of the rift valley and was transferred to adjacent valley walls. Thus, the brittle-ductile deformation associated with formation of the felsic, pla-

gioclase-rich, and amphibole veins took place relatively early near the ridge axis. The hydrothermal overprinting of the early felsic veins and the formation of the lower-temperature diopside veins probably took place as the section moved across the rift valley floor and brittle deformation became dominant. Uplift of the crust into the rift valley walls would have increased brittle fracturing and reopened existing veins, leading to the development of the late-stage prehnite, smectite, and chlorite veins. The latest oxidative alteration associated with carbonate veins presumably took place after the Atlantis Bank had been unroofed and uplifted into the transverse ridge on the edge of the fracture zone.

SUMMARY AND CONCLUSIONS

Veins in Hole 735B record the cooling history and paths of fluid circulation in a segment of lower ocean crust formed at a very slow spreading ridge. Vein assemblages span the entire range of temperature from late magmatic (+800°C) to ambient seawater and record the tectonic evolution of the crust as it formed at the spreading axis, migrated across the rift valley, and was uplifted into the transverse ridge along the edge of the fracture zone. Felsic and plagioclase-rich veins, particularly those with myrmekitic textures, are clearly magmatic. Although most of these veins have a significant hydrothermal overprint that obscures their origin, their textures, mineralogies, and chemical compositions argue strongly for an original late magmatic origin. The monomineralic amphibole veins in the highly deformed sequence at the top of the section formed as seawater gained access to the hot crust during brittle-ductile deformation associated with a major detachment fault that unroofed the lower crust and presumably caused rapid cooling. As the crustal section migrated away from the ridge axis and across the rift valley floor, the original magmatic veins acted as conduits for the hydrothermal fluids, and new veins also developed as brittle deformation continued. Most of the hydrothermal veins record declining fluid temperatures as indicated by precipitation of albite on plagioclase rims, deposition of late-stage quartz in the groundmass, and alteration of original minerals to greenschist assemblages. A number of veins also have discrete fractures that are filled with smectite ± zeolite ± carbonate. Both groundmass alteration of the host rocks and vein intensity decrease markedly downhole, indicating little penetration of fluids below ~1000 mbsf.

Chemical maps indicate very little interaction between vein fluids and the host rock, and most groundmass alteration appears to be associated with intense shearing in zones of crystal-plastic deformation. Detachment faulting played a major role not only in the tectonic evolution of this crustal segment but also in the timing and extent of alteration. Compared to gabbros formed at the fast-spreading East Pacific Rise, sampled in ODP Holes 894F and 894G, the Hole 735B section is more highly deformed and has a wider variety of igneous and hydrothermal veins.

ACKNOWLEDGMENTS

We thank Captain Ed Oonk and the crew of *JOIDES Resolution* for a very successful cruise. Henry Dick and James Natland provided an excellent working environment on the ship, allowing the shipboard party to log and sample a tremendous volume of core. Jay Miller, ODP Sci-

ence Representative, and Henry Dick assisted with the manuscript editing and revision. Mr. Xu-Feng Hu, Dalhousie University, carried out most of microprobe analyses and assisted with preparation of the illustrations. Dr. D. Rhede, GeoForschungsZentrum, kindly produced the chemical maps, and Dr. K. Hahne, GeoForschungsZentrum, prepared the vein samples for chemical analysis.

This research used samples and/or data provided by the Ocean Drilling Program (ODP). ODP is sponsored by the U.S. National Science Foundation (NSF) and participating countries under management of Joint Oceanographic Institutions (JOI), Inc. Funding for this research was provided by the GeoForschungsZentrum and the Natural Sciences and Engineering Research Council of Canada.

REFERENCES

Bird, D.K., Rogers, D., and Manning, C.E., 1986. Mineralized fracture systems of the Skaergaard Intrusion, East Greenland. *Medd. Groenl.: Geosci.,* 16:68.

Bird, D.K., Schiffman, P., Elders, W.A., Williams, A.E., and McDowell, D., 1984. Calc-silicate mineralization in active geothermal systems. *Econ. Geol.,* 79:671–695.

Currie, K.L., 1997. A revised computer program for amphibole classification. *Can. Mineral.,* 35:1351–1352.

Deer, W.A., Howie, R.A., and Zussman, J., 1992. *An Introduction to the Rock-Forming Minerals* (2nd ed.): London (Longman).

Dick, H.J.B., Meyer, P.S., Bloomer, S., Kirby, S., Stakes, D., and Mawer, C., 1991. Lithostratigraphic evolution of an in-situ section of oceanic Layer 3. *In* Von Herzen, R.P., Robinson, P.T., et al., *Proc. ODP, Sci. Results,* 118: College Station, TX (Ocean Drilling Program), 439–538.

Dick, H.J.B., Natland, J.H., Alt, J.C., Bach, W., Bideau, D., Gee, J.S., Haggas, S., Hertogen, J.G.H., Hirth, G., Holm, P.M., Ildefonse, B., Iturrino, G.J., John, B.E., Kelley, D.S., Kikawa, E., Kingdon, A., LeRoux, P.J., Maeda, J., Meyer, P.S., Miller, D.J., Naslund, H.R., Niu, Y., Robinson, P.T., Snow, J., Stephen, R.A., Trimby, P.W., Worm, H.-U., and Yoshinobu, A., 2000. A long in situ section of the lower ocean crust: results of ODP Leg 176 drilling at the Southwest Indian Ridge. *Earth Planet. Sci. Lett.,* 179:31–51.

Dick, H.J.B., Robinson, P.T., and Meyer, P.S., 1992. The plutonic foundation of a slow-spreading ridge. *In* Duncan, R., Rea, D., Kidd, R., von Rad, U., and Weissel, J. (Eds.), *Synthesis of Results from Scientific Drilling in the Indian Ocean.* Geophys. Monogr., Am. Geophys. Union, 70:1–50.

Früh-Green, G.L., Plas, A., and Dell' Angelo, L.N., 1996. Mineralogic and stable isotope record of polyphase alteration of upper crustal gabbros of the East Pacific Rise (Hess Deep, Site 984). *In* Mével, C., Gillis, K.M., Allan, J.F., and Meyer, P.S. (Eds.), *Proc. ODP, Sci. Results,* 147: College Station, TX (Ocean Drilling Program), 235–254.

Holland, T., and Blundy, J., 1994. Non-ideal interactions in calcic amphiboles and their bearing on amphibole–plagioclase thermometry. *Contrib. Mineral. Petrol.,* 116:433–447.

Leake, B.E., Woolley, A.R., Arps, C.E.S, Birch, W.D., Gilbert, M.C., et al., 1997. Nomenclature of amphiboles: report of the subcommittee on amphiboles of the International Mineralogical Association, Commission on New Minerals and Mineral Names. *Can. Mineral.,* 35:219–246.

Manning, C.E., and Bird, D.K., 1986. Hydrothermal clinopyroxenes of the Skaergaard intrusion. *Contrib. Mineral. Petrol.,* 92:437–447.

Manning, C.E., and MacLeod, C.J., 1996. Fracture-controlled metamorphism of Hess Deep gabbros, Site 894: constraints on the roots of mid-ocean-ridge hydrothermal systems at fast-spreading centers. *In* Mével, C., Gillis, K.M., Allan, J.F., and Meyer, P.S. (Eds.), *Proc. ODP, Sci. Results,* 147: College Station, TX (Ocean Drilling Program), 189–212.

Manning, C.E., Weston, P.E., and Mahon, K.I., 1999. Rapid high-temperature metamorphism of East Pacific Rise gabbros from Hess Deep. *Earth Planet. Sci. Lett.,* 144:123–132.

Mével, C., Gillis, K.M., Allan, J.F., and Meyer, P.S. (Eds.), 1996. *Proc. ODP, Sci. Results,* 147: College Station, TX (Ocean Drilling Program).

Phipps Morgan, J., and Chen, Y.J., 1993. The genesis of oceanic crust: magma injection, hydrothermal circulation, and crustal flow. *J. Geophys. Res.,* 98:6283–6297.

Plyushina, L.P., 1982. Geothermometry and geobarometry of plagioclase-hornblende bearing assemblages. *Contrib. Mineral. Petrol.,* 80:140–146.

Robinson, P.T., Dick, H.J.B., and Von Herzen, R.P., 1991. Metamorphism and alteration in oceanic layer 3: Hole 735B. *In* Von Herzen, R.P., Robinson, P.T., et al., *Proc. ODP, Sci. Results,* 118: College Station, TX (Ocean Drilling Program), 541–552.

Robinson, P.T., Von Herzen, R., et al., 1989. *Proc. ODP, Init. Repts.,* 118: College Station, TX (Ocean Drilling Program).

Shipboard Scientific Party, 1989. Introduction and explanatory notes. *In* Robinson, P.T., Von Herzen, R., et al., *Proc. ODP, Init. Repts.,* 118: College Station, TX (Ocean Drilling Program), 3–24.

————, 1999. Leg 176 summary. *In* Dick, H.J.B., Natland, J.H., Miller, D.J., et al., *Proc. ODP, Init. Repts.,* 176: College Station, TX (Ocean Drilling Program), 1–70.

Spear, F.S., 1980. NaSiCaAl exchange equilibrium between plagioclase and amphibole: an empirical model. *Contrib. Mineral. Petrol.,* 72:33–41.

Stakes, D., Mével, C., Cannat, M., and Chaput, T., 1991. Metamorphic stratigraphy of Hole 735B. *In* Von Herzen, R.P., Robinson, P.T., et al., *Proc. ODP, Sci. Results,* 118: College Station, TX (Ocean Drilling Program), 153–180.

Vanko, D.A., and Stakes, D.S., 1991. Fluids in oceanic layer 3: evidence from veined rocks, Hole 735B, Southwest Indian Ridge. *In* Von Herzen, R.P., Robinson, P.T., et al., *Proc. ODP, Sci. Results,* 118: College Station, TX (Ocean Drilling Program), 181–215.

Figure F1. Map showing location of Hole 735B on Atlantis Bank, Southwest Indian Ridge. F.Z. = fracture zone.

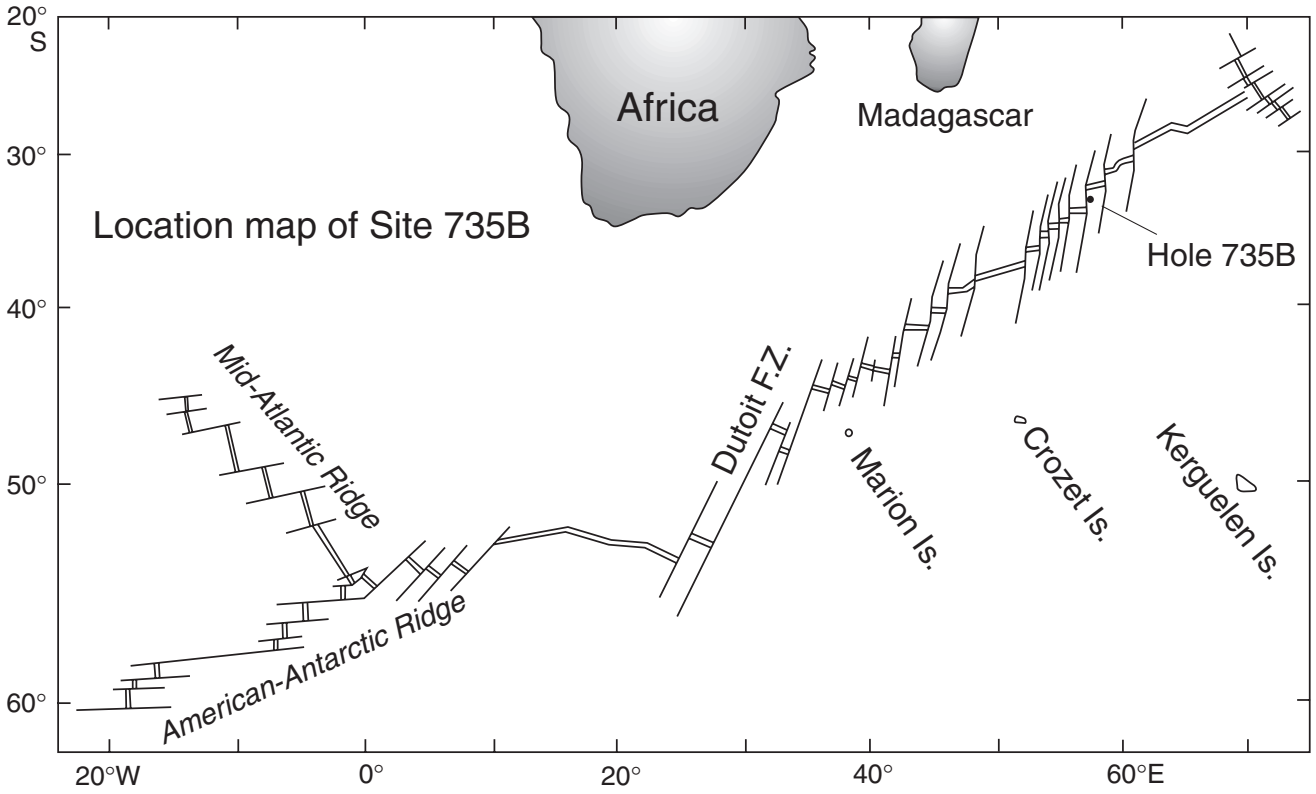

Figure F2. Pie diagram showing estimated area percentages of different vein types in Hole 735B.

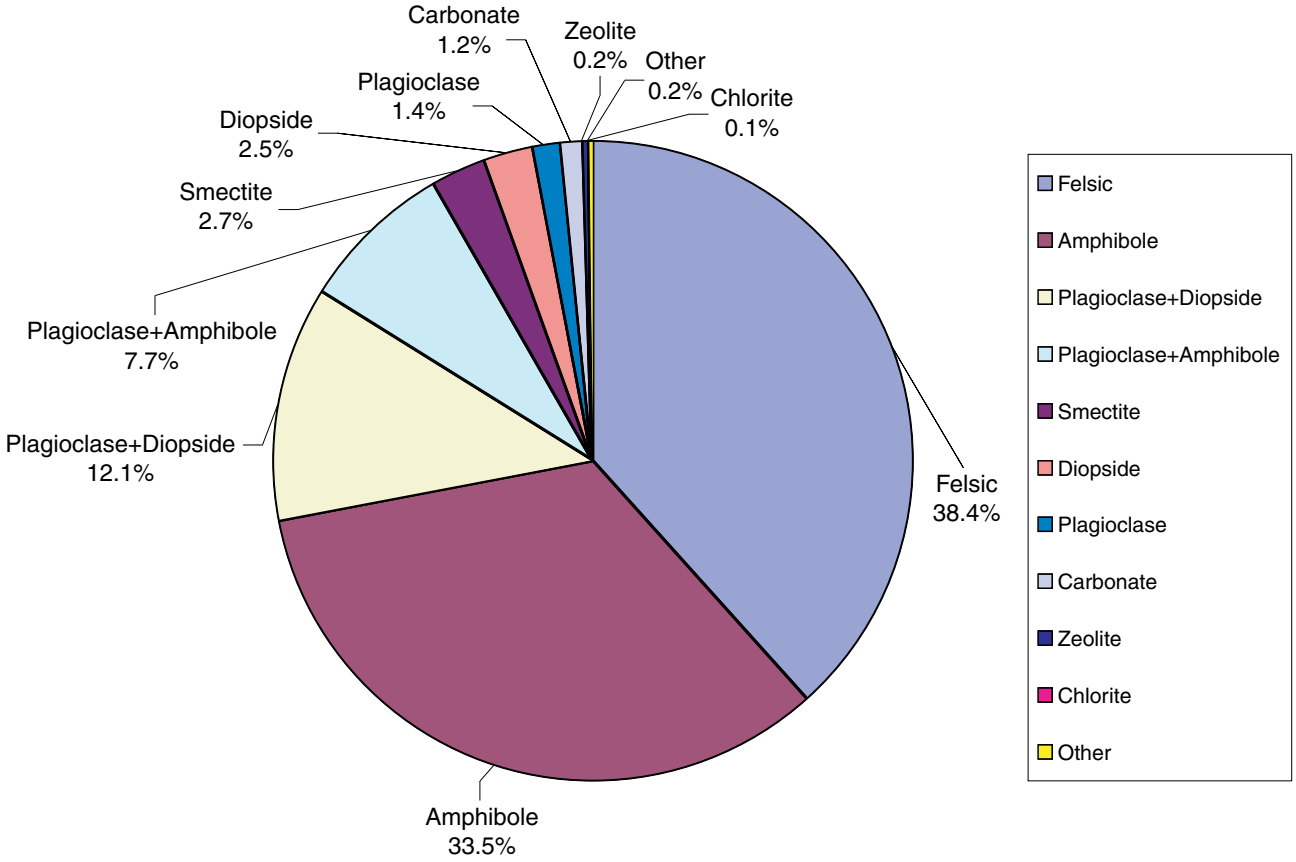

Figure F3. Downhole plots of vein abundance in Hole 735B (data from upper 500 m is after Dick et al., 1991; that from remainder of the core is after Shipboard Scientific Party, 1999). Carbonate and smectite veins are grouped together because they commonly form mixed assemblages, particularly in the lower parts of the core.

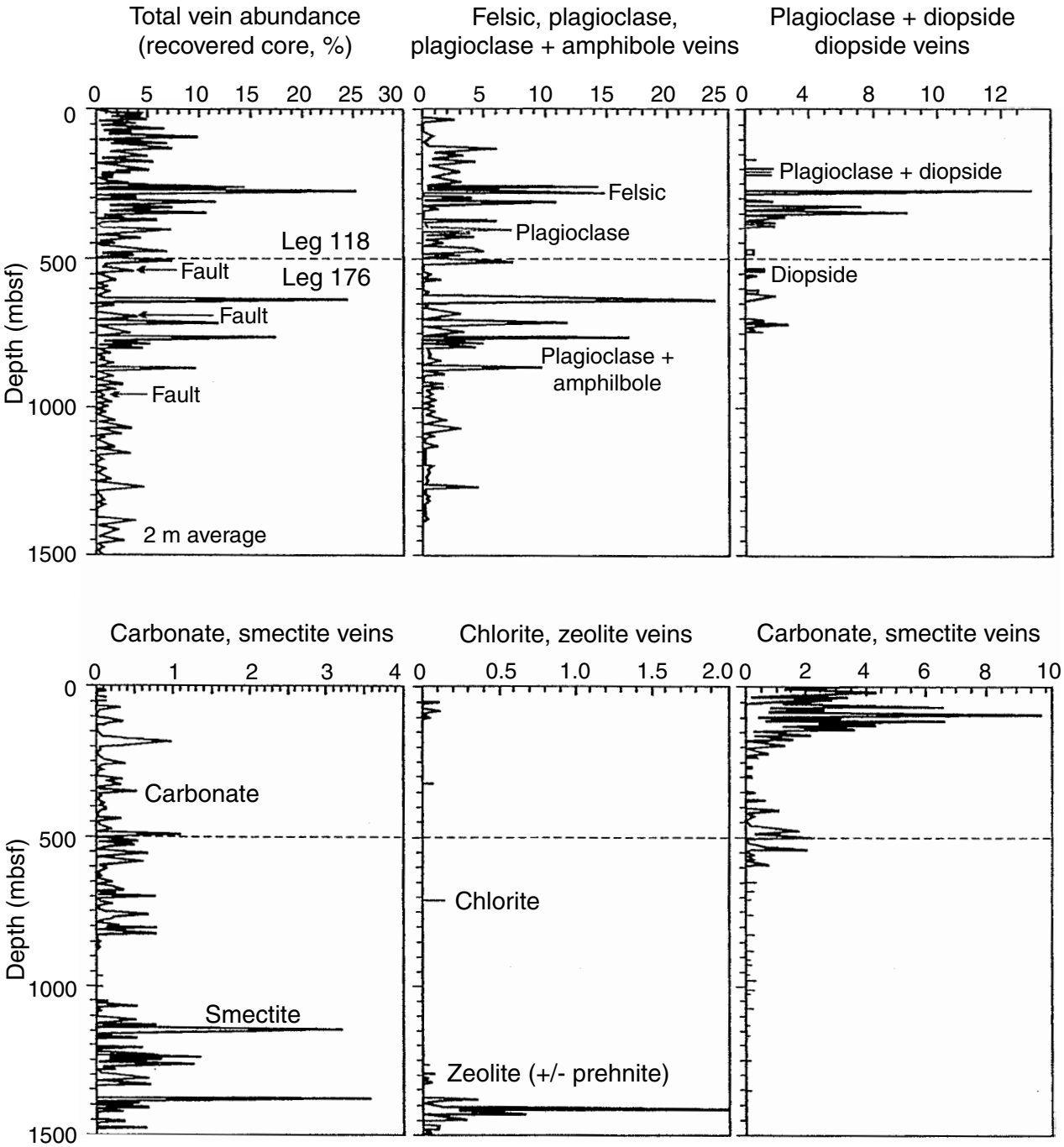

Figure F4. Compositions of vein plagioclase in Hole 735B. Representative analyses of the vein plagioclase are given in Table T2, p. 39. Ab = albite, Or = orthoclase, An = anorthite.

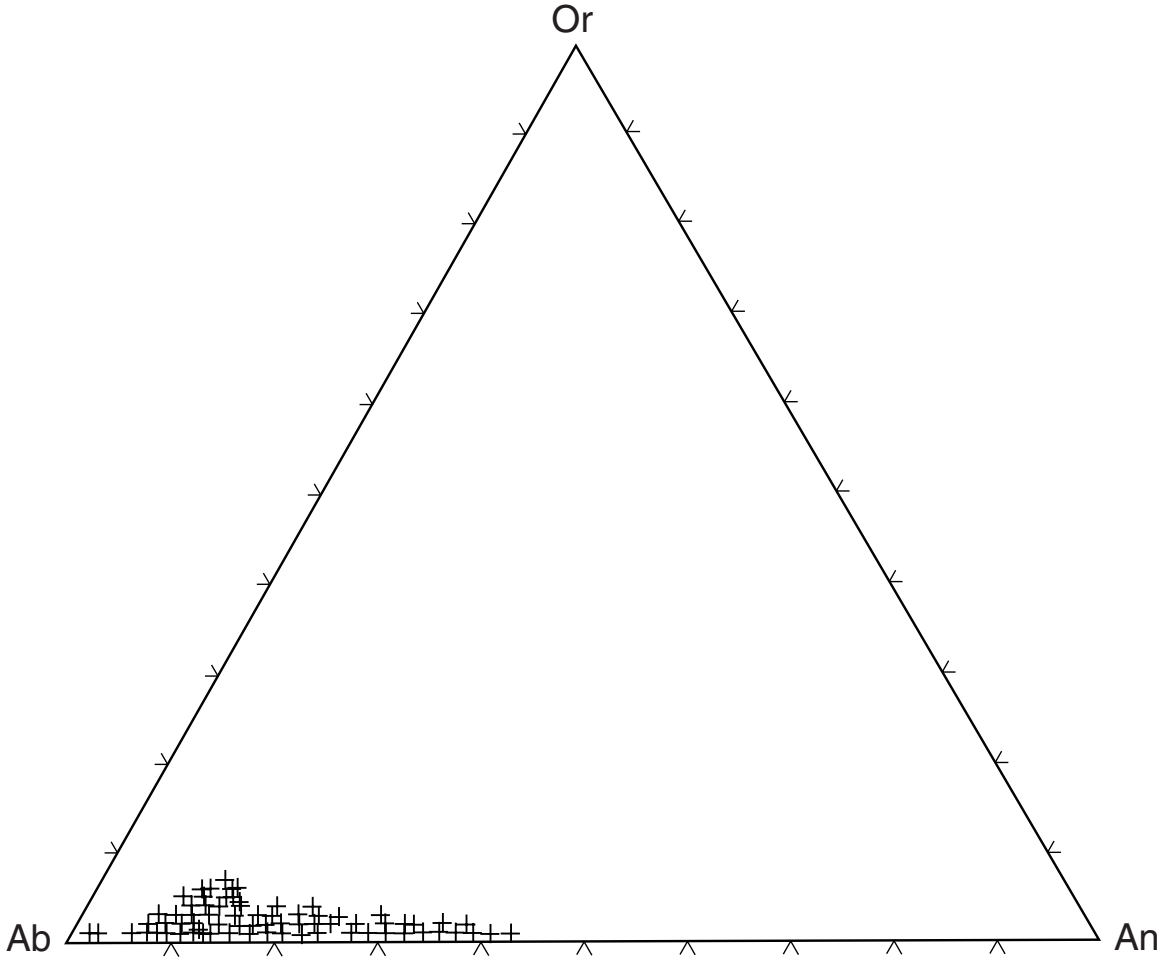

Figure F5. Classification of (**A**) brown and greenish brown vein amphiboles and (**B**) green vein amphibole in Hole 735B (after Leake et al., 1997 using the computer program of Currie, 1997). The brown and brownish green amphibole is chiefly edenite and magnesiohornblende, whereas the green amphibole is chiefly actinolite with lesser amounts of edenite. Representative analyses of vein amphiboles and their cation proportions are given in Tables **T3,** p. 43, and **T4,** p. 44.

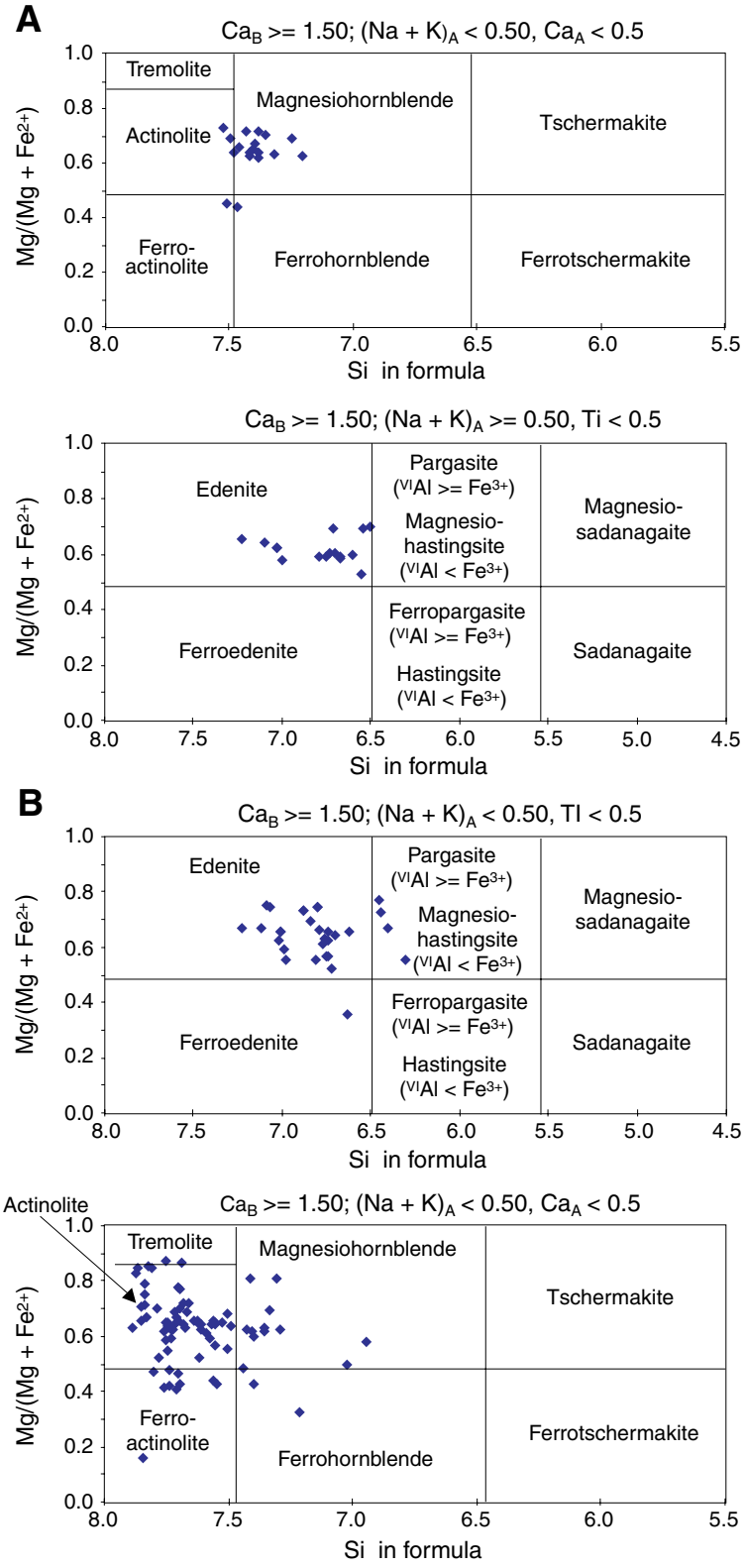

Figure F6. Pyroxene quadrilateral showing compositions of vein diopside in Hole 735B. Representative analyses of vein diopside are given in Table T5, p. 47. En = enstatite, Di = diopside, Wo = wollastonite, Hd = hedenbergite, Fs = ferrosilite.

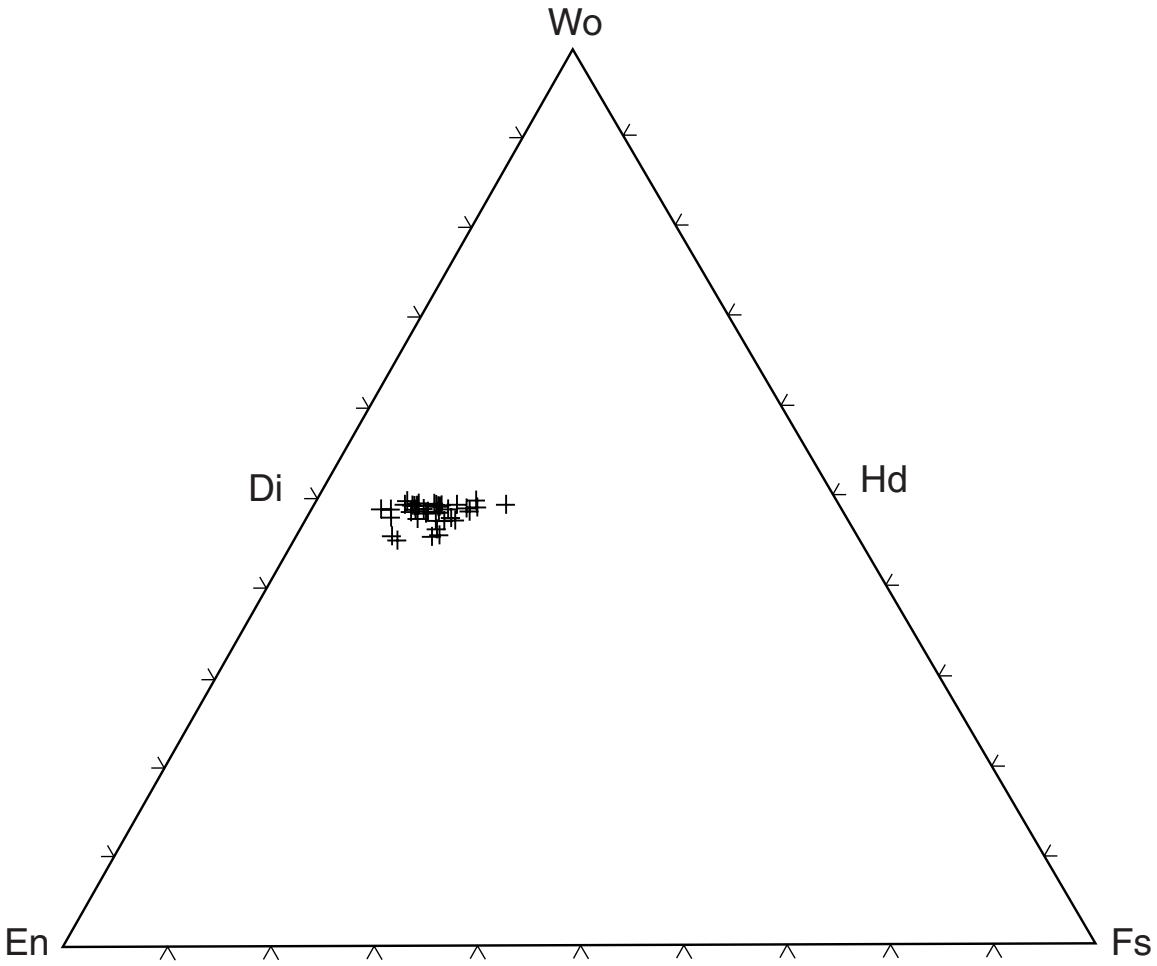

Figure F7. Plot of Fe_2O_3 vs. Al_2O_3 in vein epidote from Hole 735B showing a strong negative correlation.

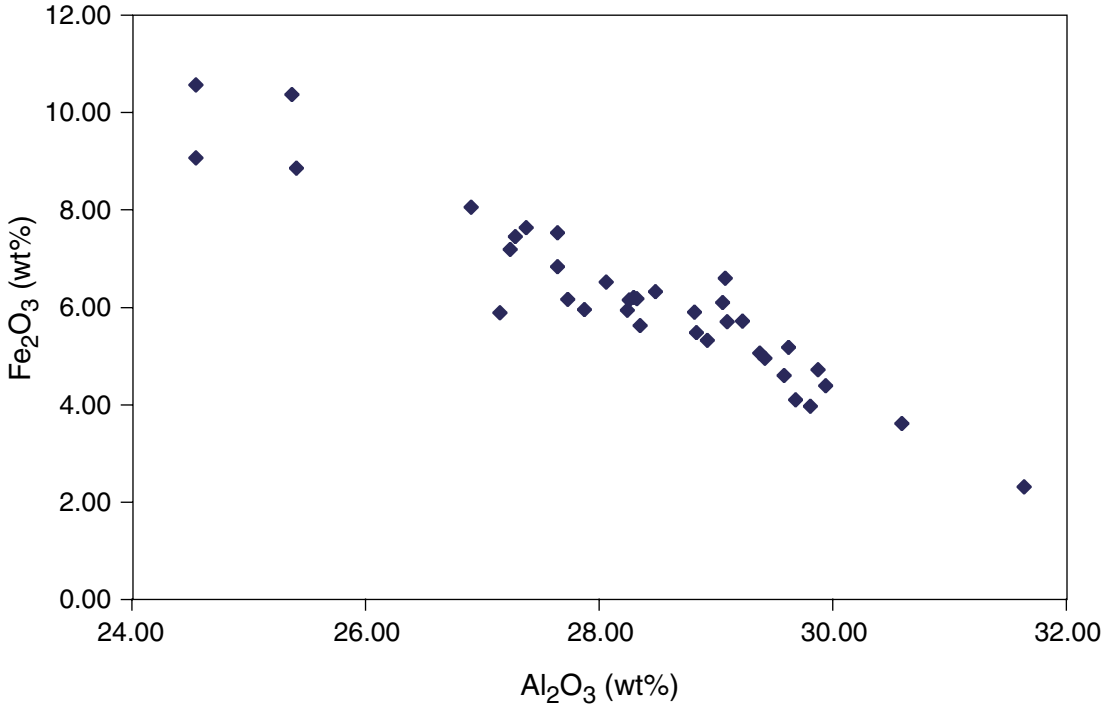

Figure F8. Chemical map showing relative abundances of (**A**) Ca, (**B**) Si, (**C**) Al, and (**D**) Mg in a strongly zoned felsic vein with a myrmekitic texture (Sample 176-735B-124R-1, 111–115 cm). The vein margins are marked by sharp changes in Al and are delineated by solid black lines. Very narrow bands of amphibole are present along the vein margins followed inward by zones of sodic plagioclase about 2 mm wide (green bands in [C]). The myrmekitic intergrowths of quartz and plagioclase (Myr) form parallel bands clearly illustrated in (B). The center of the vein is consists chiefly of greenish brown amphibole (Am) separated from the myrmekite by bands of pure plagioclase. Scale bars = 5 mm.

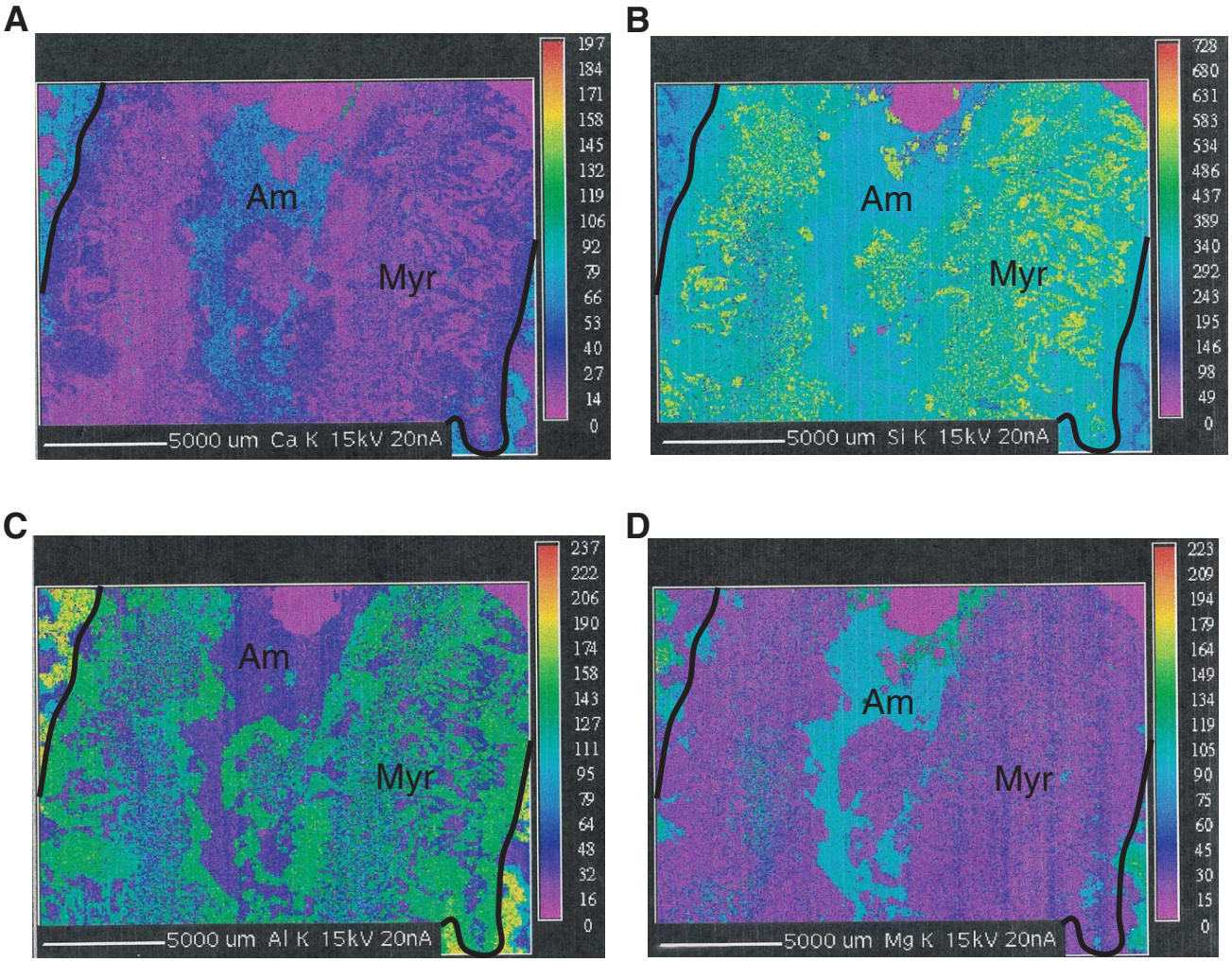

Figure F9. Chemical map showing relative abundances of (**A**) Mg, (**B**) Si, (**C**) Al, and (**D**) Na in a plagioclase + diopside vein (Sample 176-735B-123R-6, 140–144 cm). The vein boundary in the upper left (delineated by solid black line) is marked by distinct changes in Al, Si, and Na, reflecting changes in plagioclase composition. The boundary in the lower right is against epoxy. Most of the vein is filled with sodic plagioclase (Pl), but the distinct band along the center is filled with diopside (Di) in a matrix of black to dark brown aphanitic material. Scale bars = 5 mm.

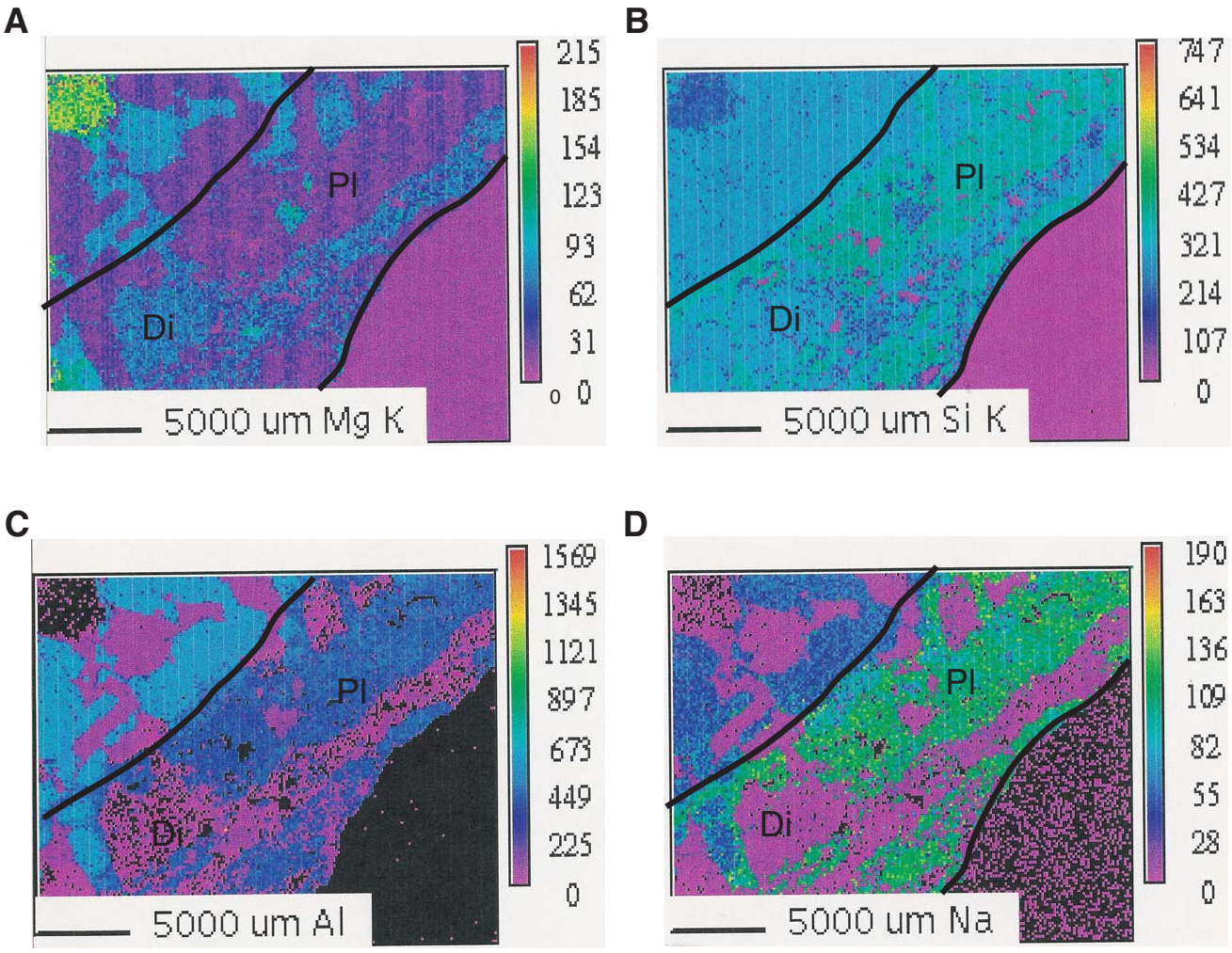

Figure F10. Chemical map showing variations of (**A**) Al and (**B**) Na in large, zoned plagioclase crystals in a plagioclase-rich vein (Sample 176-735B-161R-7, 77–83 cm). The vein margin in the lower right (delineated by solid black line) is marked by a distinct change in plagioclase composition from calcic plagioclase (An) in the host rock to more sodic plagioclase (Pl) in the vein. The large, subhedral plagioclase crystals in the vein have relatively uniform cores and strongly zoned, relatively sodic rims. The spaces between the plagioclase grains may be open or filled with minor amphibole or quartz. Scale bars = 5 mm.

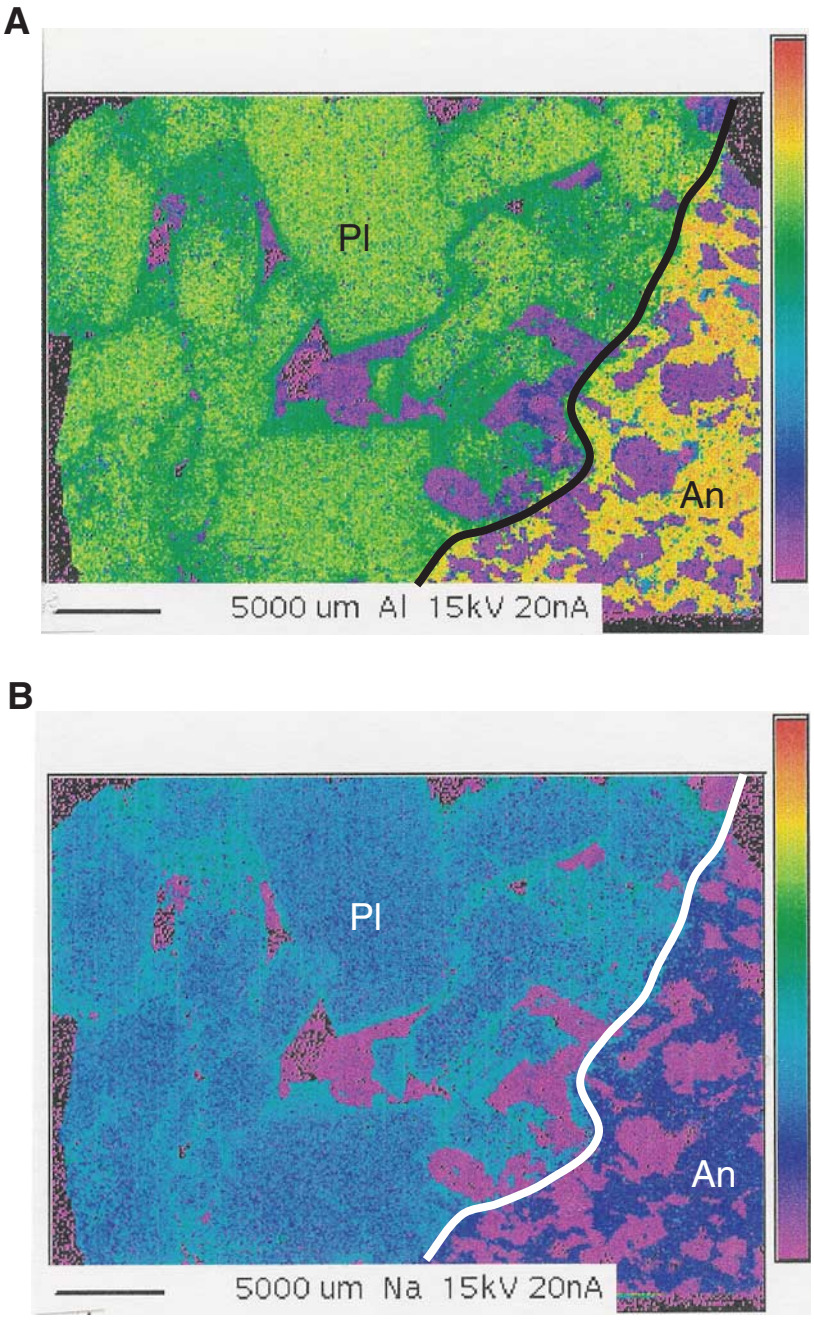

Figure F11. Chemical map showing variations in Al in a plagioclase-rich vein (Sample 176-735B-120R-2, 99–104 cm). The vein margin on the right side (delineated by solid black line) is marked by a significant change in plagioclase composition from calcic plagioclase (An) in the host rock to more sodic plagioclase (Pl) in the vein. Large, subhedral, zoned plagioclase crystals are concentrated along the vein wall. The low-Al zone (blue color) in the center of the vein consists of dark aphanitic material. Note the rim of chlorite on the large clinopyroxene grain (red color) in the upper right corner. Scale bar = 5 mm. Ap = apatite.

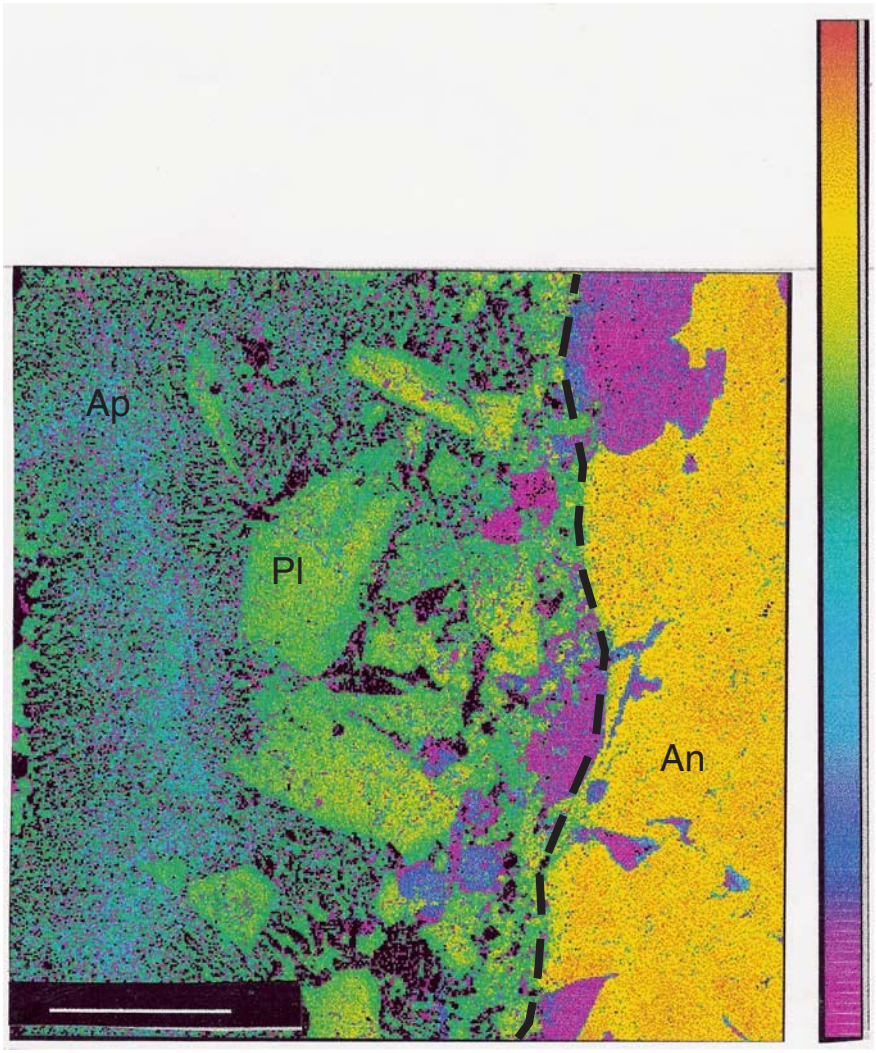

Figure F12. Histogram of formation temperatures calculated from plagioclase-amphibole pairs in veins from Hole 735B using the geothermometer of Holland and Blundy (1994).

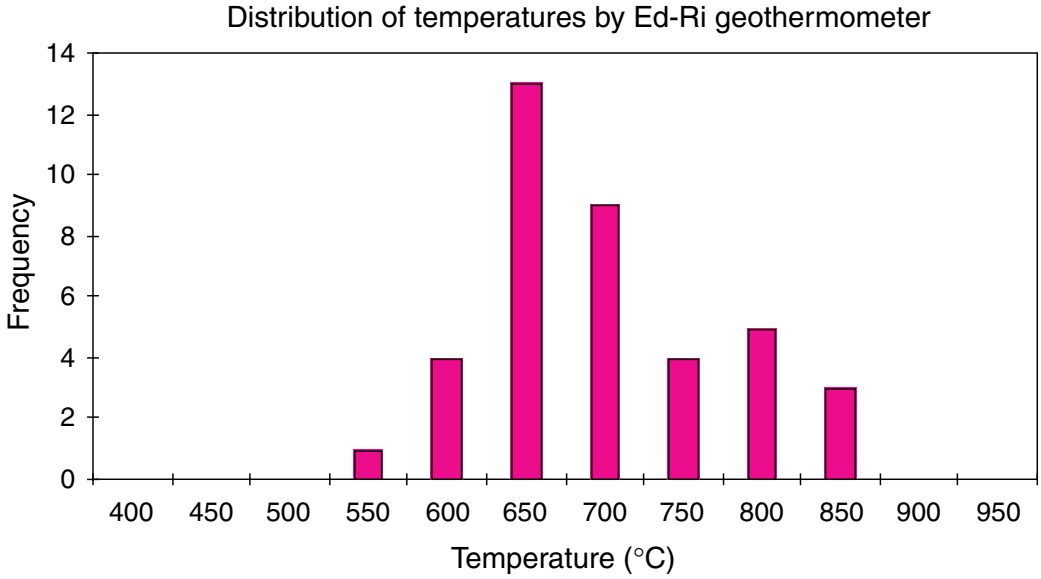

Table T1. Number and area of different vein types in the lower 1053 m of Hole 735B, Leg 176.

Vein type	Number	Vein (%)	Area (cm^2)	Area (%)
Smectite	1316	47.13	684.44	15.17
Amphibole	471	16.87	208.14	4.61
Amphibole + plagioclase	269	9.63	871.45	19.31
Carbonate	255	9.14	81.97	1.86
Plagioclase	138	4.94	223.08	4.94
Felsic	114	4.08	2023.45	44.85
Zeolite	51	1.83	26.93	0.60
Diopside + plagioclase	40	1.43	171.32	3.80
Smectite + carbonate	35	1.25	24.89	0.55
Diopside	27	0.97	16.59	0.37
Smectite + zeolite	22	0.79	63.93	1.42
Chlorite	17	0.61	9.95	0.22
Amphibole + chlorite	13	0.47	37.68	0.84
Quartz	8	0.29	20.60	0.46
Diopside + amphibole	5	0.18	5.90	0.13
Carbonate + oxide	4	0.14	14.40	0.32
Epidote	3	0.11	14.15	0.31
Smectite + amphibole	2	0.07	8.10	0.18
Amphibole + carbonate	1	0.04	2.60	0.06
Chlorite + zeolite	1	0.04	2.40	0.05

Table T2. Representative microprobe analyses of feldspar from veins, Hole 735B. (Continued on next three pages.)

Core, section, interval (cm):	19R-1, 140–146	22R-1, 82–90	22R-1, 82–90	28R-4, 141–144	87R-7, 0–7	87R-7, 0–7	43R-4, 129–133	43R-4, 129–133	44R-1, 35–47	44R-1, 35–47	121R-3, 48–52	121R-3, 48–52	58R-3, 0–8	58R-3, 0–8	47R-2, 92–100	47R-2, 92–100	63R-1, 106–107
Number of analyses:	2	2	1	1	2	2	3	1	1	2	1	1	2	5	1	1	2
Vein type:	Na-Pl	Na-Pl	Na-Pl	Na-Pl	Na-Pl	Na-Pl	Pl-Di	Pl-Di	Pl-Di	Pl-Di	Pl-Di	Pl-Di	Pl-Am-Ep	Pl-Am-Ep	Pl-Am-Ep	Pl-Am-Ep	Pl-Ep-Cl
Location:	Homo	Homo	Homo	Homo	Homo	Homo	Core	Rim	Rim	Core	Rim	Core	Rim	Core	Rim	Core	Rim
Major element oxide (wt%):																	
SiO_2	62.65	62.06	63.16	57.49	61.71	63.46	63.06	64.80	64.75	62.38	70.53	65.22	64.54	63.49	65.46	59.37	64.30
TiO_2	0.00	0.00	0.00	0.04	0.00	0.01	0.01	0.01	0.00	0.00	0.00	0.04	0.00	0.02	0.00	0.05	0.01
Al_2O_3	22.84	23.98	23.08	26.47	22.69	22.08	23.13	22.04	22.05	23.51	19.70	21.92	22.44	22.90	21.81	25.43	22.41
Fe_2O_3	0.24	0.05	0.05	0.16	0.21	0.13	0.30	0.06	0.22	0.05	0.23	0.00	0.09	0.12	0.20	0.11	0.26
CaO	4.39	5.60	4.41	7.97	4.61	3.15	4.64	2.98	3.13	4.78	0.21	3.71	2.66	3.90	2.92	7.47	3.95
Na_2O	9.26	8.28	8.79	7.38	10.18	10.48	8.73	9.66	9.17	8.78	8.46	8.44	9.96	9.17	9.43	6.94	9.06
K_2O	0.04	0.02	0.05	0.03	0.05	0.05	0.03	0.03	0.58	0.03	0.00	0.00	0.01	0.15	0.04	0.21	0.38
BaO	0.01	0.00	0.04	0.02	0.00	0.00	0.00	0.00	0.01	0.00	0.01	0.10	0.00	0.00	0.00	0.00	0.00
Total:	99.44	99.99	99.58	99.56	99.43	99.35	99.90	99.56	99.92	99.53	99.13	99.41	99.70	99.76	99.87	99.58	100.37
Number of ions based on 8 O:																	
Si	2.7898	2.7490	2.7998	2.5877	2.7642	2.8257	2.7902	2.8611	2.8563	2.7721	3.0569	2.8759	2.8469	2.8093	2.8774	2.6572	2.8299
Ti	0.0000	0.0000	0.0000	0.0014	0.0000	0.0003	0.0002	0.0002	0.0000	0.0000	0.0000	0.0012	0.0000	0.0008	0.0000	0.0017	0.0004
Al^{IV}	1.1988	1.2510	1.2002	1.4042	1.1979	1.1488	1.2053	1.1389	1.1437	1.2279	0.9431	1.1241	1.1531	1.1901	1.1226	1.3411	1.1623
Al^{VI}	0.0000	0.0008	0.0056	0.0000	0.0000	0.0097	0.0009	0.0077	0.0028	0.0035	0.0634	0.0149	0.0134	0.0040	0.0071	0.0000	0.0000
Al ions	1.1988	1.2519	1.2058	1.4042	1.1979	1.1585	1.2062	1.1466	1.1464	1.2315	1.0065	1.1390	1.1665	1.1941	1.1297	1.3411	1.1623
Fe^{+3}	0.0081	0.0017	0.0017	0.0054	0.0069	0.0042	0.0098	0.0019	0.0073	0.0015	0.0075	0.0000	0.0030	0.0039	0.0067	0.0036	0.0085
Ca	0.2092	0.2657	0.2094	0.3843	0.2210	0.1503	0.2200	0.1408	0.1481	0.2274	0.0097	0.1751	0.1259	0.1850	0.1376	0.3583	0.1861
Na	0.7992	0.7110	0.7554	0.6440	0.8839	0.9046	0.7487	0.8266	0.7846	0.7566	0.7110	0.7212	0.8519	0.7868	0.8036	0.6020	0.7729
K	0.0024	0.0011	0.0028	0.0017	0.0029	0.0027	0.0019	0.0015	0.0324	0.0016	0.0000	0.0000	0.0006	0.0087	0.0023	0.0119	0.0216
Ba	0.0002	0.0000	0.0007	0.0004	0.0000	0.0000	0.0000	0.0000	0.0002	0.0000	0.0001	0.0017	0.0000	0.0001	0.0000	0.0000	0.0000
Total:	5.0077	4.9804	4.9757	5.0291	5.0768	5.0464	4.9770	4.9786	4.9754	4.9906	4.7917	4.9141	4.9947	4.9887	4.9574	4.9759	4.9817
An	20.7	27.2	21.7	37.4	20.1	14.2	22.7	14.6	15.9	23.1	1.3	19.5	12.9	19.1	14.6	37.3	19.4

Notes: Pl = plagioclase, Na-Pl = sodic plagioclase, Di = diopside, Am = amphibole, Ep = epidote, Bi = biotite, Qz = quartz, Cl = chlorite, Myr = myrmekite, Ap = apatite, Pr = prehnite, Sm = smectite. Inter = intermediate, Homo = unzoned grain.

Table T2 (continued).

Core, section, interval (cm):	64R-2, 100–105	64R-2, 100–105	124R-1, 111–116	124R-1, 111–116	124R-1, 111–116	124R-1, 111–116	124R-1, 111–116	118R-1, 76–82	118R-1, 76–82	118R-1, 76–82	118R-1, 76–82	119R-5, 62–68	119R-5, 62–68	119R-5, 62–68	45R-3, 107–112	45R-4-3, 107–112	122R-4, 0–5
Number of analyses:	1	1	1	1	1	1	1	1	1	1	1	1	1	1	1	2	1
Vein type:	Pl-Ep-Cl	Pl-Ep-Cl	Myr	Myr	Myr	Myr	Myr	Pl-Am	Pl-Am	Pl-Am	Pl-Am	Pl-Am	Pl-Am	Pl-Am	Pl-Am	Pl-Am	Pl-Am
Location:	Core	Core	Homo	Homo	Homo	Homo	Homo	Rim	Core	Core	Rim	Core	Inter	Rim	Rim	Core	Rim
Major element oxide (wt%):																	
SiO_2	57.96	58.97	66.66	66.57	67.83	70.33	63.46	63.55	63.36	63.97	64.35	62.37	66.06	68.39	64.50	61.91	68.55
TiO_2	0.05	0.00	0.00	0.00	0.00	0.07	0.16	0.00	0.00	0.03	0.00	0.00	0.01	0.03	0.03	0.02	0.04
Al_2O_3	26.39	25.91	20.96	20.99	20.07	19.40	22.68	22.25	22.32	22.27	21.79	23.31	20.84	19.83	21.86	23.76	19.68
Fe_2O_3	0.01	0.00	0.18	0.19	0.19	0.17	0.22	0.22	0.27	0.18	0.13	0.39	0.15	0.05	0.08	0.09	0.15
CaO	8.46	6.67	2.72	2.68	1.54	0.09	4.75	4.39	4.59	4.30	4.11	5.42	2.51	1.12	3.02	4.96	0.95
Na_2O	6.98	7.83	8.13	8.70	9.53	9.28	7.88	8.88	8.66	8.96	8.90	8.35	9.41	9.88	9.53	8.48	10.71
K_2O	0.02	0.03	0.62	0.49	0.11	0.07	0.33	0.38	0.45	0.26	0.20	0.02	0.15	0.00	0.12	0.03	0.00
BaO			0.00	0.00	0.00	0.00	0.00	0.00	0.00	0.01	0.11	0.14	0.02	0.04	0.04	0.02	0.03
Total:	99.88	99.41	99.27	99.62	99.27	99.41	99.48	99.66	99.64	99.97	99.58	99.99	99.16	99.33	99.19	99.27	100.12
Number of ions based on 8 O:																	
Si	2.5977	2.6430	2.9339	2.9250	2.9764	3.0514	2.8135	2.8209	2.8148	2.8272	2.8511	2.7666	2.9187	2.9944	2.8610	2.7591	2.9876
Ti	0.0017	0.0000	0.0000	0.0000	0.0000	0.0023	0.0054	0.0000	0.0000	0.0009	0.0000	0.0000	0.0005	0.0010	0.0012	0.0007	0.0015
Al^{IV}	1.3939	1.3570	1.0661	1.0750	1.0236	0.9486	1.1850	1.1641	1.1684	1.1600	1.1378	1.2188	1.0812	1.0056	1.1390	1.2409	1.0111
Al^{VI}	0.0000	0.0116	0.0212	0.0119	0.0144	0.0434	0.0000	0.0000	0.0000	0.0000	0.0000	0.0000	0.0042	0.0175	0.0039	0.0070	0.0000
Al ions	1.3939	1.3686	1.0873	1.0870	1.0380	0.9920	1.1850	1.1641	1.1684	1.1600	1.1378	1.2188	1.0854	1.0231	1.1429	1.2479	1.0111
Fe^{+3}	0.0003	0.0000	0.0059	0.0062	0.0064	0.0056	0.0072	0.0072	0.0090	0.0060	0.0042	0.0130	0.0050	0.0015	0.0027	0.0030	0.0051
Ca	0.4062	0.3203	0.1282	0.1259	0.0723	0.0040	0.2257	0.2087	0.2187	0.2036	0.1951	0.2574	0.1186	0.0524	0.1433	0.2366	0.0445
Na	0.6067	0.6803	0.6940	0.7412	0.8104	0.7807	0.6777	0.7639	0.7456	0.7678	0.7643	0.7179	0.8061	0.8385	0.8197	0.7323	0.9054
K	0.0011	0.0017	0.0346	0.0276	0.0063	0.0037	0.0185	0.0213	0.0256	0.0144	0.0115	0.0009	0.0082	0.0000	0.0068	0.0020	0.0000
Ba	0.0000	0.0000	0.0000	0.0000	0.0000	0.0000	0.0000	0.0000	0.0000	0.0001	0.0019	0.0024	0.0004	0.0008	0.0007	0.0004	0.0005
Total:	5.0076	5.0139	4.8839	4.9129	4.9098	4.8398	4.9331	4.9861	4.9822	4.9801	4.9659	4.9770	4.9429	4.9117	4.9784	4.9819	4.9556
An	40.1	32.0	15.6	14.5	8.2	0.5	25.0	21.5	22.7	21.0	20.3	26.4	12.9	5.9	14.9	24.4	4.7

Table T2 (continued).

Core, section, interval (cm):	122R-4, 0–5	122R-4, 0–5	122R-4, 0–5	122R-4, 0–5	135R-3, 68–72	135R-3, 68–72	135R-3, 68–72	137R-1, 45–49	137R-1, 45–49	137R-1, 45–49	120R.1, 85–91	120R-2, 85–91	121R-1, 81–86	121R-1, 81–86	121R-8, 1–8	121R-8, 1–8
Number of analyses:	1	1	1	1	2	1	1	2	1	1	1	3	3	3	1	1
Vein type:	Pl-Am	Pl-Am	Pl-Am	Pl-Am	Pl-Am-Bi	Pl-Am-Bi	Pl-Am-Bi	Pl-Am-Bi-Qz	Pl-Am-Bi-Qz	Pl-Am-Bi-Qz	Pl-Di-Am-Ep	Pl-Di-Am-Ep	Pl-Ep-Cl	Pl-Ep-Cl	Pl	Pl
Location:	Inter	Inter	Inter	Core	Core	Inter	Rim	Core	Inter	Rim	Core	Rim	Core	Rim	Core	Inter
Major element oxide (wt%):																
SiO_2	67.20	65.93	64.17	63.91	60.72	62.93	66.19	57.76	61.20	65.86	58.80	66.97	67.95	69.73	61.87	63.59
TiO_2	0.11	0.06	0.00	0.03	0.08	0.00	0.03	0.00	0.00	0.00	0.00	0.03	0.02	0.03	0.04	0.06
Al_2O_3	19.76	21.13	22.23	22.63	24.07	22.74	21.03	26.08	23.77	21.06	25.14	20.52	20.24	19.56	23.60	22.20
Fe_2O_3	0.18	0.06	0.17	0.21	0.30	0.33	0.15	0.27	0.17	0.25	0.34	0.18	0.18	0.13	0.24	0.18
CaO	1.63	2.76	4.31	4.57	6.47	4.69	2.58	9.01	6.22	2.69	7.84	2.05	1.76	0.60	6.01	4.60
Na_2O	10.00	9.00	9.08	8.47	7.94	8.07	9.32	6.45	7.67	8.98	6.73	9.74	9.45	9.05	7.71	8.25
K_2O	0.14	0.37	0.42	0.44	0.30	0.54	0.05	0.17	0.38	0.24	0.10	0.02	0.01	0.01	0.22	0.27
BaO	0.00	0.02	0.01	0.00	0.00	0.00	0.00	0.17	0.16	0.07	0.10	0.03	0.04	0.11	0.04	0.00
Total:	99.02	99.33	100.39	100.26	99.87	99.30	99.35	99.92	99.57	99.14	99.05	99.54	99.64	99.22	99.72	99.14
Number of ions based on 8 O:																
Si	2.9663	2.9094	2.8282	2.8170	2.7098	2.8027	2.9161	2.5957	2.7350	2.9110	2.6508	2.9418	2.9710	3.0368	2.7522	2.8292
Ti	0.0036	0.0019	0.0000	0.0010	0.0026	0.0000	0.0009	0.0000	0.0000	0.0000	0.0000	0.0011	0.0006	0.0008	0.0014	0.0019
Al^{IV}	1.0282	1.0906	1.1546	1.1758	1.2660	1.1936	1.0839	1.3815	1.2520	1.0890	1.3357	1.0574	1.0286	0.9632	1.2369	1.1642
Al^{VI}	0.0000	0.0083	0.0000	0.0000	0.0000	0.0000	0.0078	0.0000	0.0000	0.0081	0.0000	0.0047	0.0142	0.0408	0.0000	0.0000
Al ions	1.0282	1.0989	1.1546	1.1758	1.2660	1.1936	1.0917	1.3815	1.2520	1.0972	1.3357	1.0621	1.0429	1.0040	1.2369	1.1642
Fe^{+3}	0.0060	0.0019	0.0055	0.0069	0.0101	0.0112	0.0051	0.0093	0.0058	0.0082	0.0116	0.0059	0.0059	0.0043	0.0081	0.0061
Ca	0.0772	0.1304	0.2036	0.2157	0.3093	0.2239	0.1215	0.4336	0.2976	0.1274	0.3788	0.0965	0.0824	0.0279	0.2863	0.2193
Na	0.8562	0.7702	0.7757	0.7240	0.6866	0.6964	0.7957	0.5622	0.6644	0.7694	0.5881	0.8291	0.8009	0.7641	0.6645	0.7115
K	0.0079	0.0210	0.0238	0.0245	0.0173	0.0307	0.0028	0.0098	0.0219	0.0136	0.0055	0.0013	0.0005	0.0006	0.0124	0.0151
Ba	0.0000	0.0004	0.0002	0.0000	0.0000	0.0000	0.0001	0.0030	0.0027	0.0012	0.0018	0.0005	0.0007	0.0020	0.0007	0.0000
Total:	4.9452	4.9340	4.9916	4.9649	5.0016	4.9585	4.9339	4.9950	4.9794	4.9280	4.9725	4.9384	4.9048	4.8406	4.9625	4.9472
An	8.3	14.5	20.8	23.0	31.1	24.3	13.3	43.5	30.9	14.2	39.2	10.4	9.3	3.5	30.1	23.6

Table T2 (continued).

Core, section, interval (cm):	121R-8, 1–8	121R-8, 1–8	159R-7, 66–72	159R-7, 66–72	159R-7, 66–72	188R-5, 13–18	70R-1, 39–49	183R-3, 69–78	183R-3, 69–78	184R-2, 10–13
Number of analyses:	1	1	2	1	2	2	1	1	1	1
Vein type:	Pl	Pl	Pl-Qz-Ap	Pl-Qz-Ap	Pl-Qz-Ap	Pl-Pr-Sm	Pl-Di	Pl-Sm	Pl-Sm	Felsic
Location:	Inter	Rim	Core	Inter	Rim	Homo	Homo	Homo	Homo	Homo
Major element oxide (wt%):										
SiO_2	67.78	69.33	60.20	60.81	67.15	67.73	64.29	62.15	62.61	65.18
TiO_2	0.00	0.07	0.07	0.00	0.05	0.09	0.03	0.04	0.01	0.00
Al_2O_3	20.28	19.20	24.22	24.04	20.01	19.81	19.29	18.69	19.23	18.20
Fe_2O_3	0.27	0.26	0.27	0.20	0.00	0.19	0.23	0.06	0.00	0.00
CaO	1.78	0.51	6.49	6.04	0.71	0.30	0.55	0.07	0.02	0.05
Na_2O	9.35	9.83	8.50	8.70	11.69	12.16	1.02	0.19	0.29	0.20
K_2O	0.23	0.00	0.19	0.27	0.14	0.02	14.11	15.69	15.64	16.16
BaO	0.25	0.00	0.00	0.13	0.00	0.00	0.00	2.28	1.71	0.13
Total:	99.96	99.20	99.95	100.18	99.75	100.29	99.52	99.18	99.51	99.92
Number of ions based on 8 O:										
Si	2.9641	3.0295	2.6914	2.7108	2.9529	2.9620	2.9634	2.9483	2.9434	3.0117
Ti	0.0000	0.0024	0.0023	0.0000	0.0015	0.0028	0.0010	0.0015	0.0004	0.0000
Al^{IV}	1.0359	0.9705	1.2761	1.2628	1.0372	1.0210	1.0366	1.0451	1.0566	0.9883
Al^{VI}	0.0094	0.0184	0.0000	0.0000	0.0000	0.0000	0.0113	0.0000	0.0086	0.0028
Al ions	1.0453	0.9889	1.2761	1.2628	1.0372	1.0210	1.0479	1.0451	1.0652	0.9911
Fe^{+3}	0.0087	0.0086	0.0092	0.0066	0.0000	0.0061	0.0080	0.0022	0.0000	0.0000
Ca	0.0835	0.0237	0.3110	0.2885	0.0336	0.0139	0.0272	0.0038	0.0009	0.0026
Na	0.7930	0.8326	0.7369	0.7521	0.9963	1.0306	0.0911	0.0175	0.0261	0.0175
K	0.0130	0.0000	0.0109	0.0153	0.0077	0.0013	0.8293	0.9494	0.9381	0.9527
Ba	0.0044	0.0000	0.0000	0.0023	0.0000	0.0000	0.0000	0.0424	0.0315	0.0023
Total:	4.9120	4.8857	5.0377	5.0383	5.0291	5.0377	4.9680	5.0101	5.0058	4.9779
An	9.5	2.8	29.7	27.7	3.3	1.3	23.0	17.8	3.5	13.1

Table T3. Representative microprobe analyses of brown and greenish-brown amphibole veins, Hole 735B.

Core, section, interval (cm):	12R-1, 50–55	26R-3, 87–91	47R-2, 92–100	47R-2, 92–100	58R-1, 95–102	70R-1, 39–49	119R-5, 62–68	123R-8, 27–32	124R-1, 111–116	130R-3, 52–59	130R-3, 52–59	135R-3, 68–72	137R-3, 112–116	141R-1, 50–55	159R-4, 120–125	163R-6, 15–20	168R-2, 140–146
Number of analyses:	1	1	2	2	1	1	1	2	2	2	1	2	4	2	1	3	2
Major element oxide (wt%):																	
SiO_2	44.00	45.94	49.29	49.62	50.81	47.33	53.08	44.77	48.54	44.69	51.41	45.44	50.62	51.22	48.50	51.56	50.49
TiO_2	2.35	0.15	0.60	0.58	0.82	1.95	0.04	3.59	1.44	2.38	0.86	2.29	0.95	1.06	1.32	0.74	1.07
Al_2O_3	9.92	10.07	3.97	4.68	3.51	6.64	1.28	9.35	5.40	8.12	3.28	7.64	3.76	3.51	4.97	3.32	4.28
FeO	17.28	11.82	21.38	14.18	14.23	14.58	20.46	11.24	13.83	15.71	15.03	15.68	15.50	13.44	14.98	11.96	12.81
MnO	0.26	0.20	0.30	0.13	0.18	0.30	0.45	0.08	0.39	0.27	0.35	0.35	0.29	0.00	0.64	0.42	0.50
MgO	10.98	15.14	9.67	14.23	15.20	13.51	13.56	14.49	14.47	12.60	14.93	13.17	14.83	16.21	14.18	17.24	16.49
CaO	10.90	11.53	10.22	11.66	10.84	10.19	8.17	11.52	10.48	10.53	11.10	10.59	10.78	10.69	10.38	11.22	10.97
Na_2O	2.53	2.43	1.34	0.96	1.14	2.14	0.36	3.07	2.33	2.40	1.05	2.28	1.05	1.11	1.79	1.04	1.40
K_2O	0.38	0.18	0.17	0.12	0.29	0.24	0.00	0.31	0.23	0.30	0.20	0.29	0.22	0.14	0.14	0.18	0.18
F	0.00	0.00	0.03	0.05	0.03	0.05	0.00	0.00	0.00	0.00	0.00	0.00	0.00	0.00	0.00	0.00	0.00
Cl	0.00	0.00	0.32	0.24	0.12	0.00	0.02	0.00	0.04	0.02	0.08	0.02	0.00	0.00	0.00	0.01	0.01
Total:	98.59	97.47	97.29	96.46	97.18	96.93	97.43	98.43	97.16	97.04	98.27	97.76	98.01	97.39	96.90	97.69	98.20
Ions:	15.727	15.763	15.305	15.317	15.339	15.521	15.074	15.766	15.571	15.695	15.315	15.682	15.347	15.315	15.494	15.359	15.439
Si T	6.555	6.715	7.488	7.361	7.461	7.024	7.862	6.522	7.164	6.710	7.482	6.763	7.401	7.445	7.203	7.445	7.301
Al^{IV}	1.445	1.285	0.513	0.639	0.539	0.976	0.138	1.478	0.837	1.290	0.518	1.237	0.600	0.556	0.797	0.552	0.699
Al^{VI}	0.297	0.450	0.200	0.180	0.068	0.185	0.085	0.128	0.103	0.147	0.045	0.104	0.049	0.046	0.073	0.016	0.031
Ti^{VI}	0.263	0.016	0.069	0.066	0.091	0.218	0.004	0.393	0.161	0.270	0.094	0.256	0.105	0.117	0.147	0.078	0.117
FeM_2	0.914	0.706	1.210	0.891	0.908	0.859	1.193	0.670	0.868	0.910	0.948	0.922	0.965	0.856	0.937	0.797	0.830
MgM_2	0.526	0.827	0.522	0.864	0.934	0.738	0.717	0.810	0.870	0.674	0.913	0.719	0.882	0.982	0.843	1.113	1.024
MnM_1	0.033	0.025	0.038	0.017	0.022	0.038	0.056	0.010	0.049	0.035	0.043	0.044	0.036	0.000	0.081	0.051	0.062
FeM_1	1.016	0.607	1.215	0.706	0.673	0.768	0.981	0.595	0.681	0.857	0.703	0.823	0.734	0.622	0.731	0.522	0.576
MgM_1	1.951	2.368	1.747	2.278	2.305	2.194	1.963	2.396	2.271	2.110	2.254	2.134	2.231	2.378	2.189	2.427	2.364
FeM_4	0.223	0.131	0.292	0.162	0.167	0.182	0.361	0.106	0.159	0.207	0.178	0.208	0.197	0.156	0.193	0.126	0.145
MgM_4	0.000	0.104	0.000	0.028	0.088	0.057	0.314	0.000	0.043	0.038	0.072	0.072	0.121	0.154	0.108	0.171	0.168
CaM_4	1.740	1.765	1.665	1.834	1.705	1.620	1.296	1.798	1.658	1.695	1.731	1.690	1.679	1.666	1.652	1.703	1.688
NaM_4	0.076	0.000	0.123	0.000	0.039	0.141	0.029	0.157	0.139	0.061	0.019	0.031	0.004	0.025	0.048	0.000	0.000
K_A	0.072	0.034	0.033	0.023	0.054	0.045	0.000	0.058	0.043	0.058	0.037	0.055	0.041	0.026	0.027	0.034	0.033
Na_A	0.655	0.689	0.272	0.275	0.285	0.475	0.074	0.709	0.527	0.638	0.278	0.627	0.295	0.289	0.468	0.291	0.394
Ca_A	0.000	0.041	0.000	0.020	0.000	0.000	0.000	0.000	0.000	0.000	0.000	0.000	0.011	0.000	0.000	0.034	0.011
Mg#	0.53	0.70	0.45	0.64	0.66	0.62	0.54	0.70	0.65	0.59	0.64	0.60	0.63	0.68	0.63	0.72	0.70
Mineral	eden	eden	fe-hbl	mg-hbl	mg-hbl	eden	act	eden	eden	eden	mg-hbl	eden	mg-hbl	mg-hbl	mg-hbl	mg-hbl	mg-hbl

Note: act = actinolite, eden = edenite, mg-hbl = magnesiohornblende, fe-hbl = ferrohornblende. Cation proportions and classification after Leake et al. (1997) and Currie (1997).

Table T4. Representative microprobe analyses of green amphibole from veins, Hole 735B. (Continued on next two pages.)

Core, section, interval (cm):	19R-5, 62–73	20R-2, 13–21	22R-2, 82–90	27R-1, 115–121	27R-3, 32–34	31R-3, 4–10	31R-3, 4–10	37R-2, 113–117	42R-3, 27–31	45R-3, 107–112	45R-3, 107–112	47R-2, 92–100	47R-2, 92–100	57R-3, 124–130	57R-3, 124–130	57R-4, 123–133	60R-4, 112–120	63R-1, 106–107
Number of analyses:	1	2	2	1	4	2	1	1	1	3	1	2	1	1	1	1	2	1
Major element oxide (wt%):																		
SiO_2	53.03	47.23	46.07	45.01	46.91	52.96	55.66	48.97	52.64	49.23	45.65	49.86	41.74	54.76	47.11	55.24	53.32	51.74
TiO_2	0.15	0.23	0.25	0.93	0.50	0.32	0.00	0.50	0.08	0.16	0.20	0.57	0.38	0.28	1.67	0.01	0.22	0.30
Al_2O_3	3.07	8.20	10.08	8.91	9.69	2.10	2.25	5.08	2.25	6.53	7.39	4.90	10.16	1.26	6.20	2.49	2.03	3.66
FeO	14.08	16.41	14.09	16.16	9.66	15.54	5.61	14.48	17.89	11.15	18.74	15.23	21.65	10.42	15.19	5.83	12.57	16.10
MnO	0.18	0.24	0.13	0.15	0.14	0.18	0.19	0.10	0.18	0.14	0.17	0.13	0.30	0.12	0.29	0.09	0.06	0.18
MgO	15.14	12.35	13.20	12.02	15.39	14.39	21.19	13.49	12.21	16.99	10.35	13.26	6.79	17.75	14.13	21.21	15.97	13.17
CaO	12.20	11.21	11.93	11.80	11.80	11.21	11.90	12.21	12.34	10.43	11.40	11.76	10.94	12.00	10.35	12.21	11.96	11.98
Na_2O	0.69	1.95	2.20	2.27	2.28	0.66	0.64	1.43	0.35	1.93	1.37	1.04	2.14	0.45	1.67	0.66	0.60	0.62
K_2O	0.04	0.06	0.24	0.10	0.20	0.04	0.06	0.07	0.03	0.10	0.09	0.07	0.61	0.05	0.22	0.04	0.03	0.02
F	0.00	0.00	0.00	0.00	0.06	0.00	0.00	0.00	0.00	0.06	0.20	0.08	0.76	0.14	0.30	0.00	0.12	0.13
Cl	0.00	0.00	0.00	0.00	0.28	0.00	0.00	0.06	0.01	0.15	0.06	0.06	0.04	0.05	0.02	0.00	0.03	0.00
Total:	98.59	97.88	98.20	97.36	96.92	97.40	97.51	96.41	97.98	96.87	95.63	96.96	95.52	97.29	97.17	97.81	96.90	97.91
Ions:																		
Si T	7.625	6.983	6.751	6.740	6.837	7.739	7.752	7.291	7.748	7.162	7.023	7.376	6.636	7.835	7.014	7.690	7.746	7.575
Al^{IV}	0.375	1.017	1.250	1.260	1.163	0.261	0.248	0.709	0.252	0.838	0.977	0.625	1.364	0.165	0.986	0.310	0.255	0.425
Al^{VI}	0.145	0.411	0.492	0.312	0.503	0.102	0.121	0.183	0.138	0.280	0.363	0.230	0.540	0.047	0.102	0.099	0.093	0.207
Ti^{IV}	0.000	0.000	0.000	0.000	0.000	0.000	0.000	0.000	0.000	0.000	0.000	0.000	0.000	0.000	0.000	0.000	0.000	0.000
Ti^{IV}	0.016	0.025	0.028	0.105	0.056	0.036	0.000	0.056	0.009	0.018	0.023	0.063	0.045	0.030	0.187	0.001	0.025	0.033
FeM_2	0.892	0.923	0.795	0.932	0.584	0.978	0.400	0.917	1.100	0.708	1.064	0.927	1.099	0.711	0.919	0.415	0.831	0.978
MgM_2	0.947	0.642	0.686	0.651	0.858	0.886	1.479	0.844	0.754	0.994	0.550	0.780	0.316	1.212	0.792	1.485	1.053	0.782
MnM_1	0.022	0.030	0.016	0.019	0.017	0.022	0.022	0.013	0.022	0.017	0.022	0.017	0.040	0.015	0.037	0.011	0.007	0.022
FeM_1	0.656	0.896	0.771	0.896	0.506	0.742	0.223	0.735	0.907	0.525	1.094	0.785	1.512	0.447	0.766	0.231	0.575	0.813
MgM_1	2.322	2.074	2.214	2.085	2.478	2.236	2.754	2.253	2.070	2.457	1.884	2.200	1.447	2.538	2.197	2.758	2.419	2.165
FeM_4	0.145	0.212	0.161	0.196	0.088	0.181	0.030	0.151	0.195	0.123	0.253	0.173	0.267	0.088	0.206	0.032	0.122	0.180
MgM_4	0.000	0.019	0.000	0.000	0.031	0.017	0.166	0.000	0.000	0.233	0.000	0.000	0.000	0.036	0.147	0.159	0.000	0.000
CaM_4	1.879	1.775	1.855	1.857	1.843	1.755	1.776	1.948	1.946	1.622	1.807	1.851	1.864	1.839	1.647	1.809	1.862	1.879
NaM_4	0.000	0.006	0.000	0.000	0.063	0.051	0.028	0.003	0.004	0.022	0.000	0.030	0.023	0.036	0.000	0.000	0.030	0.012
K_A	0.007	0.011	0.045	0.019	0.037	0.008	0.011	0.013	0.006	0.019	0.018	0.014	0.124	0.009	0.042	0.007	0.005	0.004
Na_A	0.192	0.553	0.625	0.659	0.582	0.137	0.145	0.410	0.096	0.521	0.409	0.267	0.637	0.089	0.482	0.178	0.141	0.164
Ca_A	0.000	0.001	0.018	0.036	0.000	0.000	0.000	0.000	0.000	0.004	0.072	0.012	0.000	0.000	0.004	0.012	0.000	0.000
Si	7.625	6.983	6.751	6.740	6.837	7.739	7.752	7.291	7.748	7.162	7.023	7.376	6.636	7.835	7.014	7.690	7.746	7.575
Mg#	0.66	0.57	0.63	0.57	0.74	0.62	0.87	0.62	0.55	0.73	0.50	0.61	0.36	0.75	0.62	0.87	0.69	0.59
Mineral	act	eden	eden	eden	eden	act	act	mg-hbl	act	eden	fe-hbl	mg-hbl	fe-eden	act	eden	act	act	act

Note: act = actinolite, fe-act= ferroactinolite, eden = edenite, fe-eden = ferroedenite, mg-hbl = magnesiohornblende, fe-hbl = ferrohornblende, parg = pargasite, fe-anth = ferroanthophyllite. Cation proportions and classification after Leake et al. (1997) and Currie (1997).

Table T4 (continued).

Core, section, interval (cm):	63R-1, 106–107	70R-1, 39–49	70R-1, 39–49	71R-2, 115–125	87R-7, 0–7	90R-4, 84–86	91R-3, 67–72	99R-4, 68–74	118R-1, 76–82	118R-6, 100–105	119R-5, 62–68	119R-5, 62–68	121R-3, 48–52	121R-8, 1–8	122R-3, 135–139	122R-4, 0–5	130R-3, 52–59	130R-3, 52–59
Number of analyses:	2	1	1	1	2	1	1	2	2	2	1	1	4	1	2	2	1	1
Major element oxide (wt%):																		
SiO_2	47.24	53.83	55.89	50.88	44.74	53.82	52.07	50.43	53.05	50.42	51.16	48.50	56.49	49.58	51.33	51.65	46.99	46.26
TiO_2	1.57	0.68	0.03	0.37	2.05	0.30	0.16	0.21	0.30	0.26	0.25	0.61	0.29	1.28	0.84	0.19	0.77	0.21
Al_2O_3	6.32	1.94	1.88	4.27	11.02	2.50	5.70	2.74	1.95	3.95	1.01	4.15	1.09	5.06	3.29	2.37	8.03	5.94
FeO	13.78	12.28	6.20	17.51	9.60	12.07	8.27	22.60	16.98	20.12	30.32	22.66	7.68	13.43	14.85	21.78	15.71	25.27
MnO	0.32	0.09	0.10	0.13	0.15	0.13	0.06	0.24	0.28	0.59	0.70	0.14	0.16	0.16	0.29	0.17	0.23	0.17
MgO	14.70	16.20	19.33	12.20	16.08	17.17	19.26	9.31	13.76	11.45	10.92	9.49	20.87	15.07	14.63	9.81	12.24	6.87
CaO	10.37	10.55	13.11	11.76	11.73	11.27	11.63	11.56	11.06	9.86	2.28	10.40	11.42	10.94	11.07	12.28	12.25	11.16
Na_2O	2.21	1.04	0.19	0.57	2.85	0.79	1.32	0.47	0.79	0.92	0.27	1.17	0.62	2.08	1.48	0.39	1.51	0.56
K_2O	0.23	0.07	0.01	0.06	0.12	0.00	0.08	0.04	0.04	0.03	0.02	0.20	0.01	0.30	0.23	0.00	0.25	0.14
F	0.11	0.05	0.09	0.00	0.00	0.00	0.00	0.00	0.00	0.00	0.00	0.00	0.00	0.00	0.00	0.00	0.00	0.00
Cl	0.00	0.08	0.00	0.00	0.00	0.06	0.01	0.06	0.09	0.04	0.10	0.19	0.02	0.02	0.07	0.02	0.07	0.02
Total:	96.85	96.80	96.83	97.75	98.33	98.11	98.56	97.67	98.30	97.64	97.04	97.50	98.66	97.92	98.07	98.66	98.04	96.58
Ions:																		
Si T	7.007	7.790	7.864	7.502	6.453	7.682	7.306	7.638	7.743	7.527	7.875	7.395	7.834	7.229	7.490	7.700	6.945	7.217
Al^{IV}	0.993	0.210	0.136	0.498	1.548	0.318	0.694	0.363	0.257	0.474	0.125	0.605	0.166	0.771	0.510	0.301	1.055	0.783
Al^{VI}	0.111	0.121	0.175	0.244	0.326	0.102	0.249	0.128	0.079	0.221	0.058	0.141	0.012	0.099	0.056	0.115	0.343	0.309
Ti^{IV}	0.000	0.000	0.000	0.000	0.000	0.000	0.000	0.000	0.000	0.000	0.000	0.000	0.000	0.000	0.000	0.000	0.000	0.000
Ti^{IV}	0.176	0.074	0.003	0.041	0.222	0.032	0.017	0.024	0.033	0.029	0.029	0.070	0.030	0.140	0.092	0.021	0.086	0.025
FeM_2	0.856	0.792	0.439	1.026	0.577	0.784	0.543	1.315	1.053	1.144	1.490	1.280	0.534	0.845	0.942	1.283	0.904	1.329
MgM_2	0.857	1.013	1.383	0.688	0.876	1.081	1.191	0.534	0.836	0.607	0.423	0.510	1.424	0.915	0.910	0.581	0.667	0.338
MnM_1	0.040	0.011	0.012	0.016	0.018	0.016	0.007	0.031	0.036	0.075	0.091	0.018	0.019	0.020	0.036	0.022	0.029	0.022
FeM_1	0.684	0.569	0.258	0.923	0.490	0.534	0.360	1.263	0.814	1.059	1.496	1.282	0.303	0.647	0.703	1.189	0.859	1.612
MgM_1	2.276	2.420	2.705	2.061	2.493	2.450	2.632	1.706	2.151	1.866	1.413	1.700	2.678	2.333	2.261	1.790	2.112	1.365
FeM_4	0.170	0.125	0.033	0.210	0.091	0.122	0.067	0.285	0.207	0.310	0.917	0.328	0.055	0.145	0.167	0.244	0.179	0.356
MgM_4	0.118	0.061	0.000	0.000	0.088	0.122	0.205	0.000	0.008	0.076	0.671	0.000	0.212	0.027	0.011	0.000	0.000	0.000
CaM_4	1.648	1.636	1.976	1.857	1.777	1.723	1.728	1.854	1.729	1.578	0.376	1.699	1.696	1.709	1.731	1.947	1.904	1.750
NaM_4	0.065	0.177	0.024	0.000	0.044	0.032	0.000	0.000	0.057	0.037	0.036	0.026	0.038	0.118	0.091	0.000	0.000	0.000
K_A	0.043	0.013	0.002	0.011	0.022	0.000	0.014	0.009	0.007	0.005	0.004	0.039	0.002	0.056	0.043	0.000	0.047	0.028
Na_A	0.573	0.114	0.028	0.163	0.753	0.187	0.359	0.140	0.167	0.230	0.044	0.320	0.131	0.470	0.328	0.114	0.433	0.169
Ca_A	0.000	0.000	0.000	0.000	0.036	0.000	0.020	0.021	0.000	0.000	0.000	0.000		0.000	0.000	0.016	0.036	0.115
Si	7.007	7.790	7.864	7.502	6.453	7.682	7.306	7.638	7.743	7.527	7.875	7.395	7.834	7.229	7.490	7.700	6.945	7.217
Mg#	0.66	0.70	0.85	0.55	0.75	0.72	0.81	0.42	0.59	0.50	0.39	0.43	0.83	0.67	0.64	0.45	0.58	0.33
Mineral	eden	act	act	act	parg	act	mg-hbl	fe-act	act	act	fe-anth	fe-hbl	act	eden	act	fe-act	mg-hbl	fe-hbl

Table T4 (continued).

Core, section, interval (cm):	133R-7, 95–100	135R-3, 68–72	135R-3, 68–72	137R-1, 45–49	140R-6, 40–44	144R-6, 35–47	144R-6, 35–47	149R-4, 82–87	156R-6, 42–46	161R-3, 128–135	161R-3, 128–135	192R-6, 44–50
Number of analyses:	1	2	1	1	4	1	1	6	1	1	1	2
Major element oxide (wt%):												
SiO_2	54.19	52.36	45.44	51.93	46.23	49.66	51.09	52.93	53.01	52.19	50.58	54.35
TiO_2	0.21	0.58	2.05	0.56	0.44	0.26	0.13	0.09	0.15	0.13	0.34	0.26
Al_2O_3	1.93	2.54	7.29	2.58	8.75	1.12	2.05	2.48	1.33	1.30	4.17	1.76
FeO	13.41	15.05	17.61	15.64	13.36	31.47	22.14	14.23	20.67	19.32	15.82	9.95
MnO	0.33	0.35	0.32	0.35	0.24	0.41	0.13	0.37	0.80	0.43	0.21	0.26
MgO	16.52	15.52	12.14	14.41	14.84	3.41	9.11	15.51	15.40	11.98	14.20	19.01
CaO	11.68	11.06	10.55	11.38	12.86	11.29	12.47	11.32	6.07	11.91	11.72	11.54
Na_2O	0.69	0.83	1.99	0.52	1.76	0.09	0.28	0.63	0.38	0.30	0.90	0.96
K_2O	0.07	0.16	0.40	0.12	0.40	0.00	0.01	0.07	0.00	0.01	0.04	0.04
F	0.00	0.00	0.00	0.00	0.00	0.00	0.00	0.00	0.00	0.00	0.00	0.00
Cl	0.03	0.06	0.02	0.05	0.18	0.00	0.01	0.05	0.00	0.03	0.06	0.02
Total:	99.05	98.51	97.81	97.54	99.04	97.70	97.43	97.68	97.82	97.60	98.05	98.15
Ions:												
Si T	7.720	7.583	6.815	7.614	6.739	7.844	7.739	7.681	7.796	7.779	7.407	7.698
Al^{IV}	0.280	0.416	1.185	0.386	1.261	0.156	0.261	0.319	0.204	0.221	0.593	0.294
Al^{VI}	0.044	0.019	0.104	0.060	0.242	0.052	0.105	0.106	0.027	0.007	0.127	0.009
Ti^{IV}	0.000	0.000	0.000	0.000	0.000	0.000	0.000	0.000	0.000	0.000	0.000	0.000
Ti^{IV}	0.022	0.061	0.231	0.062	0.048	0.031	0.015	0.010	0.017	0.015	0.037	0.020
FeM_2	0.872	0.960	1.015	0.989	0.828	1.728	1.325	0.913	1.192	1.217	0.982	0.686
MgM_2	1.061	0.961	0.649	0.889	0.882	0.189	0.555	0.972	0.764	0.761	0.854	1.295
MnM_1	0.040	0.044	0.041	0.043	0.030	0.055	0.017	0.046	0.100	0.054	0.026	0.031
FeM_1	0.586	0.683	0.946	0.740	0.655	2.160	1.245	0.652	0.925	0.956	0.764	0.407
MgM_1	2.374	2.274	2.014	2.216	2.316	0.785	1.736	2.302	1.975	1.990	2.210	2.562
FeM_4	0.139	0.181	0.248	0.188	0.146	0.269	0.234	0.162	0.425	0.235	0.191	0.086
MgM_4	0.073	0.115	0.051	0.044	0.026	0.000	0.000	0.087	0.637	0.000	0.036	0.156
CaM_4	1.783	1.705	1.695	1.768	1.828	1.902	2.000	1.755	0.938	1.853	1.772	1.752
NaM_4	0.005	0.000	0.006	0.000	0.000	0.000	0.000	0.003	0.000	0.000	0.000	0.008
K_A	0.013	0.029	0.077	0.022	0.075	0.000	0.002	0.013	0.000	0.002	0.007	0.008
Na_A	0.186	0.234	0.573	0.148	0.496	0.028	0.082	0.174	0.108	0.087	0.256	0.258
Ca_A	0.000	0.011	0.000	0.020	0.179	0.009	0.024	0.006	0.019	0.049	0.066	0.000
Si	7.720	7.583	6.815	7.614	6.739	7.844	7.739	7.681	7.796	7.779	7.407	7.698
Mg#	0.69	0.65	0.55	0.62	0.66	0.16	0.42	0.66	0.57	0.53	0.62	0.77
Mineral	act	act	eden	act	eden	fe-act	fe-act	act	anth	act	mg-hbl	act

Table T5. Representative microprobe analyses of diopside from veins, Hole 735B.

Core, section, interval (cm):	35R-3, 74–78	43R-4, 129–133	43R-4, 129–133	44R-1, 35–47	63R-1, 106–107	63R-6, 98–106	63R-6, 98–106	64R-4, 66–70	66R-3, 128–132	66R-3, 128–132	68R-2, 68–75	70R-1, 39–49	71R-2, 115–125	84R-1, 88–98	87R-6, 31–41	92R-2, 49–53	92R-2, 49–53	163R-6, 15–20
Number of analyses:	2	1	3	4	1	3	1	1	2	2	2	2	1	3	2	1	1	2
Major element oxide (wt%):																		
SiO_2	52.58	51.42	53.43	52.88	53.35	53.48	52.94	53.90	53.35	53.48	53.73	53.01	53.22	52.15	52.89	53.27	53.36	52.93
TiO_2	0.05	0.18	0.03	0.01	0.03	0.03	0.00	0.00	0.00	0.03	0.02	0.03	0.02	0.05	0.17	0.00	0.00	0.06
Al_2O_3	0.27	1.79	0.46	0.39	0.54	0.27	0.11	0.28	0.42	0.75	0.34	0.38	0.23	0.58	0.95	1.19	0.04	0.36
FeO	8.20	11.29	6.44	7.36	5.67	6.68	10.01	5.00	6.01	7.43	6.75	8.45	6.50	9.54	6.26	4.37	8.09	8.52
Cr_2O_3	0.00	0.00	0.00	0.02	0.12	0.01	0.00	0.03	0.01	0.04	0.01	0.03	0.02	0.01	0.07	0.01	0.04	0.10
MnO	0.22	0.08	0.09	0.12	0.03	0.13	0.17	0.04	0.07	0.10	0.16	0.16	0.06	0.15	0.16	0.15	0.01	0.62
MgO	13.78	10.83	14.31	14.16	14.73	14.30	12.13	15.72	15.07	13.38	14.10	13.06	14.36	12.71	15.91	15.98	13.87	14.18
CaO	22.27	23.26	24.02	23.54	24.62	24.46	23.68	24.60	23.93	23.72	23.80	23.42	24.45	23.87	22.61	24.47	24.05	22.29
Na_2O	1.96	0.37	0.45	0.66	0.20	0.30	0.29	0.23	0.34	0.47	0.35	0.55	0.32	0.28	0.27	0.33	0.15	0.69
Total:	99.35	99.22	99.23	99.14	99.28	99.66	99.33	99.80	99.17	99.39	99.24	99.10	99.18	99.34	99.27	99.78	99.60	99.75
Number of ions based on 6 O:																		
Si	1.9831	1.9626	1.9950	1.9863	1.9846	1.9929	2.0063	1.9890	1.9889	1.9988	2.0057	1.9987	1.9917	1.9764	1.9656	1.9633	1.9980	1.9826
Ti	0.0003	0.0011	0.0002	0.0001	0.0002	0.0002	0.0000	0.0000	0.0000	0.0001	0.0001	0.0002	0.0001	0.0003	0.0010	0.0000	0.0000	0.0004
Al^{IV}	0.0000	0.0000	0.0000	0.0000	0.0000	0.0000	0.0000	0.0000	0.0000	0.0000	0.0000	0.0000	0.0000	0.0000	0.0000	0.0000	0.0000	0.0000
Al^{VI}	0.0120	0.0804	0.0201	0.0171	0.0237	0.0118	0.0049	0.0122	0.0182	0.0330	0.0148	0.0167	0.0101	0.0257	0.0416	0.0517	0.0016	0.0159
Al ions	0.0120	0.0804	0.0201	0.0171	0.0237	0.0118	0.0049	0.0122	0.0182	0.0330	0.0148	0.0167	0.0101	0.0257	0.0416	0.0517	0.0016	0.0159
Fe^{+2}	0.2585	0.3604	0.2010	0.2313	0.1762	0.2082	0.3172	0.1542	0.1873	0.2322	0.2107	0.2666	0.2035	0.3022	0.1945	0.1347	0.2532	0.2670
Cr	0.0003	0.0000	0.0000	0.0010	0.0075	0.0008	0.0000	0.0019	0.0003	0.0025	0.0006	0.0021	0.0013	0.0009	0.0044	0.0003	0.0027	0.0064
Mn	0.0071	0.0027	0.0027	0.0039	0.0009	0.0042	0.0055	0.0013	0.0021	0.0032	0.0051	0.0051	0.0019	0.0049	0.0049	0.0048	0.0002	0.0196
Mg	0.7751	0.6161	0.7969	0.7929	0.8167	0.7941	0.6853	0.8648	0.8372	0.7456	0.7844	0.7344	0.8012	0.7182	0.8812	0.8779	0.7741	0.7918
Ca	0.8998	0.9510	0.9609	0.9475	0.9812	0.9764	0.9614	0.9725	0.9555	0.9499	0.9517	0.9461	0.9803	0.9692	0.9002	0.9663	0.9646	0.8946
Na	0.4233	0.0786	0.0974	0.1412	0.0421	0.0645	0.0643	0.0488	0.0730	0.1009	0.0764	0.1212	0.0691	0.0596	0.0564	0.0684	0.0325	0.1475
Total:	3.9362	3.9742	3.9768	3.9801	3.9910	3.9886	3.9806	3.9958	3.9895	3.9654	3.9730	3.9699	3.9900	3.9978	3.9934	3.9989	3.9944	3.9782
En	40.1	32.0	40.7	40.2	41.4	40.1	34.9	43.4	42.3	38.7	40.3	37.7	40.4	36.1	44.6	44.4	38.9	40.5
Fe	13.4	18.7	10.3	11.7	8.9	10.5	16.2	7.7	9.5	12.0	10.8	13.7	10.3	15.2	9.8	6.8	12.7	13.7
Wo	46.5	49.3	49.1	48.1	49.7	49.3	49.0	48.8	48.3	49.3	48.9	48.6	49.4	48.7	45.6	48.8	48.4	45.8
Mg#	75.0	63.1	79.9	77.5	82.3	79.2	68.4	84.9	81.7	76.3	78.8	73.4	79.7	70.4	81.9	86.7	75.4	74.8

Table T6. Representative microprobe analyses of mica from Hole 735B veins.

Core, section, interval (cm):	135R-3, 68–72	135R-3, 68–72	135R-3, 68–72	137R-1, 45–49	137R-4, 112–116	137R-4, 112–116	137R-4, 112–116	138R-4, 59–63	141R-1, 50–55	149R-4, 82–87	149R-4, 82–87	161R-2, 114–119	161R-2, 114–119	161R-2, 114–119	163R-6, 15–20	168R-2, 140–146
Number of analyses:	1	1	1	3	4	1	1	4	1	1	1	3	1	1	3	2
Major element oxide (wt%):																
SiO_2	37.51	37.32	37.37	37.10	37.44	36.30	35.37	37.72	37.38	38.44	37.77	36.45	37.30	36.73	37.15	37.39
TiO_2	3.95	4.29	4.25	4.66	4.60	2.83	4.24	4.15	3.67	0.28	3.82	4.19	1.27	3.18	3.84	3.69
Al_2O_3	12.08	12.21	11.95	12.27	12.19	13.07	11.88	11.88	12.39	13.18	12.29	12.41	12.67	12.22	12.48	12.28
FeO	21.16	21.12	20.02	20.48	19.94	25.59	24.47	20.04	17.89	18.96	20.07	21.68	20.77	21.23	18.50	18.23
MnO	0.09	0.21	0.08	0.08	0.13	0.15	0.14	0.20	0.12	0.05	0.10	0.09	0.07	0.10	0.12	0.21
MgO	11.95	11.38	12.32	11.82	12.03	8.57	8.14	12.56	14.51	15.18	12.27	10.94	13.09	10.88	13.50	14.26
CaO	0.01	0.09	0.05	0.00	0.07	0.01	1.10	0.04	0.07	0.00	0.00	0.03	0.10	0.09	0.02	0.01
Na_2O	0.23	0.22	0.27	0.39	0.27	0.22	0.24	0.37	0.27	0.38	0.26	0.45	0.38	0.47	0.36	0.40
K_2O	9.15	9.18	8.67	8.97	9.07	8.70	8.56	8.89	9.21	8.58	8.86	8.73	8.71	8.58	9.03	9.03
BaO	0.29	0.00	0.19	0.12	0.10	0.15	0.06	0.17	0.26	0.03	0.04	0.20	0.00	0.27	0.16	0.05
La_2O_3	0.12	0.00	0.14	0.09	0.06	0.05	0.14	0.07	0.25	0.00	0.00	0.09	0.00	0.04	0.22	0.09
Cl	0.15	0.15	0.06	0.02	0.05	0.08	0.09	0.08	0.03	0.34	0.06	0.20	0.38	0.33	0.23	0.22
Total:	96.54	96.03	95.30	95.98	95.90	95.64	94.35	96.09	96.01	95.08	95.48	95.26	94.35	93.79	95.41	95.63
Number of ions based on 22 (O, OH):																
Si	5.7313	5.7205	5.7363	5.6740	5.7117	5.7033	5.6520	5.7459	5.6642	5.8455	5.7690	5.6619	5.7974	5.7812	5.6803	5.6843
Ti	0.4536	0.4946	0.4904	0.5362	0.5281	0.3349	0.5095	0.4756	0.4178	0.0321	0.4384	0.4894	0.1486	0.3770	0.4416	0.4217
Al^{IV}	2.1751	2.2054	2.1612	2.2118	2.1924	2.2967	2.2374	2.1337	2.2117	2.1545	2.2128	2.2724	2.2026	2.2188	2.2489	2.2001
Al^{VI}	0.0000	0.0000	0.0000	0.0000	0.0000	0.1229	0.0000	0.0000	0.0000	0.2072	0.0000	0.0000	0.1175	0.0484	0.0000	0.0000
Fe^{+2}	2.7042	2.7072	2.5703	2.6184	2.5440	3.3613	3.2687	2.5530	2.2670	2.4102	2.5630	2.8158	2.6988	2.7941	2.3657	2.3177
Mn	0.1199	0.2742	0.1065	0.1105	0.1674	0.1996	0.1933	0.2647	0.1497	0.0623	0.1348	0.1251	0.0873	0.1400	0.1614	0.2701
Mg	2.7218	2.6005	2.8192	2.6940	2.7358	2.0078	1.9391	2.8516	3.2766	3.4407	2.7933	2.5345	3.0322	2.5527	3.0772	3.2307
Ca	0.0024	0.0154	0.0080	0.0006	0.0114	0.0012	0.1877	0.0065	0.0120	0.0000	0.0000	0.0050	0.0173	0.0149	0.0038	0.0010
Na	0.0689	0.0665	0.0804	0.1141	0.0813	0.0657	0.0753	0.1083	0.0804	0.1114	0.0777	0.1363	0.1135	0.1447	0.1079	0.1191
K	1.7830	1.7951	1.6976	1.7494	1.7652	1.7432	1.7453	1.7271	1.7799	1.6646	1.7266	1.7309	1.7276	1.7223	1.7614	1.7521
Ba	0.0353	0.0000	0.0228	0.0137	0.0115	0.0187	0.0081	0.0199	0.0305	0.0036	0.0043	0.0242	0.0000	0.0331	0.0195	0.0059
La	0.0066	0.0000	0.0077	0.0053	0.0035	0.0031	0.0083	0.0041	0.0139	0.0000	0.0000	0.0052	0.0000	0.0025	0.0125	0.0048
Cl	0.0388	0.0381	0.0146	0.0063	0.0133	0.0220	0.0239	0.0209	0.0081	0.0888	0.0150	0.0539	0.0992	0.0876	0.0608	0.0580
Total:	15.8021	15.8794	15.7003	15.7281	15.7524	15.8584	15.8247	15.8905	15.9036	15.9321	15.7197	15.8007	15.9429	15.8296	15.8802	16.0075
Mg#	50.2	49.0	52.3	50.7	51.8	37.4	37.2	52.8	59.1	58.8	52.1	47.4	52.9	47.7	56.5	58.2

Table T7. Representative microprobe analyses of chlorite from veins, Hole 735B. (Continued on next page.)

Core, section, interval (cm):	19R-1, 140–146	31R-3, 4–10	31R-3, 4–10	37R-2, 113–117	57R-4, 123–133	58R-3, 0–8	63R-1, 106–107	63R-1, 106–107	64R-2, 100–105	64R-4, 66–70	67R-2, 113–125	69R-5, 31–41	119R-5, 62–68	120R-2, 99–104	120R-2, 99–104	120R-4, 55–60	121R-1, 81–86
Number of analyses:	2	1	1	2	1	2	1	2	2	1	1	1	1	1	1	2	3
Color:	Green	Colorless	Colorless	Colorless	Colorless	Green	Lt Green	Lt Green	Green	Green	Green	Lt Green	Green	Green	Green	Green	Green
Major element oxide (wt%):																	
SiO_2	24.85	29.74	29.11	26.37	25.99	30.52	26.72	26.67	26.00	26.56	25.51	27.19	26.65	25.68	27.12	25.71	25.48
TiO_2	0.10	0.00	0.00	0.02	0.09	0.02	0.01	0.00	0.00	0.03	0.09	0.00	0.08	0.00	0.02	0.00	0.06
Al_2O_3	19.16	20.10	18.11	18.70	18.65	19.70	18.57	18.57	19.53	18.35	19.35	19.49	16.70	17.70	16.79	18.16	18.43
FeO	27.85	17.25	13.30	24.62	25.48	17.11	20.43	22.22	24.68	24.77	26.28	19.12	26.16	28.22	27.92	31.00	31.32
MnO	0.19	0.23	0.08	0.28	1.45	0.24	0.80	1.03	0.50	1.30	1.05	0.27	0.32	0.61	0.39	0.28	0.40
MgO	14.04	18.64	25.34	15.99	14.51	19.18	19.06	17.68	16.00	15.33	14.98	20.15	14.82	11.94	12.45	11.65	11.37
CaO	0.05	0.74	0.00	0.09	0.02	0.35	0.02	0.04	0.01	0.02	0.01	0.03	0.06	0.21	0.15	0.05	0.08
Na_2O	0.05	0.51	0.00	0.07	0.08	1.01	0.01	0.05	0.10	0.04	0.05	0.00	0.12	0.19	0.21	0.15	0.16
K_2O	0.01	0.00	0.00	0.02	0.01	0.00	0.03	0.00	0.02	0.01	0.00	0.00	0.00	0.01	0.01	0.01	0.00
Total:	86.30	87.21	85.94	86.16	86.29	88.14	85.66	86.25	86.81	86.41	87.32	86.25	84.93	84.57	85.06	87.00	87.30
Number of ions based on 36 (O, OH):																	
Si	5.4282	6.0035	5.8554	5.6517	5.6261	6.0884	5.6462	5.6546	5.5345	5.7061	5.4685	5.6343	5.8583	5.7538	5.9976	5.6575	5.6022
Ti	0.0157	0.0000	0.0000	0.0027	0.0139	0.0033	0.0018	0.0000	0.0000	0.0048	0.0145	0.0000	0.0136	0.0000	0.0035	0.0002	0.0091
Al^{IV}	2.5718	1.9965	2.1446	2.3483	2.3739	1.9116	2.3538	2.3454	2.4655	2.2939	2.5315	2.3657	2.1417	2.2462	2.0024	2.3425	2.3978
Al^{VI}	2.3601	2.7854	2.1487	2.3762	2.3846	2.7198	2.2719	2.2946	2.4343	2.3523	2.3572	2.3942	2.1854	2.4278	2.3786	2.3680	2.3786
Al ions	4.9319	4.7820	4.2933	4.7245	4.7585	4.6315	4.6257	4.6400	4.8998	4.6462	4.8887	4.7599	4.3271	4.6740	4.3810	4.7105	4.7764
Fe^{+2}	5.0859	2.9117	2.2370	4.4208	4.6123	2.8541	3.6096	3.9399	4.3928	4.4498	4.7107	3.3130	4.8085	5.2867	5.1658	5.7045	5.7580
Mn	0.0359	0.0393	0.0136	0.0510	0.2665	0.0398	0.1438	0.1851	0.0893	0.2365	0.1906	0.0474	0.0593	0.1148	0.0732	0.0514	0.0742
Mg	4.5698	5.6096	7.5989	5.0979	4.6828	5.7053	6.0039	5.5876	5.0777	4.9099	4.7873	6.2249	4.8574	3.9870	4.1063	3.8209	3.7269
Ca	0.0114	0.1600	0.0000	0.0212	0.0038	0.0753	0.0056	0.0087	0.0023	0.0046	0.0023	0.0067	0.0152	0.0515	0.0359	0.0107	0.0194
Na	0.0232	0.1996	0.0000	0.0279	0.0345	0.3905	0.0059	0.0194	0.0393	0.0167	0.0208	0.0000	0.0507	0.0835	0.0908	0.0630	0.0691
Total:	20.1021	19.7057	19.9982	19.9976	19.9984	19.7881	20.0425	20.0354	20.0356	19.9747	20.0834	19.9861	19.9902	19.9513	19.8542	20.0189	20.0354
Mg#	47.3	65.8	77.3	53.5	50.4	66.7	62.5	58.6	53.6	52.5	50.4	65.3	50.3	43.0	44.3	40.1	39.3

Table T7 (continued).

Core, section, interval (cm):	121R-8, 1–8	121R-8, 1–8	140R-6, 40–44	141R-1, 50–55	144R-6, 35–47	168R-2, 140–146	168R-2, 140–146
Number of analyses:	1	1	2	2	1	1	1
Color:	Green	Green	Green	Green	Green	Green	Green
Major element oxide (wt%):							
SiO_2	29.13	26.52	27.43	28.08	25.33	26.61	27.20
TiO_2	0.09	0.09	0.00	0.05	0.03	0.03	0.00
Al_2O_3	17.93	18.22	18.54	17.34	18.03	18.88	17.73
FeO	18.90	28.70	19.83	25.63	33.36	25.12	23.79
MnO	0.18	0.41	0.22	0.28	0.42	0.48	0.28
MgO	21.39	13.65	20.47	16.79	9.98	15.44	16.71
CaO	0.03	0.02	0.07	0.23	0.03	0.00	0.02
Na_2O	0.02	0.01	0.08	0.06	0.14	0.17	0.15
K_2O	0.00	0.00	0.00	0.01	0.00	0.01	0.00
Total:	87.67	87.63	86.63	88.45	87.31	86.74	85.89
Number of ions based on 36 (O, OH):							
Si	5.9104	5.7072	5.6862	5.8733	5.6350	5.6767	5.8157
Ti	0.0134	0.0152	0.0000	0.0074	0.0043	0.0042	0.0000
Al^{IV}	2.0896	2.2928	2.3138	2.1267	2.3650	2.3233	2.1843
Al^{VI}	2.1991	2.3277	2.2154	2.1470	2.3615	2.4250	2.2824
Al ions	4.2887	4.6205	4.5292	4.2737	4.7265	4.7482	4.4667
Fe^{+2}	3.2077	5.1629	3.4390	4.4821	6.2062	4.4818	4.2536
Mn	0.0302	0.0748	0.0391	0.0491	0.0794	0.0864	0.0508
Mg	6.4703	4.3802	6.3255	5.2338	3.3084	4.9122	5.3277
Ca	0.0068	0.0052	0.0149	0.0519	0.0069	0.0000	0.0057
Na	0.0096	0.0035	0.0314	0.0230	0.0622	0.0713	0.0621
Total:	19.9371	19.9695	20.0652	19.9942	20.0289	19.9809	19.9823
Mg#	66.9	45.9	64.8	53.9	34.8	52.3	55.6

Table T8. Representative microprobe analyses of quartz from veins, Hole 735B.

Core, section, interval (cm):	54R-4, 69–78	90R-4, 55–58	99R-4, 68–74	118R-1, 76–82	124R-1, 111–116	130R-3, 52–59	135R-3, 68–72	137R-1, 45–49	138R-4, 59–63	142R-1, 76–80	149R-4, 82–87	156R-6, 42–46	159R-4, 120–125	159R-7, 66–72	161R-2, 114–119	163R-6, 15–20	168R-6, 140–146
Number of analyses:	1	3	5	5	3	3	2	2	2	2	3	2	1	1	2	2	2
Major element oxide (wt%):																	
SiO_2	100.22	100.19	99.38	100.37	100.40	100.44	100.29	99.76	100.39	100.17	99.61	99.84	100.40	99.70	99.33	99.67	99.06
TiO_2	0.04	0.06	0.02	0.05	0.06	0.00	0.02	0.02	0.01	0.02	0.05	0.08	0.00	0.07	0.03	0.05	0.11
Al_2O_3	0.07	0.01	0.00	0.00	0.00	0.00	0.00	0.01	0.00	0.00	0.03	0.00	0.00	0.00	0.00	0.00	0.00
FeO	0.05	0.00	0.05	0.05	0.05	0.01	0.05	0.07	0.07	0.08	0.03	0.06	0.00	0.02	0.00	0.01	0.03
CaO	0.03	0.00	0.01	0.00	0.00	0.00	0.00	0.00	0.01	0.02	0.00	0.00	0.00	0.00	0.00	0.00	0.00
Total:	100.41	100.25	99.47	100.47	100.50	100.45	100.36	99.86	100.49	100.29	99.72	99.97	100.40	99.79	99.36	99.73	99.20

Table T9. Representative microprobe analyses of epidote from veins, Hole 735B.

Core, section, interval (cm):	37R-2, 113–117	42R-3, 27–31	43R-4, 129–133	44R-1, 35–47	44R-1, 35–47	47R-2 92–100	57R-3, 124–130	57R-4, 123–133	60R-4, 112–120	63R-1, 106–107	63R-6, 98–106	64R-2, 100–105	67R-2, 113–125	68R-2, 68–75	120R-1, 85–91	122R-4, 0–5	138R-4, 59–63
Number of analyses:	2	1	1	2	1	3	1	1	1	3	1	2	2	2	1	1	1
Major element oxide (wt%):																	
SiO_2	38.37	38.41	38.43	38.25	38.77	38.10	37.93	38.23	37.79	38.38	38.58	38.74	38.20	38.75	38.71	38.11	38.29
TiO_2	0.07	0.09	0.06	0.04	0.10	0.07	0.04	0.01	0.06	0.07	0.06	0.10	0.11	0.04	0.07	0.37	0.14
Al_2O_3	27.58	29.42	28.06	27.27	29.68	28.30	29.88	27.37	29.10	29.11	30.59	30.73	29.07	29.59	26.47	24.55	25.41
Fe_2O_3	6.70	4.95	6.52	7.44	4.10	6.00	4.72	7.63	5.71	5.28	3.62	3.14	6.35	5.06	8.26	9.07	8.86
MnO	0.04	0.23	0.02	0.08	0.17	0.06	0.28	0.05	0.08	0.16	0.11	0.16	0.17	0.18	0.07	0.00	0.18
MgO	0.00	0.00	0.00	0.01	0.06	0.00	0.00	0.00	0.00	0.01	0.00	0.05	0.00	0.00	0.07	0.13	0.01
CaO	23.85	23.34	23.33	23.37	23.64	23.44	23.02	23.05	23.68	23.34	24.27	24.28	23.44	23.03	24.07	23.87	24.16
Total:	98.53	98.36	98.35	98.37	98.46	97.88	97.77	98.24	98.34	98.28	97.23	97.19	97.34	96.63	97.72	96.09	97.05
Number of ions based on 12.5 O:																	
Si	3.0212	3.0055	3.0227	3.0205	3.0225	3.0095	2.9826	3.0201	2.9711	3.0089	2.9860	2.9944	2.9775	3.0202	3.0322	3.0502	3.0339
Ti	0.0040	0.0052	0.0038	0.0026	0.0058	0.0039	0.0026	0.0008	0.0038	0.0040	0.0035	0.0058	0.0062	0.0021	0.0044	0.0224	0.0081
Al^{IV}	0.0000	0.0000	0.0000	0.0000	0.0000	0.0060	0.0174	0.0000	0.0289	0.0002	0.0140	0.0056	0.0225	0.0000	0.0000	0.0000	0.0000
Al^{VI}	2.5594	2.7130	2.6010	2.5382	2.7268	2.6285	2.7515	2.5489	2.6671	2.6893	2.7763	2.7933	2.6479	2.7176	2.4427	2.3156	2.3727
Al ions	2.5594	2.7130	2.6010	2.5382	2.7268	2.6345	2.7689	2.5489	2.6960	2.6895	2.7903	2.7989	2.6705	2.7176	2.4427	2.3156	2.3727
Fe^{+3}	0.3972	0.2915	0.3858	0.4423	0.2402	0.3564	0.2791	0.4537	0.3376	0.3114	0.2108	0.1829	0.3725	0.2965	0.4876	0.5463	0.5282
Mn	0.0026	0.0155	0.0016	0.0056	0.0115	0.0040	0.0186	0.0032	0.0051	0.0108	0.0072	0.0105	0.0112	0.0116	0.0043	0.0000	0.0123
Mg	0.0000	0.0000	0.0000	0.0008	0.0071	0.0000	0.0000	0.0000	0.0000	0.0016	0.0000	0.0058	0.0000	0.0000	0.0078	0.0154	0.0016
Ca	2.0122	1.9565	1.9655	1.9769	1.9746	1.9832	1.9392	1.9513	1.9948	1.9607	2.0124	2.0108	1.9573	1.9230	2.0195	2.0467	2.0509
Total:	7.9967	7.9873	7.9804	7.9869	7.9884	7.9914	7.9910	7.9780	8.0085	7.9869	8.0102	8.0091	7.9951	7.9709	7.9985	7.9967	8.0077

Table T10. Representative microprobe analyses of prehnite from veins, Hole 735B.

Core, section, interval (cm):	168R-7, 131–135	188R-5, 13–18	202R-3, 7–12	202R-3, 7–12	202R-3, 7–12	203R-2, 11–16	205R-1, 123–128	205R-4, 40–45	206R-4, 139–144	206R-4, 139–144	207R-4, 102–107
Number of analyses:	5	2	2	2	2	1	2	3	2	1	2
Major element oxide (wt%):											
SiO_2	43.45512	43.03785	43.29455	43.04625	43.273	43.0891	43.19925	43.22076667	42.9374	43.0476	43.21255
Al_2O_3	23.41566	23.22165	24.0392	24.15385	23.84585	22.3996	23.4575	23.83323333	23.47915	22.5933	23.3665
FeO	0.23066	0.8783	0.29475	0.34375	0.52295	2.4047	0.7681	0.181466667	1.1147	1.8023	0.22015
MnO	0.02678	0.01495	0.05355	0.05755	0.02845	0.0003	0.0996	0.040966667	0.0403	0	0.02105
MgO	0.6048	0.04315	0	0.1088	0.02295	0.0632	0.3468	0.0566	0.18835	0.0765	0.30365
CaO	26.46558	27.78155	27.6795	27.82065	27.46635	27.1898	27.35615	26.99063333	27.4752	27.5195	26.03595
Na_2O	0.05392	0.1023	0.1026	0.02625	0.032	0.0964	0.01035	0.169533333	0.04275	0.1939	0.095
Total:	94.1986	95.07975	95.46415	95.5571	95.19155	95.2431	95.23775	94.4932	95.27785	95.2331	93.15985
Number of ions based on 24 (O, OH):											
Si	6.056959304	5.994232857	5.986118396	5.94880341	5.996045443	6.010669101	5.990707292	6.02547836	5.963950123	6.00669747	6.080739975
Al^{IV}	1.943040696	2.005767143	2.013881604	2.05119659	2.003954557	1.989330899	2.009292708	1.97452164	2.036049877	1.99330253	1.919260025
Al^{VI}	1.903314776	1.806022962	1.903307804	1.882784699	1.890046681	1.69320905	1.824787041	1.941136146	1.807521939	1.722206248	1.955863414
Al ions	3.846355472	3.811790105	3.917189408	3.933981289	3.894001238	3.682539949	3.834079749	3.915657786	3.843571817	3.715508777	3.875123439
Fe^{+3}	0.024183231	0.092050007	0.03070182	0.03574735	0.054576279	0.252417937	0.080037155	0.019019176	0.116495941	0.189242123	0.023282569
Ca	3.951867978	4.14534846	4.099945107	4.118944516	4.077261099	4.063341548	4.06443569	4.030761252	4.088616104	4.113857779	3.925197485
Total:	13.87936599	14.04342143	14.03395473	14.03747657	14.02188406	14.00896854	13.96925989	13.99091657	14.01263398	14.02530615	13.90434347

Table T11. Representative microprobe analyses of ilmenite from veins, Hole 735B.

Core, section, interval (cm):	37R-2, 113–117	66R-3, 128–132	70R-2, 14–16	90R-4, 55–58	118R-1, 76–82	120R-4, 55–60	121R-3, 48–52	124R-1, 111–116	130R-3, 52–59	133R-7, 95–100	137R-4, 112–116	139R-2, 0–5	149R-4, 82–87	159R-7, 66–72	161R-2, 114–119	163R-6, 15–20	168R-2, 140–146
Number of analyses:	3	1	1	3	1	2	2	1	1	1	1	2	1	1	1	2	1
Major element oxide (wt%):																	
SiO_2	0.03	0.67	0.01	0.22	0.29	0.20	0.22	0.12	0.17	0.27	0.11	0.14	0.14	0.12	0.18	0.29	0.17
TiO_2	49.72	50.50	49.92	50.94	48.96	48.91	48.61	47.88	47.87	47.68	47.91	47.73	45.99	47.97	47.94	49.54	48.98
Fe_2O_3	6.77	ND	ND	ND	ND	ND	ND	ND	ND	ND	ND	ND	ND	ND	ND	ND	ND
FeO	41.42	45.89	45.20	45.95	48.64	48.86	48.44	50.19	49.90	50.02	49.28	50.13	51.70	49.97	49.75	47.48	47.59
MnO	0.84	1.36	2.45	1.67	1.05	0.71	0.99	0.83	1.06	0.97	1.91	1.09	1.16	0.91	1.15	1.98	2.15
MgO	0.54	0.88	0.76	0.28	0.18	0.53	0.63	0.12	0.06	0.08	0.05	0.06	0.13	0.04	0.14	0.07	0.25
Total:	99.32	99.30	98.34	99.06	99.13	99.22	98.87	99.14	99.06	99.01	99.25	99.15	99.11	99.02	99.16	99.35	99.14
Number of ions based on 6 O:																	
Si	0.0018	0.0340	0.0005	0.0111	0.0152	0.0105	0.0113	0.0062	0.0091	0.0143	0.0056	0.0071	0.0072	0.0065	0.0093	0.0148	0.0089
Ti	1.9910	1.9290	1.9401	1.9596	1.9036	1.8990	1.8938	1.8770	1.8775	1.8705	1.8771	1.8728	1.8228	1.8820	1.8772	1.9177	1.9053
Fe^{+3}	0.0435	ND	ND	ND	ND	ND	ND	ND	ND	ND	ND	ND	ND	ND	ND	ND	ND
Fe^{+2}	1.8439	1.9488	1.9530	1.9649	2.1025	2.1089	2.0981	2.1875	2.1758	2.1815	2.1465	2.1872	2.2785	2.1796	2.1659	2.0435	2.0582
Mn	0.0377	0.0585	0.1072	0.0725	0.0460	0.0312	0.0432	0.0365	0.0467	0.0426	0.0841	0.0480	0.0517	0.0403	0.0506	0.0865	0.0941
Mg	0.0425	0.0666	0.0585	0.0213	0.0139	0.0410	0.0483	0.0096	0.0044	0.0063	0.0041	0.0049	0.0099	0.0030	0.0105	0.0051	0.0193
Total:	3.9603	4.0370	4.0594	4.0294	4.0812	4.0905	4.0948	4.1168	4.1134	4.1152	4.1173	4.1200	4.1700	4.1115	4.1135	4.0675	4.0858

Note: ND = not determined.

Table T12. Representative microprobe analyses of zeolites from veins, Hole 735B.

Core, section, interval (cm):	37R-2, 113–117	57R-4, 123–133	84R-6, 31–41	122R-3, 135–139	123R-6, 140–144	161R-3, 128–135	168R-7, 131–135	178R-4, 74–77	203R-2, 11–16	57R-4, 123–133	64R-2, 100–105	71R-2, 115–125	120R-1, 85–91	121R-3, 48–52	207R-4, 102–107
Number of analyses:	1	2	1	2	2	3	1	4	5	2	2	1	2	2	2
Mineral:	Nat	Nat	Nat	Nat	Nat	Nat	Nat	Nat	Nat	Thom	Thom	Thom	Thom	Thom	Thom
Major element oxide (wt%):															
SiO_2	50.33	45.52	46.49	49.21	53.29	50.14	50.37	50.56	51.19	39.21	39.83	38.43	41.87	42.39	38.42
Al_2O_3	22.52	26.57	26.49	29.07	28.73	27.98	28.27	28.45	28.67	29.39	28.94	29.54	28.24	27.93	29.38
CaO	0.01	1.05	0.52	2.41	0.62	0.76	0.24	0.69	0.57	11.65	11.58	11.90	10.99	10.86	12.53
Na_2O	13.58	14.08	15.35	5.19	6.56	8.60	9.50	8.57	8.19	4.65	4.95	4.23	2.32	2.43	2.81
K_2O	0.03	0.08	0.02	0.03	0.04	0.01	0.04	0.01	0.00	0.04	0.04	0.00	0.00	0.02	0.02
F	0.07	0.00	0.00	0.00	0.00	0.00	0.00	0.00	0.00	0.03	0.00	0.00	0.00	0.00	0.00
Cl	0.00	0.02	0.00	0.01	0.02	0.00	0.03	0.00	0.00	0.04	0.00	0.00	0.01	0.00	0.01
Total:	86.53	87.41	88.87	85.88	89.20	87.48	88.39	88.28	88.62	85.23	85.33	84.10	83.42	83.63	83.14
Number of ions based on 40 O:															
Si	26.1981	23.8237	23.9551	25.0055	25.9286	25.2446	25.1504	25.2055	25.3399	21.2799	21.5221	21.0678	22.6814	22.8879	21.2075
Al^{IV}	13.8019	16.1763	16.0449	14.9945	14.0714	14.7554	14.8496	14.7945	14.6601	18.7201	18.4333	18.9322	17.3186	17.1121	18.7925
Al^{VI}	0.0148	0.2190	0.0420	2.4126	2.4017	1.8458	1.7894	1.9244	2.0652	0.0807	0.0000	0.1537	0.7090	0.6638	0.3197
Ca	0.0028	0.5909	0.2871	1.3120	0.3250	0.4123	0.1310	0.3699	0.3032	6.7740	6.7022	6.9891	6.3785	6.2807	7.4090
Na	13.7072	14.2847	15.3340	5.1155	6.1906	8.3919	9.1964	8.2763	7.8594	4.8927	5.1857	4.4957	2.4372	2.5472	3.0042
K	0.0198	0.0553	0.0131	0.0197	0.0280	0.0040	0.0255	0.0078	0.0012	0.0278	0.0242	0.0000	0.0000	0.0149	0.0140
Ba	0.0135	0.0000	0.0000	0.0000	0.0000	0.0000	0.0000	0.0000	0.0000	0.0061	0.0000	0.0000	0.0000	0.0000	0.0000
Total:	53.7581	55.1499	55.6762	48.8599	48.9454	50.6540	51.1423	50.5784	50.2290	51.7813	51.8675	51.6385	49.5247	49.5066	50.7469

Note: Nat = natrolite; Thom = thomsonite.

Table T13. Representative microprobe analyses of apatite and zircon from veins, Hole 735B.

Core, section, interval (cm):	135R-3, 68–72	138R-4, 59–63	139R-2, 0–5	159R-7, 66–72	163R-6, 15–20	163R-6, 15–20	168R-2, 140–146	90R-4, 55–58	119R-5, 62–68	124R-1, 111–116	133R-7, 95–100	138R-4, 59–63	161R-2, 114–119	168R-2, 140–146
Number of analyses:	1	1	3	4	1	1	1	1	1	1	1	1	1	1
Mineral:	Apatite	Apatite	Apatite	Apatite	Apatite	Apatite	Apatite	Zircon	Zircon	Zircon	Zircon	Zircon	Zircon	Zircon
Major element oxide (wt%):														
SiO_2	0.24	0.29	0.08	0.25	0.34	3.34	0.05	31.72	31.28	31.75	31.25	31.10	31.67	31.59
TiO_2	0.00	0.07	0.00	0.02	0.00	0.00	0.00	0.00	0.00	0.00	0.00	0.00	0.00	0.00
Al_2O_3	0.07	0.09	0.07	0.09	0.07	0.07	0.17	0.00	0.00	0.00	0.00	0.00	0.00	0.00
FeO	0.18	0.15	0.07	0.12	0.24	0.06	0.00	0.00	0.00	0.00	0.00	0.00	0.00	0.00
MnO	0.00	0.00	0.00	0.00	0.00	0.00	0.00	0.00	0.00	0.00	0.00	0.00	0.00	0.00
MgO	0.03	0.01	0.03	0.10	0.09	0.05	0.00	0.00	0.00	0.00	0.00	0.00	0.00	0.00
CaO	55.01	55.91	55.58	55.87	54.10	52.46	55.14	0.00	0.00	0.00	0.00	0.00	0.00	0.00
Na_2O	0.23	0.00	0.23	0.22	0.42	0.29	0.06	0.10	0.05	0.09	0.00	0.01	0.08	0.03
K_2O	0.01	0.00	0.01	0.02	0.01	0.01	0.01	0.00	0.00	0.00	0.00	0.00	0.00	0.00
P_2O_5	44.09	44.41	44.58	44.14	43.71	41.02	43.31	0.40	0.30	0.15	0.72	2.14	0.16	0.09
Cl	0.20	0.04	0.30	0.19	0.43	2.08	1.50	ND	ND	ND	ND	ND	ND	ND
ZrO_2	ND	ND	ND	ND	ND	ND	ND	67.41	68.04	68.01	67.53	66.16	68.22	68.90
Total:	100.07	100.97	100.93	101.02	99.41	99.39	100.24	99.86	100.03	100.00	99.52	99.49	100.19	100.68
Number of ions based on 16 O:														
Si								3.8977	3.8577	3.9013	3.8497	3.7901	3.8884	3.8697
Na								0.0238	0.0128	0.0225	0.0011	0.0018	0.0187	0.0070
P								0.0416	0.0310	0.0153	0.0751	0.2209	0.0171	0.0091
Ba								0.0111	0.0174	0.0000	0.0008	0.0041	0.0031	0.0031
Zr								4.0388	4.0916	4.0739	4.0557	3.9312	4.0840	4.1156

Table T14. Representative microprobe analyses of titanite from veins, Hole 735B.

Core, section, interval (cm):	28R-4, 141–144	37R-2, 113–117	42R-3, 27–31	44R-1, 35–47	58R-2, 0–10	63R-6, 98–106	66R-2, 25–31	70R-1, 39–49	87R-6, 31–41	92R-2, 49–53	120R-4, 55–60	122R-4, 0–5	123R-3, 87–94	126R-5, 102–106	139R-2, 0–5	142R-1, 76–80	159R-7, 66–72	192R-6, 44–50
Number of analyses:	1	2	1	1	1	1	1	1	1	3	9	1	2	2	1	2	1	4
Major element oxide (wt%):																		
SiO_2	30.01	30.13	30.51	30.74	30.93	30.82	30.63	30.78	30.73	30.52	30.78	30.59	30.56	30.42	30.66	30.65	30.88	30.58
TiO_2	36.17	37.29	38.22	37.16	37.49	37.63	38.66	37.41	37.64	38.19	37.75	37.62	37.77	37.77	37.59	38.26	38.85	38.45
Al_2O_3	1.97	1.01	0.40	1.26	0.70	0.57	0.29	0.37	0.39	0.69	0.40	0.52	0.26	0.43	0.56	0.63	0.95	0.47
FeO	0.71	0.88	0.96	0.46	2.01	0.69	0.95	1.36	1.30	0.56	0.74	1.78	1.42	1.19	0.74	0.34	0.75	0.69
MnO	0.04	0.02	0.00	0.00	0.00	0.00	0.00	0.00	0.00	0.00	0.04	0.00	0.00	0.00	0.00	0.00	0.00	0.03
MgO	0.00	0.00	0.00	0.00	0.00	0.00	0.00	0.00	0.00	0.07	0.03	0.00	0.01	0.03	0.01	0.03	0.00	0.03
CaO	28.34	28.33	28.17	28.61	28.15	28.86	28.78	28.20	27.85	28.34	28.67	28.28	28.21	28.41	28.94	30.00	29.00	29.13
Na_2O	0.03	0.04	0.08	0.05	0.11	0.04	0.05	0.09	0.02	0.06	0.07	0.02	0.15	0.03	0.07	0.00	0.00	0.01
La_2O_3	ND	0.00	ND	ND	ND	ND	ND	ND	ND	0.00	0.20	0.32	0.00	0.11	0.00	0.36	0.04	0.03
F	0.08	0.03	0.00	0.00	0.02	0.00	0.00	0.70	0.29	0.00	0.00	0.00	0.00	0.00	0.00	0.00	0.00	0.00
Total:	97.35	97.73	98.34	98.27	99.42	98.61	99.36	98.91	98.22	98.43	98.69	99.14	98.38	98.40	98.57	100.30	100.47	99.41
Number of ions based on 4 Si:																		
Si	4.0000	4.0000	4.0000	4.0000	4.0000	4.0000	4.0000	4.0000	4.0000	4.0000	4.0000	4.0000	4.0000	4.0000	4.0000	4.0000	4.0000	4.0000
Ti	3.6261	3.7228	3.7684	3.6372	3.6463	3.6737	3.7972	3.6565	3.6850	3.7649	3.6893	3.6999	3.7188	3.7360	3.6893	3.7558	3.7845	3.7827
Al	0.1547	0.0789	0.0311	0.0962	0.0530	0.0436	0.0223	0.0283	0.0299	0.0531	0.0308	0.0404	0.0197	0.0338	0.0433	0.0488	0.0724	0.0361
Fe^{+2}	0.0791	0.0979	0.1047	0.0496	0.2176	0.0749	0.1037	0.1478	0.1415	0.0618	0.0806	0.1942	0.1549	0.1311	0.0807	0.0369	0.0814	0.0755
Mn	0.0045	0.0018	0.0000	0.0000	0.0000	0.0000	0.0000	0.0000	0.0000	0.0001	0.0046	0.0000	0.0000	0.0000	0.0000	0.0005	0.0000	0.0031
Mg	0.0000	0.0000	0.0000	0.0000	0.0000	0.0000	0.0000	0.0000	0.0000	0.0135	0.0066	0.0000	0.0011	0.0054	0.0013	0.0062	0.0000	0.0055
Ca	4.0468	4.0295	3.9555	3.9879	3.8994	4.0133	4.0265	3.9261	3.8837	3.9801	3.9914	3.9610	3.9568	4.0032	4.0453	4.1939	4.0246	4.0814
Na	0.0039	0.0051	0.0096	0.0064	0.0143	0.0050	0.0063	0.0113	0.0025	0.0075	0.0088	0.0032	0.0194	0.0043	0.0084	0.0006	0.0000	0.0017
La	ND	0.0000	ND	ND	ND	ND	ND	ND	ND	0.0000	0.0048	0.0077	0.0000	0.0028	0.0000	0.0088	0.0009	0.0006
F	0.0337	0.0134	0.0000	0.0000	0.0096	0.0000	0.0000	0.2877	0.1194	0.0000	0.0000	0.0000	0.0000	0.0000	0.0000	0.0000	0.0000	0.0000
Total:	11.9489	11.9493	11.8693	11.7775	11.8402	11.8105	11.9561	12.0578	11.8620	11.8810	11.8120	11.8986	11.8706	11.9138	11.8682	12.0428	11.9629	11.9859

Note: ND = not determined.

Table T15. Representative microprobe analyses of clay minerals from veins, Hole 735B.

Core, section, interval (cm):	37R-2, 113–117	44R-1, 35–47	57R-4, 123–133	68R-2, 68–75	120R-1, 85–91	133R-7, 92–98	133R-7, 92–98	161R-3, 128–135	168R-5, 72–78	172R-7, 124–128	172R-7, 124–128	181R-1, 131–136	200R-6, 31–37	202R-2, 123–128	203R-2, 11–16	210R-5, 116–120
Number of analyses:	1	1	2	2	1	2	1	1	1	1	1	4	1	2	1	2
Color:	Green	Brown	Brown	Brown	Brown	Brown	Brown	Green	Brown	Brown	Brown	Brown	Green	Brown	Brown	Brown
Major element oxide (wt%):																
SiO_2	50.60	41.92	37.20	48.85	37.41	43.13	41.88	25.62	40.15	35.61	51.67	44.59	34.99	33.04	49.23	49.17
TiO_2	0.08	0.01	0.00	0.06	0.02	0.04	0.00	0.05	0.00	0.04	0.08	0.01	0.00	0.00	0.00	0.01
Al_2O_3	4.24	10.05	14.58	8.12	12.44	10.28	8.54	18.09	7.98	13.81	1.58	5.81	13.33	13.43	28.29	28.41
FeO	15.57	5.90	8.15	5.46	16.27	10.87	9.95	26.75	4.69	13.03	8.08	7.15	12.67	12.03	0.00	0.01
MnO	0.05	0.44	0.18	0.11	0.30	0.21	0.19	0.20	0.18	0.29	0.30	0.20	0.17	0.18	0.00	0.00
MgO	13.95	21.06	23.69	13.78	19.92	16.85	21.69	14.29	24.88	23.00	26.55	21.41	25.11	24.98	0.14	0.02
CaO	3.35	2.44	0.44	8.91	0.62	4.77	1.06	0.12	1.79	1.16	0.94	4.10	0.88	0.40	1.56	1.08
Na_2O	0.96	0.16	0.50	3.35	0.34	1.84	1.07	0.16	0.54	0.32	0.21	0.90	0.66	0.22	7.64	8.82
K_2O	0.00	0.30	0.46	0.02	0.05	0.03	0.04	0.00	0.03	0.02	0.04	0.02	0.00	0.01	0.00	0.03
Cl	0.00	0.03	0.03	0.11	0.03	0.07	0.02	0.03	0.00	0.00	0.51	0.01	0.05	0.00	0.03	0.00
Total:	89.00	82.37	85.22	88.77	87.40	88.09	84.45	85.31	80.25	87.26	89.97	84.21	87.86	84.29	86.89	87.55
Number of ions based on 22 O:																
Si	7.5622	6.5250	5.6932	7.1485	5.8169	6.4827	6.4923	4.4216	6.3987	5.4912	7.3358	6.8621	5.3685	5.2753	6.8631	6.8318
Ti	0.0094	0.0008	0.0000	0.0066	0.0022	0.0044	0.0000	0.0062	0.0005	0.0040	0.0082	0.0008	0.0000	0.0000	0.0000	0.0008
Al^{IV}	0.4378	1.4750	2.3068	0.8515	2.1831	1.5173	1.5077	3.5784	1.4995	2.5007	0.2646	1.1379	2.4104	2.5212	1.1369	1.1682
Al^{VI}	0.3091	0.3687	0.3235	0.5490	0.0970	0.3230	0.0528	0.1023	0.0000	0.0089	0.0000	0.2829	0.0000	0.0000	3.5116	3.4837
Al ions	0.7468	1.8437	2.6303	1.4004	2.2802	1.8403	1.5605	3.6807	1.4995	2.5096	0.2646	1.0521	2.4104	2.5211	4.6485	4.6518
Fe^{+2}	1.9456	0.7677	1.0425	0.6681	2.1159	1.3920	1.2903	3.8606	0.6244	1.6803	0.9597	0.9197	1.6257	1.6097	0.0000	0.0010
Mn	0.0063	0.0576	0.0231	0.0136	0.0399	0.0268	0.0254	0.0297	0.0245	0.0379	0.0360	0.0262	0.0221	0.0234	0.0000	0.0000
Mg	3.1086	4.8881	5.4046	3.0063	4.6180	3.8121	5.0131	3.6760	5.9109	5.2868	5.6199	4.9115	5.7440	5.9285	0.0295	0.0051
Ca	0.5361	0.4075	0.0719	1.3969	0.1035	0.7502	0.1760	0.0225	0.3062	0.1907	0.1434	0.6986	0.1451	0.0703	0.2327	0.1613
Na	0.2778	0.0480	0.1473	0.9504	0.1017	0.5261	0.3212	0.0548	0.1673	0.0954	0.0573	0.2694	0.1956	0.0705	2.0662	2.3745
K	0.0000	0.0587	0.0906	0.0037	0.0097	0.0067	0.0088	0.0000	0.0057	0.0037	0.0078	0.0049	0.0000	0.0013	0.0000	0.0055
Cl	0.0012	0.0088	0.0074	0.0273	0.0088	0.0181	0.0050	0.0074	0.0000	0.0000	0.1236	0.0031	0.0129	0.0000	0.0061	0.0000
Total:	14.1939	14.6059	15.1108	14.6218	15.0967	14.8593	14.8926	15.7595	14.9377	15.2996	14.5562	15.1169	15.5243	15.5002	13.8461	14.0319

Table T16. Representative microprobe analyses of carbonates from veins, Hole 735B.

Core, section, interval (cm):	18R-1, 139–147	18R-1, 139–147	18R-1, 139–147	18R-1, 139–147	18R-1, 139–147	37R-2, 113–117	63R-6, 98–106	64R-2, 100–105	67R-1, 88–93	67R-1, 88–93	67R-2, 113–125	70R-2, 14–16	72R-3, 10–19	81R-2, 91–95	91R-5, 81–86	92R-2, 49–53	92R-2, 49–53
Number of analyses:	1	1	1	1	1	1	2	1	1	2	1	1	1	1	3	1	1
Major element oxide (wt%):																	
SiO_2	0.00	ND	ND	ND	ND	0.16	ND	ND	ND	0.00	ND	ND	ND	ND	0.13	0.16	0.20
FeO	0.01	0.02	0.03	0.20	0.10	0.30	0.05	0.03	0.06	0.06	0.06	0.08	0.02	0.24	0.05	0.00	0.00
MnO	0.03	0.04	0.05	0.20	0.06	0.07	0.01	0.02	0.00	0.00	0.01	0.05	0.00	0.17	0.00	0.00	0.05
MgO	2.90	2.11	4.42	3.53	0.82	0.00	5.67	2.40	2.03	4.99	0.00	0.00	4.63	0.00	2.48	2.05	0.08
CaO	97.29	98.18	95.96	96.46	98.20	99.51	94.41	97.41	97.07	94.68	99.32	99.02	95.21	99.66	96.31	96.83	99.20
Na_2O	0.00	ND	ND	ND	ND	0.08	ND	ND	ND	0.00	ND	ND	ND	ND	0.05	0.09	0.28
P_2O_5	0.00	ND	ND	ND	ND	ND	ND	ND	ND	0.00	ND	ND	ND	ND	0.23	0.36	0.03
SrO	0.00	ND	ND	ND	ND	ND	ND	ND	ND	0.00	ND	ND	ND	ND	0.18	0.11	0.18
Total:	100.23	100.35	100.46	100.39	99.18	100.12	100.13	99.86	99.16	99.73	99.39	99.15	99.86	100.07	99.42	99.61	100.01

Note: ND = not determined.

Table T17. Major and trace element compositions of veins, Hole 735B. (See table note. Continued on next page.)

Core, section, interval (cm):	120R-2, 99–104	121R-1, 83–87	123R-6, 140–146	123R-8, 27–32	90R-3, 38–44	90R-4, 55–58	90R-4, 84–86	124R-1, 111–115	135R-3, 68–72	130R-3, 52–58	138R-4, 59–63	126R-5, 102–106	150R-7, 93–100	153R-1, 35–39	157R-7, 1–5	161R-7, 78–84	202R-7, 96–101
Vein type:	Plag + Diop	Plag + Diop	Plag + Diop	Plag + Amph	Felsic	Felsic	Felsic	Felsic	Felsic	Felsic	Felsic	Felsic	Felsic	Felsic	Felsic	Felsic	Felsic
Major element oxides (wt%):																	
SiO_2	53.36	62.91	59.16	64.91	74.17	70.56	60.49	72.75	64.05	69.43	70.12	61.54	66.18	59.70	66.11	62.69	61.22
TiO_2	0.06	0.27	0.26	0.31	0.12	0.15	0.19	0.23	0.15	0.27	0.10	0.17	0.47	0.25	0.31	0.08	0.14
Al_2O_3	8.49	17.44	13.27	18.82	12.86	14.31	18.60	14.79	20.36	16.18	17.32	22.10	17.31	19.72	17.12	20.69	18.57
Fe_2O_3	8.96	2.18	4.67	0.44	0.59	1.61	2.62	0.74	0.97	1.90	0.60	0.67	1.48	3.47	1.92	0.56	2.60
MnO	0.14	0.03	0.06	0.00	0.02	0.04	0.05	0.01	0.01	0.08	0.00	0.01	0.04	0.06	0.03	0.01	0.04
MgO	10.29	2.84	5.42	0.73	2.86	2.81	3.41	1.25	0.67	1.34	0.43	0.90	1.19	1.44	1.39	0.60	1.95
CaO	12.38	3.73	8.26	0.98	1.95	2.09	4.53	1.22	4.43	3.10	2.56	4.75	4.43	5.41	3.86	4.36	4.59
Na_2O	3.11	8.79	6.31	10.11	5.55	6.69	7.53	7.31	7.29	6.29	7.24	8.19	7.12	7.38	6.33	7.41	7.83
K_2O	0.03	0.01	0.01	0.02	0.02	0.02	0.04	0.08	0.40	0.22	0.36	0.24	0.28	0.32	0.43	0.23	0.17
P_2O_5	0.04	0.04	0.04	0.04	0.05	0.08	0.07	0.08	0.17	0.08	0.07	0.05	0.11	0.06	0.22	0.05	0.05
H_2O	2.35	1.20	1.23	1.02	0.59	1.07	1.08	0.59	0.49	0.62	0.44	0.53	0.75	0.87	1.12	0.93	1.21
CO_2	1.16	0.44	0.99	2.43	0.62	0.44	1.29	0.51	0.63	0.44	0.73	0.55	0.29	0.98	0.99	2.60	1.60
Total:	100.37	99.88	99.69	99.82	99.40	99.87	99.89	99.58	99.63	99.87	99.99	99.68	99.65	99.65	99.82	100.21	99.97
Trace elements determined by XRF (ppm):																	
Ba	33	33	36	50	36	44	23	70	49	34	78	30	36	25	<30	25	37
Cr	28	11	<10	<10	<10	<10	221	11	<10	<10	<10	<10	<10	<10	<10	110	18
Nb	<10	13	<10	12	<10	12	<10	11	<10	<10	11	<10	14	<10	<10	<10	<10
Ni	67	29	47	<10	25	87	86	<10	<10	<10	<10	17	10	14	<10	<10	22
Rb	<10	<10	<10	<10	<10	<10	<10	<10	<10	<10	<10	<10	<10	<10	<10	<10	<10
Sr	50	106	80	51	87	90	131	35	142	86	92	194	106	171	113	187	155
V	174	51	77	<10	<10	13	<10	<10	<10	11	<10	16	13	25	<10	<10	21
Y	31	53	86	165	28	136	61	109	84	89	37	40	44	32	63	33	19
Zn	25	29	12	<10	36	30	21	<10	358	23	10	<10	22	28	33	148	26
Zr	100	224	37	88	126	602	218	232	215	289	182	33	679	189	1720	75	76
Trace elements determined by ICP-MS (ppm):																	
Li	4.4	1	0.6	0.06	1.6	2.8	0.7	0.3	1.2	1.2	1.8	0.9	0.8	1.4	5.3	0.5	0.3
Co	31	6.6	19	0.9	2.7	9.2	13	1.1	3	5.3	1.6	2.2	3.8	8.8	5.4	1.6	6.3
Ni	58	19	39	2.4	24	79	71	3.6	7.2	7.4	3.4	5.9	5.3	9.8	9	3.5	13
Sc	20	1.8	3.8	0.26	0.48	4.1	7.1	1	3.4	5.4	1.4	2.8	2.2	3.1		2.3	0.79
Cu	2.7	3.7	5.2	5.1	10	3.8	5.6	3.9	5	5.5	4.6	4.5	9.1	4.3	5.8	3.2	7
Zn	38	17	18	9.3	33	27	24	9.2	17	17	13	12	18	30	32	12	28
Ga	15	29	23	35	18	24	26	27	33	25	26	35	27	33	27	34	28
Rb	0.3	0.3	0.2	0.1	0.4	0.3	0.2	0.2	1.4	0.6	1.4	0.8	0.5	1.2	4	0.3	0.3
Sr	55	105	86	56	90	92	131	40	145	88	89	197	104	174	111	184	156
Zr	24	17	10	9	6	11	5	37	6	11	5	5	10	4	30	3	6
Y	31	47	81	153	27	114	51	96	78	82	33	37	39	29		29	16
Nb	0.2	6.3	5.2	12	5.6	7.3	4.9	11	3.1	7.6	2.4	2.6	12	2.9	5.6	1	2.1
Mo	0.5	0.1	0.1	0.08	0.2	0.05	2.2	0.7	0.2	0.5	0.3	0.1	0.3	0.2	0.5	0.04	0.1
Cd	0	0.02	0.01	0.02	0.03	0.05	0.05	0.02	0.02	0.01	0.01	0.01	0.06	0.03	0.03	0.04	0.02
Sn	0.8	1.1	1.8	2.9	0.6	0.8	2	5	2.6	3	1.9	1.5	3.6	2.8	4.6	1	3.6
Ta	0.04	1.3	0.52	1.5	0.9	1	0.6	1.1	0.29	0.78	0.28	0.18	1	0.38	0.71	0.12	0.24
Rare earth elements determined by ICP-MS (ppm):																	
La	4.4	47	11	17	18	7.5	19	69	18	17	19	12	15	10		19	42
Ce	13	116	43	60	42	22	47	193	48	44	43	33	36	25		44	100

Table T17 (continued).

Core, section, interval (cm):	120R-2, 99–104	121R-1, 83–87	123R-6, 140–146	123R-8, 27–32	90R-3, 38–44	90R-4, 55–58	90R-4, 84–86	124R-1, 111–115	135R-3, 68–72	130R-3, 52–58	138R-4, 59–63	126R-5, 102–106	150R-7, 93–100	153R-1, 35–39	157R-7, 1–5	161R-7, 78–84	202R-7, 96–101
Vein type:	Plag + Diop	Plag + Diop	Plag + Diop	Plag + Amph	Felsic	Felsic	Felsic	Felsic	Felsic	Felsic	Felsic	Felsic	Felsic	Felsic	Felsic	Felsic	Felsic
Pr	1.9	13	7.4	10	4.9	2.6	5.8	22	7	6.1	5.3	4.4	4.4	3.1		5.5	11
Nd	8	48	35	49	17	14	24	82	31	30	23	19	21	14		22	43
Sm	2.2	8.3	9.7	13	3.1	5.3	5.8	15	8.6	7.4	4.3	4.9	4.5	3.1		4.3	6.4
Eu	0.63	1.2	1.3	1.2	0.38	1	1.3	1.5	3.6	2	2	3.7	2.2	2.8		4	1.8
Gd	3.1	7.8	11	15	3	9.3	6.3	14	11	9.4	4.6	5.7	4.8	3.4		4.5	4.4
Tb	0.57	1.2	2.1	3.1	0.51	2	1.2	2.3	2.1	1.9	0.82	0.94	1	0.58		0.79	0.52
Dy	3.9	6.8	13	21	3.6	15	7.9	14	13	12	5.1	6	5.6	4.1		5	2.9
Ho	0.99	1.6	2.9	4.9	0.86	4.1	1.9	3.2	2.9	2.9	1.1	1.4	1.5	1		1.1	0.61
Er	3.4	4.9	9.2	17	3.1	12	6.2	11	9.2	9.2	3.7	4	4.5	3.3		3.6	1.8
Tm	0.69	0.81	1.5	2.6	0.5	2.1	0.96	1.8	1.3	1.4	0.59	0.65	0.72	0.53		0.52	0.28
Yb	6	5.9	11	18	4.1	15	6.6	14	8.3	9.9	4.3	4.2	5.9	4		3.6	2.1
Lu	1.4	0.94	1.8	2.7	0.69	2.3	1.1	2.3	1.3	1.6	0.67	0.6	1.1	0.69		0.54	0.37

Note: XRF = X-ray diffraction, ICP-MS = inductively coupled plasma–mass spectroscopy.

Plate P1. Full thin section views of felsic and plagioclase + amphibole and plagioclase + diopside veins in Hole 735B. Note the sharp vein contacts in all samples. **1.** Plagioclase + quartz vein cutting gabbro (Sample 176-735B-54R-4, 69–78 cm). **2.** Large plagioclase-rich vein containing small amounts of epidote, chlorite, greenish brown amphibole, titanite, and zeolite cutting gabbro. Irregular patch in center of vein is dark brown aphanitic material (Sample 176-735B-58R-3, 0–8 cm). **3.** Plagioclase + amphibole vein cutting gabbro. Vein is zoned with plagioclase along the margins and green amphibole in the center. The vein also contains small amounts of diopside, epidote, and brown clay minerals (Sample 176-735B-45R-3, 107–112 cm). **4.** Plagioclase + amphibole vein cutting olivine gabbro. Vein consists chiefly of small, granular plagioclase crystals with a band of greenish brown amphibole in the center (Sample 176-735B-31R-3, 4–10 cm). All scale bars = 10 mm.

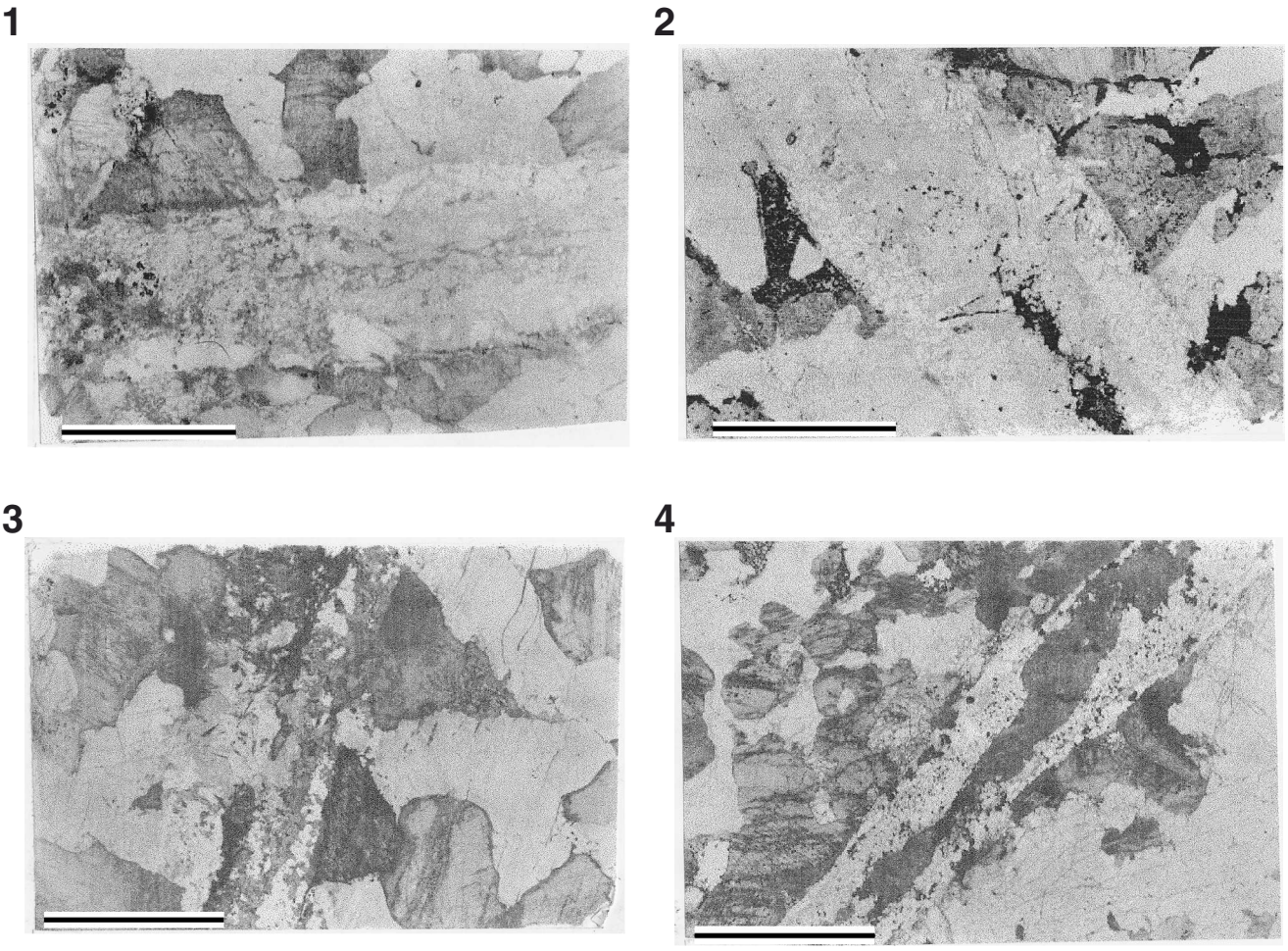

Plate P2. Photomicrographs of felsic and plagioclase-rich veins showing common presence of euhedral, strongly zoned plagioclase crystals. **1.** Euhedral plagioclase crystals in vein center, showing minor zoning and presence of dark aphanitic material between the grains (Sample 176-735B-126R-5, 101–106 cm). **2.** A large, nearly euhedral plagioclase crystal showing typically pitted and corroded core and clear rims. Note the rounded end of the pitted core in the upper left and the euhedral overgrowth of more sodic plagioclase (Sample 176-735B-153R-1, 33–39 cm). **3.** Large euhedral to subhedral, strongly zoned plagioclase in center of vein. The cores of the plagioclase grains show little pitting or corrosion. The space between the plagioclase grains (blue) is filled with late-stage quartz in optical continuity (Sample 176-735B-130R-3, 52–58 cm). **4.** Strongly corroded, subhedral plagioclase grains in felsic vein. Note the dark, pitted plagioclase cores and clear, white rims and overall porous nature of the vein (Sample 176-735B-157R-7, 1–5 cm). All scale bars = 1 mm.

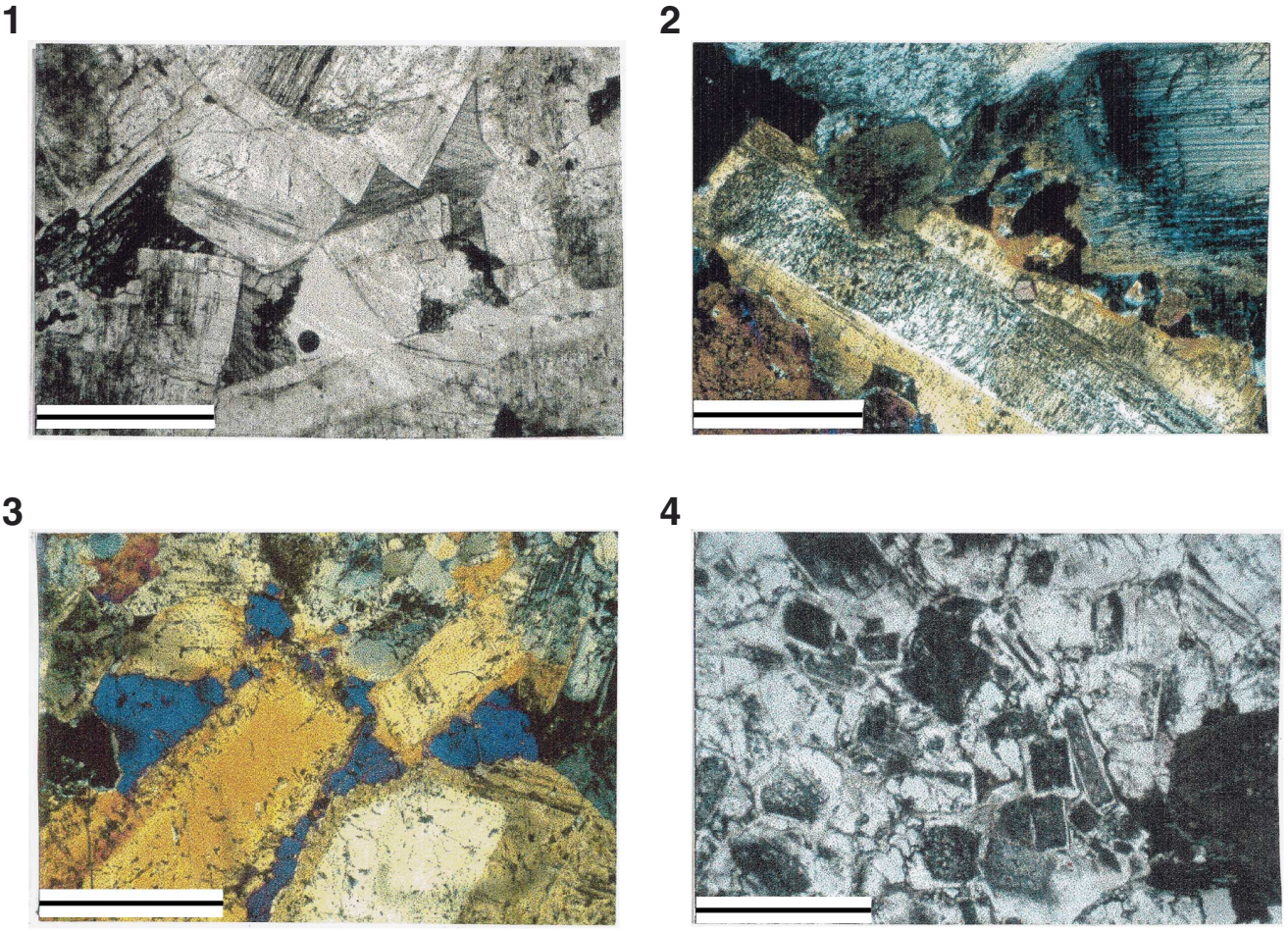

Plate P3. Photomicrographs of plagioclase + diopside and plagioclase + amphibole veins in Hole 735B. **1.** Fine-grained felsic vein with a band of green diopside along the center. Large light brown grain and smaller reddish grain are titanite. Matrix of the diopside-rich zone consists of dark, aphanitic material (Sample 176-735B-121R-1, 81–86 cm). **2.** Coarse-grained felsic vein with narrow band of green amphibole near center. Reddish brown grain is titanite (Sample 176-735B-170R-2, 15–21 cm). **3.** Well-developed plagioclase + amphibole vein with distinct mineral zoning. Note the thin band of brown amphibole where the vein cuts clinopyroxene in the host rock. This is followed inward by a band of plagioclase with a few crystals of green amphibole, followed in turn by bands of dark, aphanitic material with some small crystals of green amphibole (Sample 176-735B-192R-6, 46–51 cm). **4.** Same vein as in 3 with crossed polars. This view shows the granular nature of the plagioclase (Sample 176-735B-192R-6, 46–51 cm.). All scale bars = 1 mm.

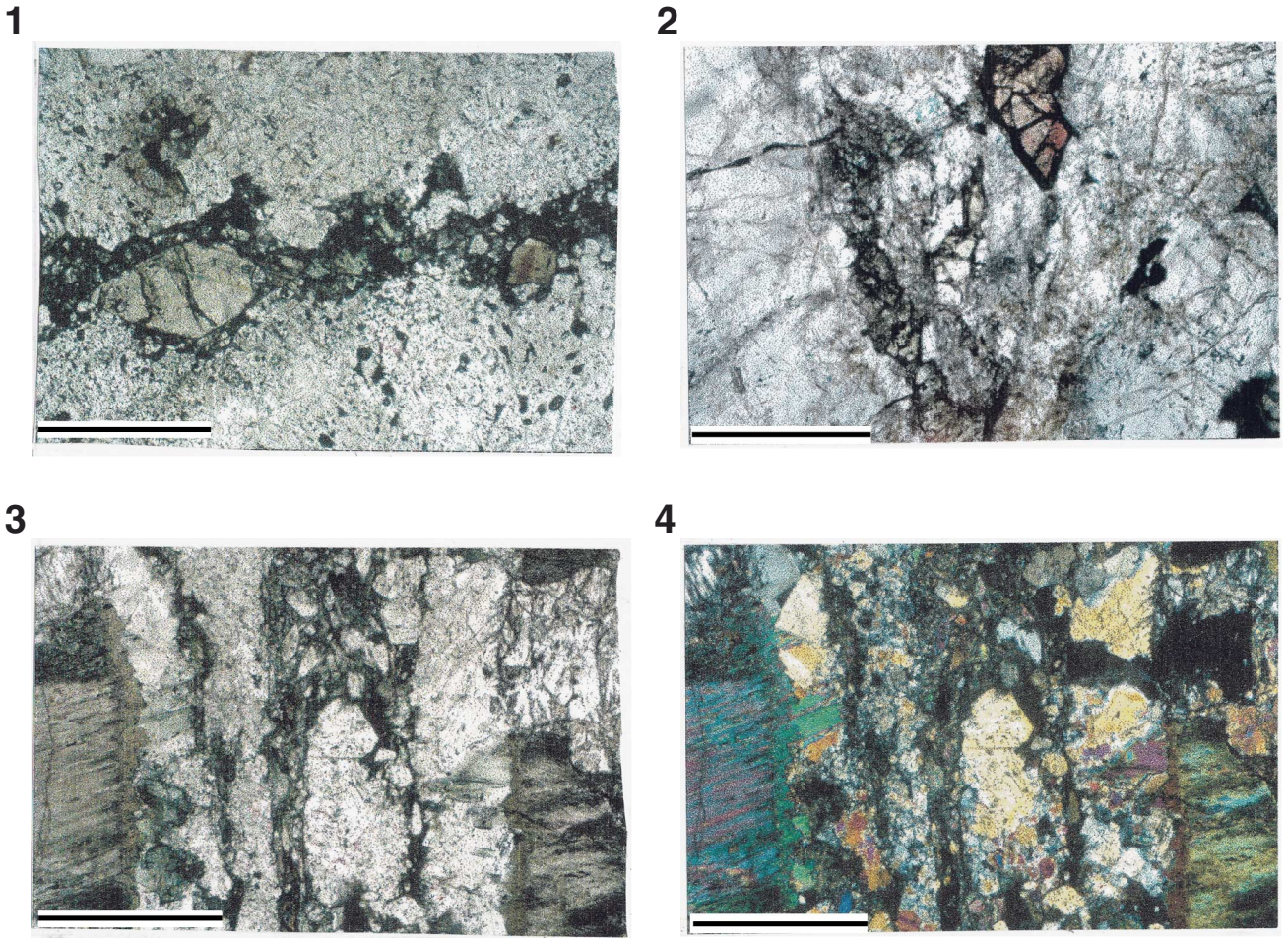

Plate P4. Photomicrographs of various vein minerals in Hole 735B. **1.** Full thin section view of an amphibole + plagioclase vein cutting slightly foliated gabbro. Note the sharp but irregular vein margins (Sample 176-735B-19R-5, 62–73 cm). **2.** Large, euhedral diopside crystals in plagioclase + diopside vein. Large crystals are located only near the vein wall. Note the Fe/Mg zoning in the crystals with the ratio increasing toward the margins (Sample 176-735B-69R-5, 31–41 cm). **3.** Narrow carbonate veins cutting olivine gabbro. Note the rather irregular vein margins and the orientation of crystals within the vein (Sample 176-735B-91R-5, 81–86 cm). **4.** Narrow natrolite vein filling crack in the center of a fine-grained felsic vein (Sample 176-735B-84R-6, 31–41 cm). All scale bars = 1 mm.

1

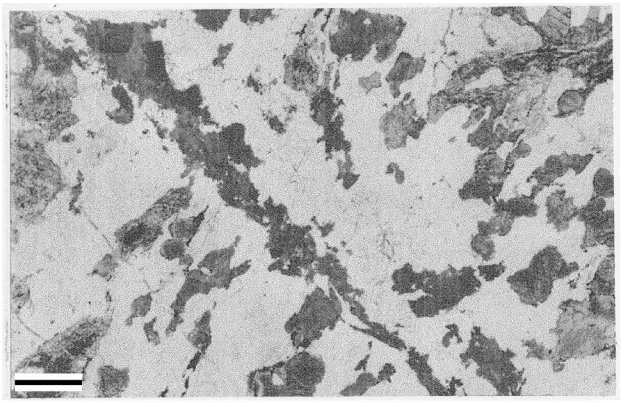

2

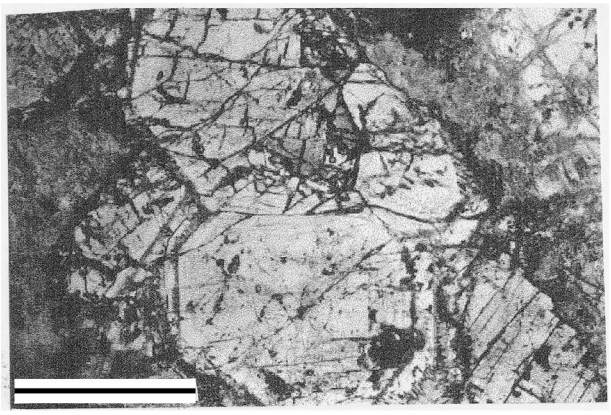

3

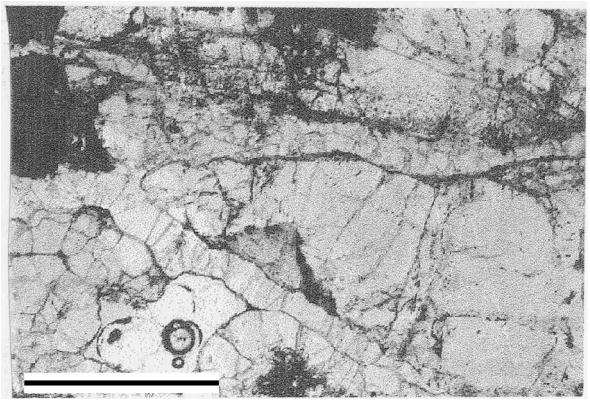

4

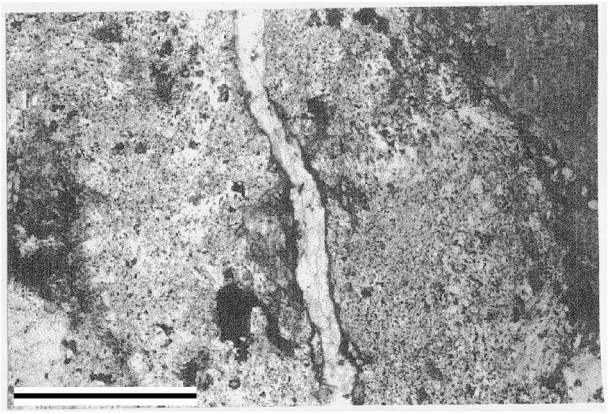

Plate P5. Photomicrographs of vein minerals in Hole 735B. **1.** A felsic patch in gabbro in which amphibole is replacing plagioclase (irregular, light gray patch on right side). The amphibole is strongly zoned from dark brown to light brown and from dark green to light green. The brown amphibole is edenite to magnesio-hornblende, and the green amphibole is actinolite and ferro-actinolite (Sample 176-735B-202R-7, 96–101 cm). **2.** Vein filled with natrolite and calcite. The natrolite forms radiating clusters of prismatic crystals growing around the calcite grain (Sample 176-735B-181R-1, 131–136 cm). **3.** A different part of the same vein as in 2. Here the natrolite forms small white crystals with square cross-sections in a matrix of light brown aphanitic material. Carbonate fills the irregular parallel crack just above the zeolite vein (Sample 176-735B-181R-1, 131–136 cm). **4.** Black to dark brown smectite vein cutting gabbro. Vein has sharp margins but tends to follow grain boundaries. At one point it has bifurcated and enclosed a piece of plagioclase. The small, white veinlet cutting the smectite is a late-stage crack filled with carbonate (Sample 176-735B-133R-7, 92–98 cm). All scale bars = 1 mm.